Role of intermediate water variability in the Caribbean and Gulf of Mexico in deglacial climate change

Dissertation

David-Willem Poggemann

Kiel 2017

ozean der zukunft
DIE KIELER MEERESWISSENSCHAFTEN

GEOMAR

SIGILLUM COLLEGII SCIENT. MATH. ET NAT. CHILONIENSIS
COMMUNE ARTIUM VINCULUM

Role of intermediate water variability in the Caribbean and Gulf of Mexico in deglacial climate change

Dissertation

zur Erlangung des Doktorgrades *Dr. rer. nat.*

an der Mathematisch-Naturwissenschaftlichen Fakultät

der Christian-Albrechts-Universität zu Kiel

vorgelegt von

David-Willem Poggemann

Kiel, 2017

Erstgutachter: Prof. Dr. Dirk Nürnberg

Zweitgutachter: Prof. Dr. Martin Frank

Eingereicht am: 04. April 2017

Tag der Disputation: 30. Mai 2017

Zum Druck genehmigt:

Der Dekan

Erklärung:

Mit Abgabe dieser Dissertationsarbeit erkläre ich,

- dass die vorliegende Arbeit, abgesehen von der Beratung durch meine Betreuer, nach Inhalt und Form meine eigene ist.
- dass diese Arbeit weder in Teilen noch in Gänze an einer anderen Hochschule im Rahmen eines Prüfungsverfahrens eingereicht wurde.
- dass ich die vorliegende Arbeit selbständig und ausschließlich unter Zuhilfenahme der angegebenen Quellen und Hilfsmittel angefertigt habe.
- dass die vorliegende Arbeit unter Beachtung der Regeln der guten wissenschaftlichen Praxis der Deutschen Forschungsgemeinschaft angefertigt wurde.
- dass Teile dieser Arbeit bereits in Fachzeitschriften veröffentlicht sind, oder in Vorbereitung zur Einreichung bei einer Fachzeitschrift stehen.

Kiel, 04. April 2017

(David-Willem Poggemann)

„I have a bad feeling about this!”

Obi-Wan Kenobi

Abstract

During the last ~ 150 years, the manmade release of greenhouse gases has effectively shaped the global climate system. But the consequences for near and far future climate evolution are discussed controversial. In particular the impact of global warming on the global oceanic system remains unclear. Despite ongoing gradually increasing surface temperatures predicted by future climate models and intensified radiative forcing, surface air temperatures stalled for about 15 years at the beginning of the 21st century. Recent studies suggest the intermediate to deep Southern Ocean (SO) to be a major sink for global heat. Other studies additionally predict a major impact of ongoing climate warming on the Atlantic Meridional Overturning Circulation (AMOC). In general, future climate predictions and the oceans role in a warming global climate are debated widely. Paleo-oceanographic studies and the reconstruction of ocean circulation changes on millennial time scales might improve our understanding of the ocean-atmosphere interaction during a global climate change.

This Ph.D.-Thesis aims to analyse the intermediate water mass circulation changes in the Atlantic Ocean in response to major perturbations of the AMOC during the last deglaciation. The approach combined the use of benthic foraminiferal based Cd_w as a proxy for past nutrient saturation, Mg/Ca to reconstruct past Intermediate Water Temperatures, $\delta^{13}C$ as a proxy for nutrient saturation and ventilation and mixed planktonic foraminiferal εNd to reconstruct past water mass distribution in the tropical Atlantic.

The results of this Ph.D.-Thesis indicate two major signal transmission pathways from the northern hemisphere into the surface SO and further into Antarctic Intermediate Water (AAIW), therefore effectively altering its geochemical and thermal properties. Triggered by rapid northern hemisphere cooling events during the last deglaciation, the atmospheric circulation pattern and the Atlantic overturning circulation changed considerably. Likely due to the postulated resulting heat accumulation in the SO, AAIW rapidly warmed in its formation areas and transferred this heat signal into the tropical intermediate W-Atlantic. The northward heat transfer via AAIW therefore might have dampened the SO warming episodes during the last deglaciation. The convincing synchronicity of the here presented Intermediate Water Temperature record from the tropical W-Atlantic to N-Atlantic AMOC strength reconstructions indicate a rather short response time delayed by a maximum of ~ 1000 years.

In contrast, the deep oceanic response time in the SO was lagged by about 2.5 thousand years to northern hemisphere cooling events. The results of this thesis indicate major oceanic circulation re-organisation in the Atlantic due to the postulated AMOC perturbations during the last deglaciation. While the AMOC today is characterised by one overturning cell, it was split into two cells separated from each other during the Last Glacial Maximum. In delayed response to weakened or even collapsed overturning in the N-Atlantic, the SO experienced enhanced upwelling of nutrient-rich deep water. The reconstructed Cd_w data from the tropical W-Atlantic presented here indicate enhanced nutrient enrichment of AAIW during these times. The reconnection of the overturning cells during the last deglaciation therefore effectively shaped the geochemical signature of AAIW. The enhanced nutrient supply to the N-Atlantic via AAIW might have fed low latitude productivity and thereby dampened the deglacial atmospheric rise of CO_2.

Comparison of nutrient and Intermediate Water Temperature reconstructions from the S-Caribbean with appropriate datasets from the Gulf of Mexico (GoM) reveals a distinct warming effect of AAIW in the Caribbean and a simultaneous cooling effect of AAIW in the GoM during the last deglaciation. While AAIW was present in the S-Caribbean permanently during the past 24 thousand years, it was likely absent from the GoM during the Last Glacial Maximum and in the Holocene. The here presented data in contrast indicate enhanced northward dispersal of AAIW into the GoM during northern hemisphere cooling events. The Cd_w reconstructions from the GoM point to enhanced nutrient supply during these times. While the heat accumulation in the SO likely fostered distinct warming of AAIW due to AMOC perturbations, the reconstructed Intermediate Water Temperatures from the GoM indicate, that AAIW was still cold enough to effectively cool the GoM at intermediate depth.

The results of this Ph.D.-Thesis show that a weakening or even collapse of the AMOC might have triggered the geochemical and thermal properties of AAIW effectively. The reconstruction of intermediate water mass distribution therefore is a powerful tool to analyse ocean circulation changes under warming climate conditions and might help to understand future climate evolution and to improve oceanic model predictions.

Zusammenfassung

Durch den verstärkten Ausstoß von Treibhausgasen in den letzten ca. 150 Jahren beeinflusst der Mensch das globale Klimasystem nachhaltig. Die Auswirkungen auf die Klimaentwicklung in naher und ferner Zukunft sind jedoch unsicher. Besonders der Einfluss des Klimawandels auf das globale Ozeansystem bleibt umstritten. Entgegen der Prognosen durch Klimamodelle und trotz weiter ansteigendem Strahlungsantrieb, pausierte der Anstieg der oberflächennahen Temperaturen für ca. 15 Jahre zu Anfang des 21. Jahrhunderts. Einige Studien deuten darauf hin, dass tiefe und Zwischen-Wassermassen im Südozean diese Wärmeenergie aufgenommen haben könnten. Zusätzlich deuten andere Ergebnisse darauf hin, dass die globale Erwärmung in Zukunft die Ausprägung der thermohalinen Zirkulation im Atlantik deutlich beeinflussen könnte. Doch generell bleiben Prognosen für die Entwicklung des Klimas und deren Wechselwirkungen mit dem Ozean umstritten. Paläo-ozeanographische Untersuchungen sowie die Rekonstruktion von Ozeanzirkulationsänderungen über Zeitspannen von mehreren zehntausend Jahren, können das Verständnis von Ozean-Atmosphäre Wechselwirkungen unter dem Einfluss eines sich ändernden Klimas verbessern.

Ziel dieser Dissertation ist es, den Einfluss von Änderungen in der atlantischen Tiefenwasserbildung (AMOC) auf die Zirkulation von atlantischen Zwischenwassermassen während des Übergangs (Termination) aus dem letzten Glazial in die heutige Warmphase, das Holozän, zu untersuchen. Dazu werden folgende geochemische Werkzeuge genutzt: Cd_w zur Rekonstruktion der Verteilung von Nährstoffen im Wasser, das Mg/Ca-Verhältnis in Foraminiferenschalen um Temperaturen im Zwischenwasser (IWT) zu rekonstruieren, $\delta^{13}C$ als Anzeiger für Änderungen in der Nährstoffkonzentration und in der Ventilation sowie εNd um die Verteilung von verschiedenen Wassermassen zu analysieren.

Die Ergebnisse aus dieser Dissertation deuten darauf hin, dass klimatische Signale, hervorgerufen durch Änderungen in der nordatlantischen Tiefenwasserbildung, im Wesentlichen über zwei verschiedene Wege in den Oberflächenozean im Südatlantik und von dort weiter in das Antarktische Zwischenwasser (AAIW) übertragen wurden. Dadurch wurden sowohl die thermische, als auch die geochemische Signatur des AAIW verändert. Ausgelöst durch rapide Kälteeinbrüche in der Nordhemisphäre während der letzten Termination, änderten sich die ozeanischen und atmosphärischen Zirkulationsmuster deutlich. Durch den resultierenden Hitzestau im Südozean erwärmte sich das AAIW bei der Bildung und transportierte dieses Wärmesignal in den Westatlantik. Diese Aufnahme von Wärme durch das AAIW könnte den Temperaturanstieg im Südozean während der letzten Termination gedämpft haben. Die zeitliche Übereinstimmung der hier präsentierten Rekonstruktionen von Temperaturen im Zwischenwasser des tropischen Westatlantiks sowie publizierten Rekonstruktionen von Änderungen in der nordatlantischen Tiefenwasserbildung deuten darauf hin, dass die Reaktion der IWT im AAIW um maximal eintausend Jahre versetzt war. Damit wäre die Reaktionszeit der thermischen Änderungen im AAIW als relativ kurz anzusehen.

Im Gegensatz dazu reagierte der tiefe Südatlantik mit einem zeitlichen Versatz von ca. zweieinhalb tausend Jahren, deutlich später auf diese Änderungen. Die Ergebnisse dieser Dissertation deuten auf erhebliche Zirkulationsänderungen im tiefen Atlantik als Reaktion auf die Ausprägungsänderungen der AMOC während der letzten Termination hin. Während die

heutige AMOC im Wesentlichen aus einer einzigen Umwälzzelle besteht, war sie im letzten Glazial durch zwei voneinander getrennte Umwälzzellen geprägt. Als während der letzten Termination die nordatlantische Tiefenwasserbildung gestört wurde, stieg zeitlich verzögert sehr nährstoffreiches Tiefenwasser im Südozean an die Oberfläche. Die hier präsentierten Cd_w-Rekonstruktionen aus dem tropischen Westatlantik deuten auf eine gleichzeitige Nährstoffanreicherung im AAIW hin. Die Verbindung der vorher voneinander getrennten Umwälzzellen während der letzten Termination hat die geochemische Signatur des AAIW deutlich verändert. Dieser verstärkte Eintrag von Nährstoffen in den Nordatlantik durch AAIW könnte die biologische Produktivität während der letzten Termination gefördert und damit den Anstieg von CO_2 in der Atmosphäre gebremst haben.

Der Vergleich der Nährstoff- und Temperaturrekonstruktionen aus der Karibik mit entsprechenden, hier präsentierten Datensätzen aus dem Golf von Mexico (GoM) deutet darauf hin, dass das AAIW während der rapiden Kältephasen in der Nordhemisphäre zwar erwärmt war, aber gleichzeitig den GoM in entsprechender Tiefe gekühlt hat. Im Gegensatz zur Südkaribik, stieß das AAIW während der letzten 24 tausend Jahre nicht permanent bis in den GoM vor und war im letzten Glazial und im Holozän dort nicht präsent. Die Ergebnisse dieser Arbeit deuten allerdings darauf hin, dass sich das AAIW während der Kältephasen weiter nach Norden und damit weiter in den GoM ausgebreitet hat. Die hier präsentierten Cd_w Rekonstruktionen deuten dementsprechend auf eine erhöhte Nährstoffzufuhr durch AAIW in den GoM zu diesen Zeiten hin. Während der Hitzestau im Südozean wahrscheinlich die Erwärmung im AAIW gesteuert hat, deuten die rekonstruierten Temperaturdaten darauf hin, dass es trotzdem kalt genug war um den GoM effektiv in der Zwischenwassertiefe zu kühlen.

Die gesamten Ergebnisse dieser Dissertation zeigen, dass eine Abschwächung oder sogar ein Kollaps der nordatlantischen Tiefenwasserbildung die geochemische und thermale Signatur des AAIW deutlich geändert haben. Die Analyse der Verbreitung und Veränderung von Zwischenwassermassen während eines sich ändernden Klimas ist damit eine nützliche Möglichkeit um neue Erkenntnisse auch über mögliche zukünftige Klimaentwicklungen zu erlangen und damit die Vorhersagen zu verbessern.

Table of Contents

Abstract V
Zusammenfassung VII
Table of Contents IX
List of Abbreviations XI
Introduction ..... - 1 -
The global thermohaline conveyor belt and the Atlantic Meridional Overturning Circulation: ..... - 1 -
Oceanographic setting in the Gulf of Mexico and in the Caribbean: ..... - 3 -
Antarctic Intermediate Water: ..... - 7 -
Glacial – deglacial AMOC perturbations: ..... - 7 -
Research questions addressed in this study: ..... - 11 -
Material & Methods ..... - 13 -
Scientific Chapter 1: Rapid Deglacial Injection of Nutrients into the tropical Atlantic via Antarctic Intermediate Water ..... - 15 -
1.1 Keywords ..... - 16 -
1.2 Abstract ..... - 16 -
1.3 Introduction ..... - 16 -
1.4 Materials and Methods ..... - 17 -
Age models ..... - 17 -
Cd/Ca measurements ..... - 18 -
Composite Cd_w-record for 1300 m water depth ..... - 18 -
$\delta^{13}C$ measurements ..... - 18 -
Data outliers ..... - 18 -
1.5 Results and Discussion ..... - 18 -
1.6 Conclusions ..... - 22 -
1.7 Acknowledgements ..... - 22 -
1.8 References ..... - 23 -
Scientific Chapter 2: Deglacial heat deprivation from the atmosphere in the Southern Ocean via Antarctic Intermediate Water ..... - 25 -
2.1 Highlights ..... - 26 -
2.2 Abstract ..... - 26 -
2.3 Introduction ..... - 27 -
2.4 Materials and Methods ..... - 29 -
Mg/Ca analyses ..... - 29 -

Table of Contents

Nd isotope measurements ..... - 30 -

2.5 Results ..... - 31 -

2.6 Discussion ..... - 32 -

2.7 Static stability check for warmed AAIW conditions ..... - 38 -

2.8 Conclusions ..... - 39 -

2.9 Acknowledgements ..... - 40 -

2.10 References ..... - 40 -

Scientific Chapter 3: Antarctic Intermediate Water effectively cooled the Gulf of Mexico during rapid deglacial northern hemisphere cooling events ..... - 45 -

3.1 Highlights ..... - 46 -

3.2 Abstract: ..... - 46 -

3.3 Introduction: ..... - 47 -

Caribbean and GoM oceanographic setting: ..... - 48 -

3.4 Material & Methods ..... - 49 -

Mg/Ca and Cd/Ca measurements: ..... - 49 -

IWT-gradient calculation: ..... - 50 -

3.5 Results ..... - 51 -

3.6 Discussion ..... - 51 -

3.7 Conclusion ..... - 56 -

3.8 Acknowledgements: ..... - 56 -

3.9 References: ..... - 56 -

General Synthesis & Outlook ..... - 59 -

Additional references ..... - 63 -

Acknowledgements ..... - 69 -

Curriculum Vitae ..... - 70 -

Supplementary material ..... - 72 -

Supplement S1 for Scientific Chapter 1 as published and available online: ..... - 72 -

Supplement S2 for Scientific Chapter 2: ..... - 82 -

Supplement S3 for Scientific Chapter 3: ..... - 95 -

List of Abbreviations

180 / 180-1 = M78/1-180-1

235 / 235-1 = M78/1-235-1

222 / 222-9 = M78/1-222-9

2198 = MD99-2198

AAIW = Antarctic Intermediate Water

AABW = Antarctic Bottom Water

ACC = Antarctic Circumpolar Current

ACR = Antarctic Cold Reversal

AMOC = Atlantic Meridional Overturning Circulation

BA = Bølling-Allerød

BWT = Bottom Water Temperature

Ca = Calcium

Cd = Cadmium

Cd_w = Cadmium water

CPDW = Circumpolar Deep Water

DFG = Deutsche Forschungsgemeinschaft

GNAIW = Glacial North Atlantic Intermediate Water

GoM = Gulf of Mexico

HS1 = Heinrich Stadial 1

IDW = Indian Deep Water

IRD = Ice rafted debris

ITCZ = Intertropical Convergence Zone

IWT = Intermediate Water Temperature

ka BP = thousand years before present

LGM = Last Glacial Maximum

Mg = Magnesium

MS = Magnetic Susceptibility

NADW = North Atlantic Deep Water

NPIW = North Pacific Intermediate Water

P = Phosphate

Pa = Protactinium

PDW = Pacific Deep Water

ppb = parts per billion

ppm = parts per million

ppt = parts per trillion

SAMW = Subantarctic Mode Water

SO = Southern Ocean

SST = Sea surface temperatures

subSST = Sea subsurface temperatures

Sv = Sverdrup

Th = Thorium

WOA13 = World Ocean Atlas 2013

YD = Younger Dryas

Introduction

The global thermohaline conveyor belt and the Atlantic Meridional Overturning Circulation:

The Intergovernmental Panel on climate Change considers the anthropogenic impact on the global climate evolution, in particular the increased release of greenhouse gases to the atmosphere, to be a major driver of the warming global climate system (e.g. Stocker et al., 2013). The use of fossil fuels has increased the atmospheric CO_2 level from a preindustrial value of ~ 280 ppm (e.g. Pearman et al., 1986) to more than 400 ppm today (Le Quéré et al., 2016). This highly elevated output of CO_2, methane and other greenhouse gases is considered to be the major reason for global climate warming during the last decades. The exact dimension of warming and its impact on the global oceanic system is debated widely in the scientific community (e.g. Zickfeld et al., 2017). Due to the slow response time of the ocean and its huge capacity to store CO_2, the future evolution of this sensitive system remains ambiguous. Predicting the influence of a warming climate on the global overturning circulation system is especially controversial. This study attempts to show how and how rapid the Atlantic Meridional Overturning Circulation (AMOC) changed under natural climate conditions unaffected by anthropogenic forcing, in order to allow a better assessment of potential ocean circulation change during the near future.

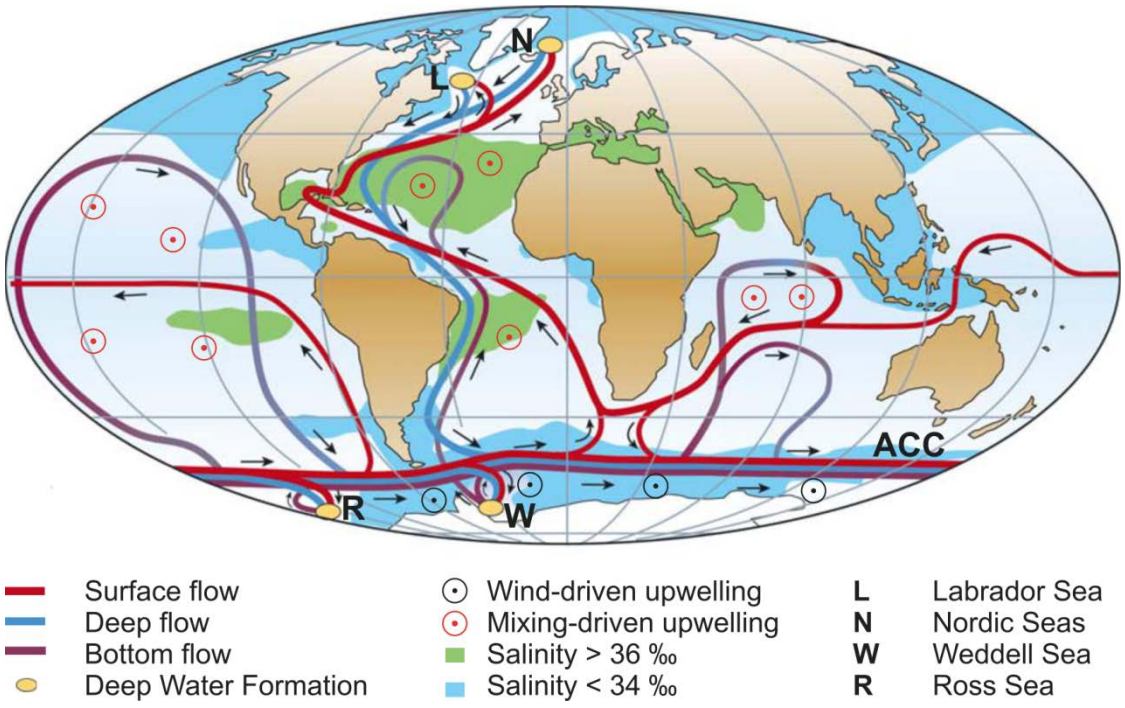

Figure 1: Simplified schematic indicating the global thermohaline circulation system. In the Atlantic ocean, warm and saline surface and subsurface waters from the (sub-)tropical W-Atlantic are transported to the N-Atlantic, where they cool, increase in density and sink to form North Atlantic Deep Water, which then flows southwards at depth. This southward flow is compensated by northward flowing Antarctic Bottom Water and Antarctic Intermediate Water that form in the Southern Ocean. (Figure from Kuhlbrodt et al., 2007)

The modern global overturning circulation connects all major ocean basins (Fig. 1), re-distributes heat, salt, CO_2 and nutrients, and is the main driver of moisture supply towards the high latitudes, therefore playing a key role in the global climate system. Overturning circulation is mainly driven by deep water formation in the N-Atlantic and in the Southern Ocean (SO) (Fig. 2) (e.g. Rahmstorf, 2002 and references therein). As main driver in the global thermohaline conveyor belt, the AMOC dynamics are of crucial interest for climate research. As northward directed (sub-)surface branch of the AMOC, the Gulf Stream transports warm and saline waters from the Caribbean and the Gulf of Mexico (GoM) to the N-Atlantic and thereby generates relatively warm climate conditions on the NW-European continent (e.g. Talley, 1996, 2013; Buckley & Marshall, 2016). The surface and subsurface waters of the Gulf Stream cool, increase in density and sink to form North Atlantic Deep Water (NADW) in the N-Atlantic which then flows southwards at a water depth between ~ 1300 and 4000 m and is characterised by low nutrient conditions and high salinities (e.g. Talley et al., 2003; Marchitto & Broecker, 2006; Kanzow et al., 2010). This deep water formation in the N-Atlantic is therefore considered to be a major driver of the AMOC system. The southward flowing NADW is compensated by northward flowing southern sourced waters, comprising Antarctic Intermediate Water (AAIW, ~ 600 – 1000 m water depth) and Antarctic Bottom Water (AABW, below ~ 5000 m water depth), both of which are formed in the SO and are characterised by low salinities and high nutrient contents (e.g. Talley, 1996; Marchitto & Broecker, 2006; Talley, 2013).The strength of deep water formation in the N-Atlantic and therefore the stability of the AMOC under a postulated ongoing future climate warming trend is debated widely. While some studies indicate a distinct weakening or even collapse of the AMOC, others point to rather minor changes (e.g. Weaver et al., 2012; Liu et al., 2017). Due to biases and uncertainties in model simulations and future climate predictions, the AMOC variability expected even in the near future remains unclear. High-resolution paleo-oceanographic studies of the glacial – interglacial AMOC variability, especially in times of abrupt climate fluctuations, may help to better understand how the AMOC functions within a changing climate system and therefore support future climate predictions.

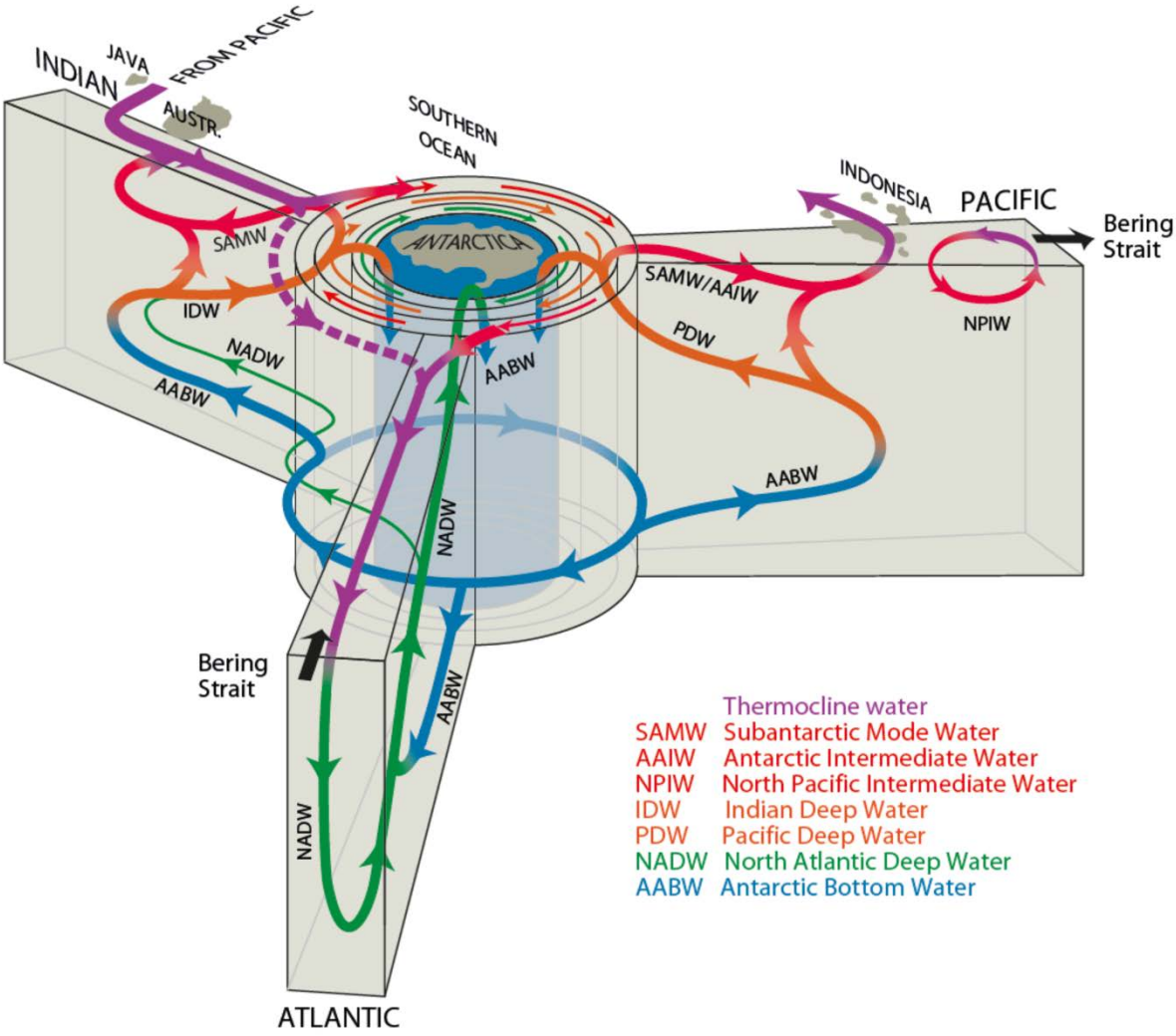

Figure 2: Schematic pattern of the modern overturning circulation in the Atlantic, Pacific and Indian Ocean with a focus on the southern hemisphere. North Atlantic Deep Water penetrates far into the Southern Ocean, mixes with Antarctic Bottom Water and wells up in the Southern Ocean. Together with waters from the Pacific, NADW contributes to the formation of southern sourced water masses. (Figure from Talley, 2013)

Oceanographic setting in the Gulf of Mexico and in the Caribbean:

Due to their position in the (sub-)tropical W-Atlantic, the GoM and the Caribbean are influenced by both, northward flowing AAIW and southward flowing NADW, and therefore are key locations to decipher changes in the AMOC system on millennial time scales. The warm and saline surface and subsurface water masses from these basins are transported northward by the Gulf Stream into the N-Atlantic where they sink and contribute to the formation of NADW (e.g. Talley, 1996; 2013). While the upper 80 m of the water column in the Caribbean are mainly relatively fresh Caribbean Water, the depth between 80 and 180 m is dominated by highly saline Subtropical Underwater (Wüst, 1964). Together these two water masses form the Caribbean thermocline (Metcalf, 1976) and are transported to the GoM via the Caribbean Current. On the intermediate to deep water depth level, both basins are influenced by nutrient depleted and saline northern sourced NADW and by nutrient

enriched and fresher southern sourced AAIW (e.g. Wüst, 1964; Merino, 1997; Sturges, 2005; Osborne et al., 2014). Paleo-oceanographic studies from the GoM and from the Caribbean can therefore provide useful reconstructions of the past AMOC evolution on millennial to centennial timescales.

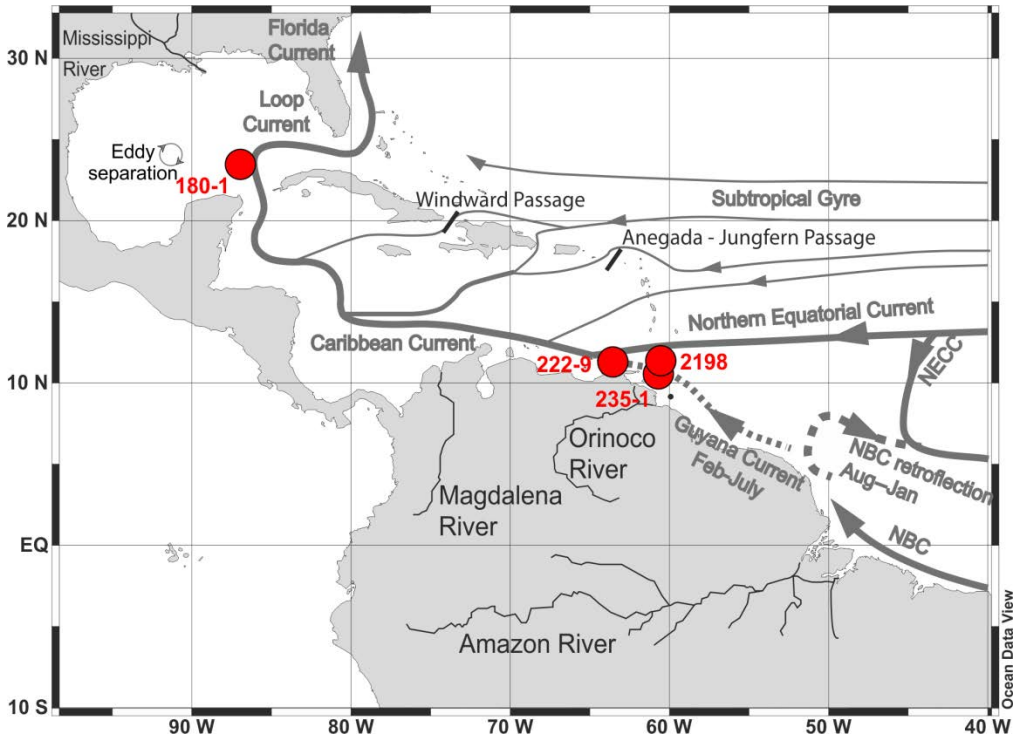

Figure 3: Map showing the locations of sediment cores analysed in this study (red circles), as well as major rivers and surface ocean currents in the Caribbean and the Gulf of Mexico. NBC = North Brazil Current; NECC = Northern Equatorial Counter Current; Sediment cores: 180-1 = M78/1-180-1; 222-9 = M78/1-222-9; 235-1 = M78/1-235-1; 2198 = MD99-2198; (Figure modified from Osborne et al., 2014)

The surface water mass distribution in the Caribbean is mainly driven by the Caribbean Current, which is an extension of the Northern Equatorial Current and the boreal spring/summer Guyana Current (e.g. Hellweger and Gordon, 2002; Johns et al., 2002; Osborne et al., 2014). On its northward pathway through the Caribbean and into the GoM, surface and subsurface waters, mainly Subtropical Underwater, are added to the Caribbean Current via the passages through the Antilles. These contributions are mainly driven by the N-Atlantic Subtropical Gyre (Fig. 3) (Johns et al., 2002). In addition, Amazon and Orinoco river discharge affect the Caribbean and GoM surface hydrography dependent on the position of the ITCZ (Müller-Karger et al., 1989). Passing the Yucatan Strait, the Caribbean Current enters the GoM as the now called Loop Current which is the dominant surface / subsurface feature in this basin. Today the Loop Current is characterised by the aperiodic shedding of anticyclonic eddies with an unstable periodicity of 3 – 18 months (e.g. Nürnberg et al., 2008; 2015). According to Chang & Oey (2010), the eddies can reach a depth of 500 – 1000 m, therefore influencing surface, subsurface and intermediate water masses. The GoM surface hydrographic setting is additionally influenced by Mississippi River discharge which is

a major source for freshwater and nutrient supply to the north-eastern shelves of the GoM (Wawrik & Paul, 2004). Both, the eddy shedding periodicity and the Mississippi River discharge changed significantly during the last deglaciation (e.g. Flower et al., 2004; Nürnberg et al., 2008; Kujau et al., 2010; Mildner et al., 2013).

Below the thermocline, the Caribbean is dominated by AAIW at intermediate depth, which is transported northwards and can be traced into the Yucatan Strait, where it is mixed up with thermocline waters (Fig. 4) (e.g. Merino, 1997; Osborne et al., 2014). Below the AAIW, the Caribbean is filled with upper NADW, which enters via the deep passages between the Antilles (e.g. Wüst, 1964; Osborne et al., 2014).

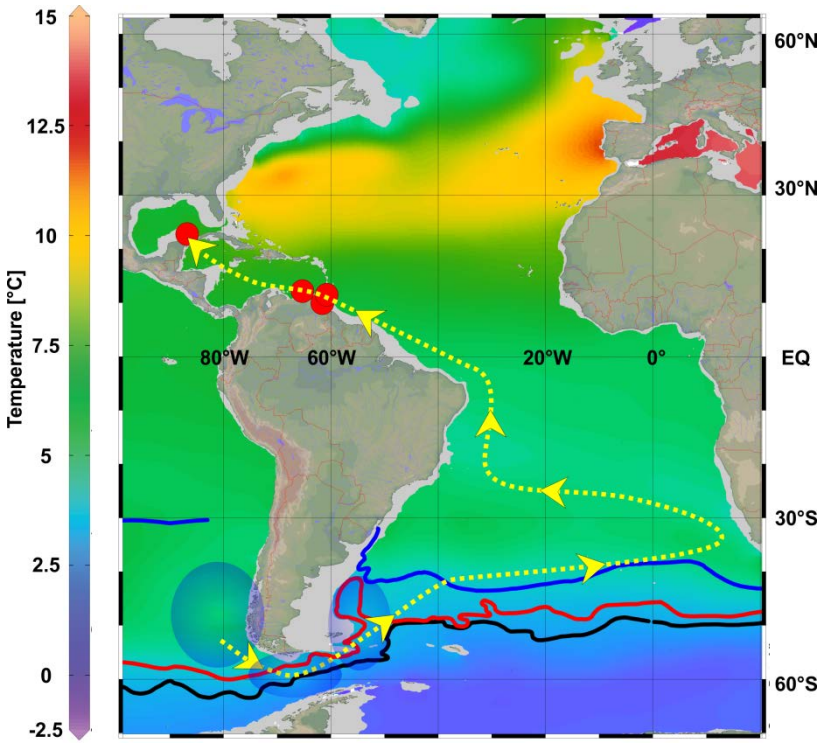

Figure 4: Simplified pathway illustration of Antarctic Intermediate Water from the Southern Ocean into the (sub-)tropical N-Atlantic (following Taft, 1963; Talley, 1996; Boebel et al., 1999; Bostock et al., 2010). Colour shading indicates intermediate water temperature at 850 m water depth (data obtained from World Ocean Atlas; Boyer et al., 2013). The pathway of AAIW is depicted by the yellow dashed line. Red circles indicate sediment core locations analysed in this thesis in the S-Caribbean and in the Gulf of Mexico. Blue line = Subtropical Front; red line = Subpolar Front; black line = Polar Front. Blue shaded ellipses indicate main formation areas of Atlantic AAIW. The figure was created using Ocean Data View (Schlitzer, 2015).

Today, the total inflow of waters into the Caribbean Sea is ~ 28 Sverdrup (Sv; 1 SV = 10^6 m^3/s) which is split between the Greater Antilles passages (~ 10 Sv), the Leeward Island passages (~ 8 Sv) and the Windward Island passages (~ 10 Sv). The highest individual contributions are found to be made via the Grenada Passage (~ 6 Sv) and the Windward Passage (~ 7 Sv) (Johns et al., 2002). All incoming water masses add up to the ~ 28 Sv outflow via the Yucatan Strait into the GoM (Johns et al., 2002). Due to the shallow sill depth

of the Florida Straits (~ 800 m), water masses below this depth return to the Caribbean basin via the Yucatan Strait (Sturges, 2005). Therefore, the deep water exchange between the GoM and the Atlantic / Caribbean is restricted and the deep water residence time in the GoM is high (~ 250 years) (DeHaan & Sturges, 2005; Rivas et al., 2005). The Anegada and the Windward passages with sill depths of 1900 m and 1700 m, respectively, are the main pathways for deep water return flow from the Caribbean into the open Atlantic (Johns et al., 2002; Sturges, 2005). The residence time of deep waters below 1800 m in the Caribbean basin is ~ 150 years (Joyce et al., 1999).

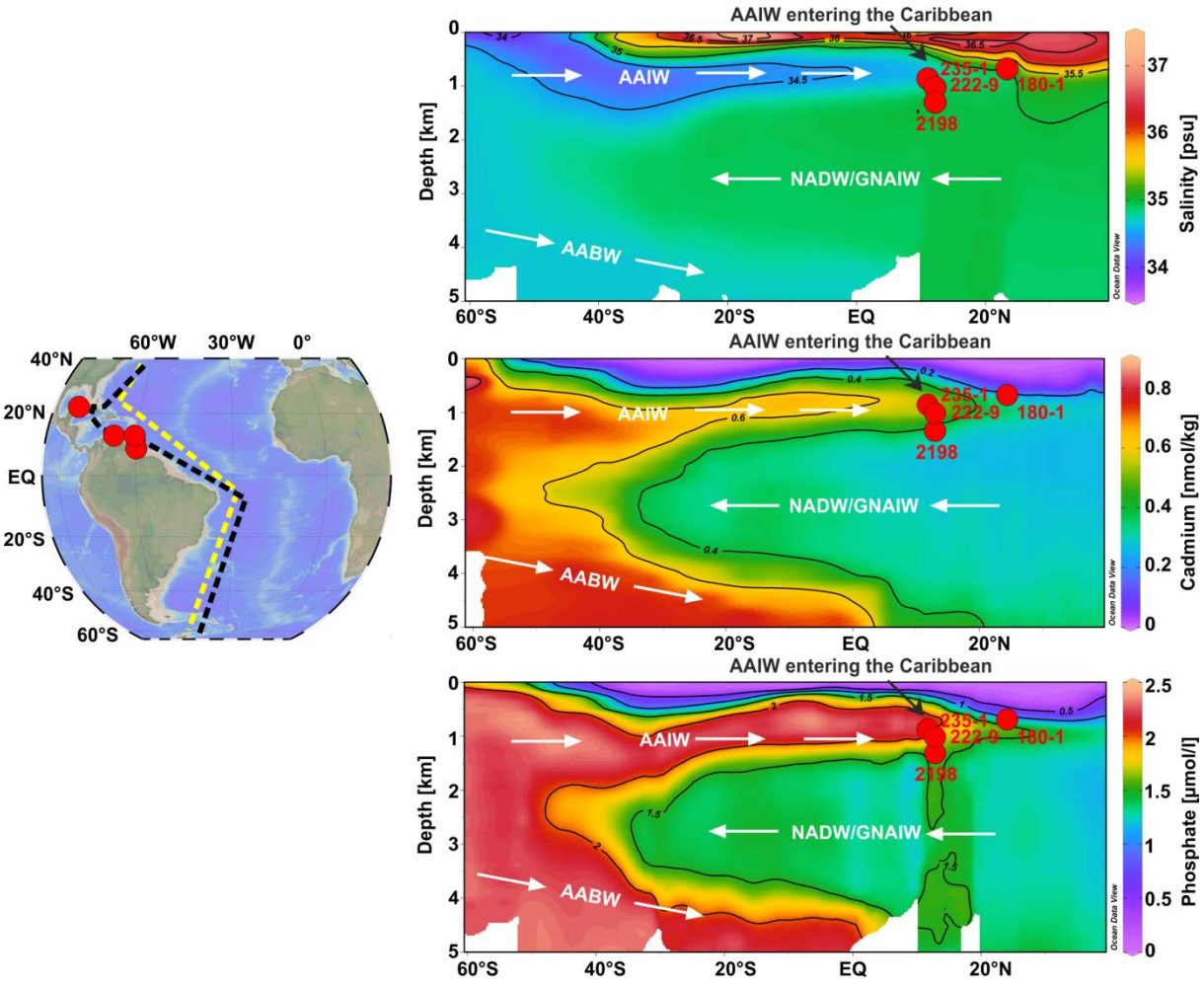

Figure 5: N-S-trending profiles through the Atlantic Ocean indicating major water masses characterised by distinct differences in salinity (top), cadmium-content (middle) and phosphate-concentrations (bottom). Map to the left indicates position of the profile sections (dashed lines): salinity- and phosphate-profiles = black (data obtained from World Ocean Atlas 2013; Boyer et al., 2013); cadmium-profile = yellow (data obtained from GEOTRACES; Mawji et al., 2015). Red circles and labels show location and depth of the sediment cores that were analysed in this thesis (180-1 = M78/1-180-1; 222-9 = M78/1-222-9; 235-1 = M78/1-235-1; 2198 = MD99-2198). Figures were created using Ocean Data View (Schlitzer, 2015). AAIW = Antarctic Intermediate Water; NADW = North Atlantic Deep Water; GNAIW = Glacial North Atlantic Intermediate Water; AABW = Antarctic Bottom Water

Antarctic Intermediate Water:

The most prominent intermediate depth water mass in the W-Atlantic with respect to oxygen, nutrients and salinity is Antarctic Intermediate Water (AAIW) (Fig. 5). Today, AAIW is mainly formed at the northernmost latitude reached by the Antarctic Circumpolar Current, between the Polar Front and the Subantarctic Front with the major formation sites of Atlantic AAIW in the areas surrounding the southernmost tip of South America (e.g. Hanawa & Talley, 1996; 2001). Here, AAIW forms from the coldest and densest Subantarctic Mode Water before it penetrates northward into the Atlantic (Fig. 4) (e.g. Bostock et al., 2010). Within the global oceanic circulation system in general and especially within the AMOC system, AAIW is a prominent distributor of nutrients, salt / freshwater, carbon, oxygen and ocean heat, and it balances the export of NADW to the S-Atlantic / SO (e.g. Saenko et al., 2003; Sloyan et al., 2010). Today, AAIW is considered to be a major sink for anthropogenic atmospheric CO_2, which then is transported equatorward (Sabine et al., 2004). AAIW is therefore an important component of the upper branch of the AMOC, connecting high and low latitude ocean basins at intermediate depth (e.g. Hartin et al., 2011; Howe et al., 2016). It therefore plays a key role in the global climate system and is a crucial part of understanding ocean dynamics under a changing climate environment.

Glacial – deglacial AMOC perturbations:

There is evidence for a bifurcation of the AMOC into two separate overturning cells during the Last Glacial Maximum (Fig. 6) (LGM, 23 – 19 ka BP; Barker et al., 2015). The upper overturning cell was driven by the formation of southward flowing Glacial North Atlantic Intermediate Water (GNAIW), which was the shallower substitute of NADW during glacial times (e.g. Lynch-Stieglitz et al., 2007; Ferrari et al., 2014). Previous studies indicate that GNAIW was characterised by low nutrient conditions and a high stable carbon isotope ($\delta^{13}C$) signature (e.g. Curry & Oppo, 2005; Marchitto & Broecker, 2006). It was likely the main contributor feeding AAIW in the SO during the LGM, and AAIW was therefore likewise depleted in nutrients (Ferrari et al., 2014; Poggemann et al., 2017). The lower overturning cell in contrast was characterised by the formation of AABW, which was cut off from the atmosphere due to a northward extension of permanent sea ice cover in the SO. In consequence the SO was dominated by a deep stable stratification (e.g. Burke & Robinson, 2012). Overall, previous studies suggest that the AMOC was slightly weaker although relatively stable during the LGM compared to modern times, as indicated by a comparable circulation pattern but not with the same structure as today (e.g. Yu et al., 1996; McManus et al., 2004; Lynch-Stieglitz et al., 2007; Böhm et al., 2015).

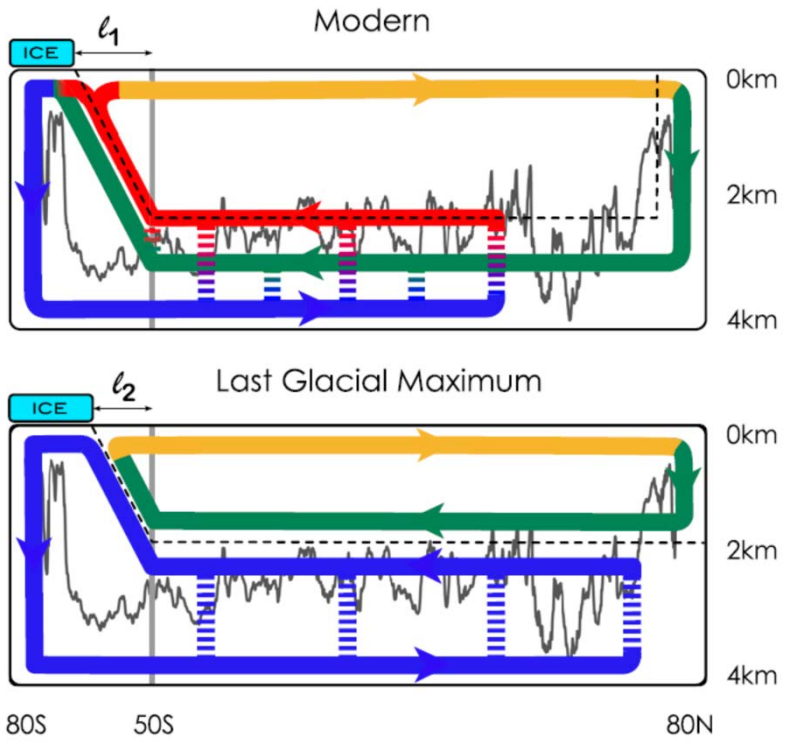

Figure 6: Simplified schematic of Atlantic overturning circulation pattern during the Holocene / modern times (top) and during the Last Glacial Maximum (bottom). The Holocene and modern circulation pattern is characterised by one major overturning cell connecting deep water formation in the N-Atlantic and in the Southern Ocean. Both southern sourced and northern sourced deep waters mix and well up in the Southern Ocean. In contrast, the Last Glacial Maximum was characterised by two overturning cells, separated from each other. Dashed black line indicates isopycnal, which separates the overturning cells. Difference in quasi-permanent sea ice extend is indicated by distance $\ell 1$ and $\ell 2$ to the Antarctic Circumpolar Current indicating enhanced sea ice extent during the LGM ($\ell 2 < \ell 1$). Ragged line indicates main bathymetric features. (Figure from Ferrari et al., 2014)

Figure 7 (Denton et al., 2010) provides a comparison of different published proxy records illustrating the differences in northern and southern hemisphere evolution during the last deglaciation. In contrast to the LGM, the last deglaciation was characterised by globally rising annual mean surface temperatures, interrupted by two major abrupt and short-term northern hemisphere cooling events (NGRIP Dating Group 2006), namely the Heinrich Stadial 1 (HS1, 18 – 14.6 ka, Barker et al., 2009) and the Younger Dryas (YD, 12.8 – 11.5 ka, Barker et al., 2009). On the northern hemisphere, the rise in global annual mean surface temperatures during the deglaciation was accompanied by a reduction in continental ice sheets to about their modern extent and a gradual rise in sea level of ~ 120 m (e.g. Denton et al., 2010). Several studies suggest large surges of meltwater to be the most likely trigger for the HS1 and the YD cooling events (e.g. Liu et al., 2009; Toucanne et al., 2009) while other studies rather view these cold events as a consequence of stadial conditions and not the driver (e.g. Barker et al., 2015). Nonetheless, the enhanced ice rafting in the N-Atlantic and times of rapid cooling in the northern hemisphere were probable closely related (Fig. 7D) (e.g. Bard et al., 2000). Published studies suggest that the postulated large meltwater and ice surges in the N-Atlantic during HS1 and in the YD most likely mixed with dense waters from the

tropical Atlantic and prevented them from sinking and forming NADW/GNAIW, hence fostering a major weakening or even collapse of the AMOC (Fig. 7F) (e.g. McManus et al., 2004; Böhm et al., 2015).Together with the expanded winter sea ice cover in the N-Atlantic (e.g. Denton et al., 2005), the synchronous southward shift of the Intertropical Convergence Zone (ITCZ) (e.g. Chiang & Bitz, 2005), the strengthening and likewise southward shift of the trade wind system and the westerly wind belt (e.g. Denton et al., 2010; Bradtmiller et al., 2016), the AMOC cessation caused major atmospheric and oceanic reorganisations. While the AMOC today (and likewise but slightly weaker during the LGM) redistributes heat from the tropical W-Atlantic and from the SO, the weakening or collapse of the AMOC during HS1 and in the YD caused a major heat accumulation in the southern hemisphere. In consequence, the SO warmed and the Antarctic sea ice retreated, thereby instigating a thermometric see saw between the hemispheres (e.g. Barker et al., 2009; Toggweiler and Lea, 2010; Landais et al., 2015). Hence, the SO and, to some extent, the Antarctic were characterised by pronounced warming episodes during northern hemisphere cooling events (e.g. Stenni et al., 2006; Lamy et al., 2007; Stenni et al., 2011) separated by the Antarctic Cold Reversal (ACR) (Fig. 7G,H,J). The southward shift of the ITCZ in contrast brought rain to normally arid regions of Brazil (Wang et al., 2004), a weakening of the Asian monsoon and enhanced precipitation in N-Australia and Indonesia (Muller et al., 2008; Griffiths et al., 2009; Denton et al., 2010). Likewise, the strengthening and southward shift of the trade wind system and of the westerly wind belt induced enhanced upwelling of nutrient rich intermediate and deep water masses in the E-Atlantic and in the SO (e.g. Anderson et al., 2009; Sikes et al., 2009; Bradtmiller et al., 2016), which entailed enhanced CO_2 outgassing from abyssal waters and therefore a rise in atmospheric CO_2 (e.g. Marcott et al., 2014; Jaccard et al. 2016). While the northern hemisphere rapid cooling events were separated by the Bølling-Allerød (BA), a period of pronounced warming, resumed deep water formation and retreat of sea ice cover, the southern hemisphere experienced an episode of distinct cooling during the ACR (NGRIP Dating Group, 2006; Stenni et al., 2006). The subsequent YD was in many ways a repetition of oceanic and atmospheric changes taken place already during HS1 and the warming in the southern hemisphere during the YD was likely necessary to raise the atmospheric CO_2 level and by this finalize the termination, hence initialize interglacial conditions (Denton et al., 2010). During the early Holocene the modern atmospheric and oceanic circulation pattern was established.

Several studies have aimed to reconstruct past AAIW dispersal in the Atlantic on glacial – interglacial timescales in relation to postulated changes in the AMOC and the fluctuations in NADW formation. While some results point to the enhanced presence and northward penetration of AAIW into the subtropical N-Atlantic at times of decreased NADW / GNAIW formation (e.g. Pahnke et al., 2008; Hendry et al., 2012), others indicate a distinct weaker advection of AAIW into the N-Atlantic during these episodes (e.g. Xie et al., 2012, 2014; Huang et al., 2014; Howe et al., 2016). The exact behaviour of AAIW during HS1 and in the YD nonetheless remains uncertain and affords further investigation.

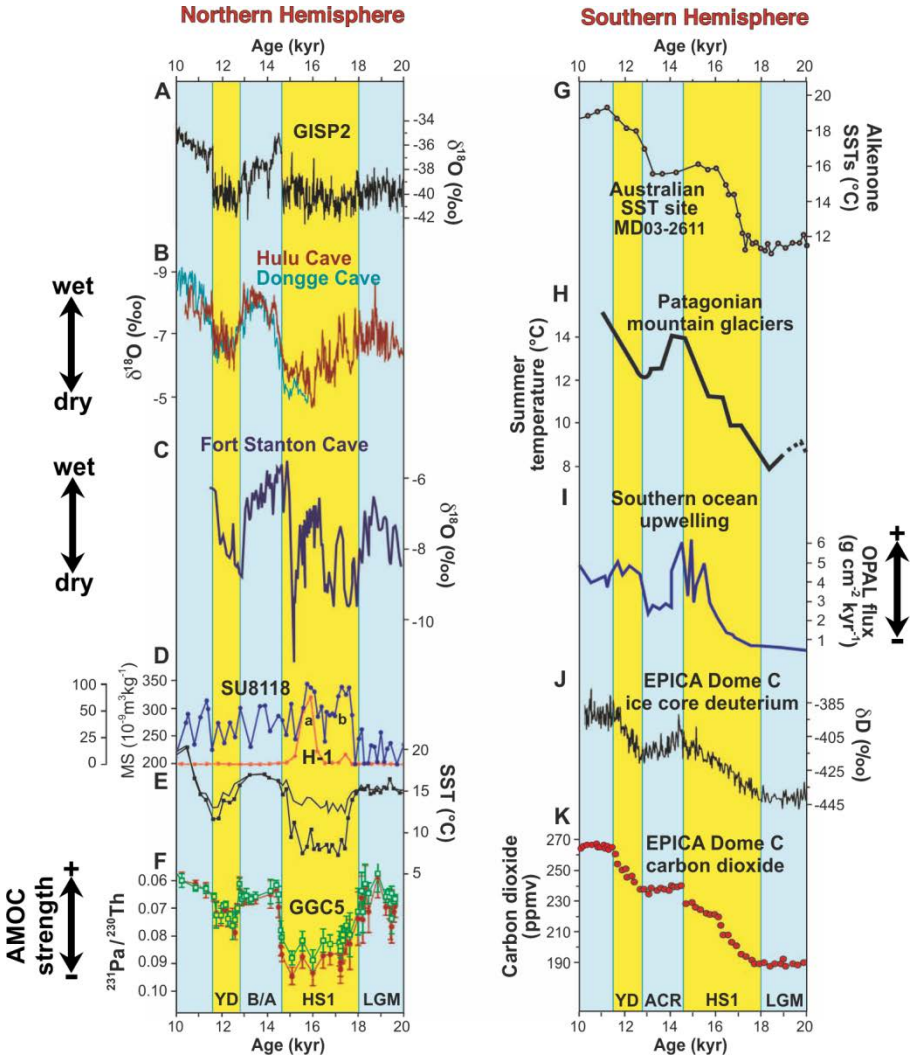

Figure 7: Comparison of various proxy records reconstructing northern hemisphere (left) and southern hemisphere (right) climate signals. **A)** Stable oxygen isotope data ($\delta^{18}O$) from a Greenland ice core (GISP2) as reference for northern hemisphere climate (Stuiver & Grootes, 2000). **B)** Stable oxygen isotope data indicating changes in the Chinese monsoon (Wang et al., 2001; Yuan et al., 2004). **C)** Stable oxygen isotope data reflecting precipitation changes in the southwestern N-America (Asmerom et al., 2010). **D)** Ice rafted debris (IRD) and magnetic susceptibility (MS) reflecting changes in ice berg rafting (Bard et al., 2000). **E)** Sea Surface Temperature (SST) reconstructions from the subtropical N-Atlantic indicating distinct cooling during HS1 and in the YD (Bard et al., 2000). **F)** Pa/Th record indicating changes in Atlantic Meridional Overturning Circulation strength (McManus et al., 2004). **G)** Alkenone based SST reconstructions south of Australia indicating distinct SST rises during HS1 and the YD (Calvo et al., 2007). **H)** Southern S-America atmospheric summer temperature evolution during the last deglacial period (Denton et al., 1999; Strelin & Denton, 2005). **I)** Southern Ocean upwelling changes derived from opal flux reconstructions (Anderson et al., 2009). **J)** Hydrogen isotope (δD) record of an Antarctic ice core (EPICA Dome C) reflecting atmospheric temperature changes over Antarctica (Monnin et al., 2001). **K)** Antarctic atmospheric CO_2 reconstructions from EPICA Dome C (Monnin et al., 2001). LGM = Last Glacial Maximum; HS1 = Heinrich Stadial 1; B/A = Bølling-Allerød; ACR = Antarctic Cold Reversal; YD = Younger Dryas. (Figure modified from Denton et al., 2010)

Research questions addressed in this study:

The following research questions are addressed within this thesis:

I. How did the northward penetration of AAIW in the (sub-)tropical Atlantic change during northern hemisphere cooling events?
II. Did the geochemical signatures of AAIW change as a result of N- and S-Atlantic overturning fluctuations during the last deglaciation?
III. How did atmospheric thermal and CO_2 changes affect the heat and carbon uptake of AAIW?
IV. Did the interaction at intermediate water depth between the Gulf of Mexico and the Caribbean change during the last deglaciation?

To answer these questions, sediment cores retrieved from the Caribbean and the Gulf of Mexico were analysed using different geochemical proxies in benthic and planktonic foraminiferal tests. The proxy records, covering the past 24 thousand years (24 ka), and their paleo-oceanographic interpretations are presented in the following scientific chapters:

Scientific Chapter 1 contains a peer-reviewed publication from the journal *Earth and Planetary Science Letters* as it was published:

"Rapid deglacial injection of nutrients into the tropical Atlantic via Antarctic Intermediate Water"

This publication describes how the shallow and the deep overturning cells reconnected during the last deglaciation and effectively shaped the nutrient budget of AAIW due to changes in the upwelling of nutrient rich deep waters in the SO.

My contribution to this publication:

- I co-sampled sediment cores M78/1-235-1 and MD99-2198 and carried out the chemical sample preparation for the measurements.
- I co-performed the element/Ca and stable carbon isotope measurements.
- I co-provided the AMS^{14}C dates and created the age model for sediment core M78/1-235-1.
- I interpreted the data a prepared the manuscript under support of my co-authors.
- I submitted and revised the manuscript according to the comments of the external reviewers.

Scientific Chapter 2 contains a manuscript that is prepared for submission to the journal *Nature Communications* with the title

"Deglacial heat deprivation from the atmosphere in the Southern Ocean via Antarctic Intermediate Water".

In this chapter evidence for a major deglacial ocean heat uptake of AAIW from the surface SO, closely related to northern hemisphere cooling events and subsequent northward transport into the (sub-)tropical N-Atlantic is presented.

My contribution to this publication:

- I sampled sediment cores M78/1-235-1 and M78/1-222-9 and carried out the chemical sample preparation for the measurements.
- I performed the element/Ca measurements.
- I provided the AMS^{14}C dates and created the age model for sediment core M78/1-222-9.
- I interpreted the data a prepared the manuscript under support of my co-authors.

Scientific Chapter 3 contains a manuscript that is prepared for submission to journal *Paleoceanography* with the title

"Antarctic Intermediate Water effectively cooled the Gulf of Mexico during rapid deglacial northern hemisphere cooling events".

This chapter points to major cooling events in the intermediate depth Gulf of Mexico during times of weakened or even collapsed AMOC which are closely related to variations in northward AAIW expansion.

My contribution to this publication:

- I sampled sediment cores M78/1-235-1 and M78/1-180-1 and carried out the chemical sample preparation for the measurements.
- I performed the element/Ca measurements.
- I provided the AMS^{14}C dates and created the age model for sediment core M78/1-180-1.
- I interpreted the data a prepared the manuscript under support of my co-authors.

All chapters are individual publications or have been prepared for potential publication in highly-ranked, peer-reviewed international scientific journals. Hence, all chapters have an individual introduction, description of the materials and methods, discussion and conclusion.

Since Scientific Chapters 2 and 3 contain manuscripts that have not yet undergone peer-review, they may be subject to revisions and improvements. Associated manuscripts, co-authored by me, are currently in preparation for publication and provide further results from surface and subsurface analyses from the same areas (main author Stefan Reißig). These co-authored manuscripts are not part of this thesis.

The study was funded by the Deutsche Forschungsgemeinschaft (DFG) via the „Cluster of Excellence – The Future Ocean" registered at the Christian-Albrechts-University of Kiel (Project number CP1142). The study was performed in close collaboration with the GEOMAR Helmholtz Centre for Ocean Research Kiel and entirely accomplished at GEOMAR.

Material & Methods

As outlined above, detailed information on the scientific approach is given in the single scientific chapters 1, 2 and 3. In the following, an only broad overview is provided. Within this study, sediment cores M78/1-180-1, M78/1-222-9, M78/1-235-1 from Meteor cruise M78 and sediment core MD99-2198 from Marian Dufresne cruise MD114 were analysed (Fig. 5). All sediment cores were sampled at centennial resolution covering the approximately past 24 ka. The samples were wet sieved using a 63 µm mesh to remove the silt and clay fractions. For (isotope) geochemical analyses benthic and/or planktonic foraminiferal tests were selected and underwent a routine cleaning procedure outlined in the appropriate scientific chapters.

To infer past oceanographic changes at intermediate depth level, several established geochemical proxies were selected for this study:

1) **Cd_w** as a proxy for past nutrient saturation:
   Several studies show that seawater cadmium (Cd_w) correlates to phosphate (PO_4), a major nutrient in seawater (e.g. Boyle & Kegwin, 1985). Since benthic foraminiferal shells incorporate Cd into their calcite ($CaCO_3$) test in proportion to the Cd concentration in seawater, the measured Cd/Ca-ratio of the foraminiferal tests can be used, to calculate past Cd_w and therefore to approximate past changes in the phosphate content of the surrounding water body (e.g. Came et al., 2003; Marchitto & Broecker, 2006). Nutrient enriched water masses like modern AAIW or AABW are characterised by high PO_4 and therefore high Cd_w concentrations. In contrast, nutrient depleted water masses like NADW and GNAIW are indicated by low PO_4 and Cd_w (e.g. Bryan & Marchitto, 2010).
2) **$\delta^{13}C$** as a proxy for past ocean ventilation:
   Although the reconstructed $\delta^{13}C$ signal obtained from benthic foraminiferal tests is influenced by many effects, e.g. species-specific vital effects, it can be used as a reliable proxy for past changes in ocean ventilation (e.g. Curry & Oppo, 2005). Water masses, which received a relatively high percentage of “young” surface waters (e.g. NADW), are typically characterised by high $\delta^{13}C$, while water masses that received larger percentages of nutrient enriched “old” water masses are typically characterised by low $\delta^{13}C$ (e.g. AAIW) (e.g. Kroopnik, 1985; Oppo et al., 2015).
3) **Mg/Ca** as a proxy for past seawater temperature reconstructions:
   Most planktonic and benthic foraminifera incorporate magnesium (Mg) into their calcite tests as a function of ambient seawater temperature. Several studies established the magnesium to calcium ratio (Mg/Ca) in fossil foraminiferal calcite tests as a robust tool to reconstruct ancient sea surface temperatures (SST), sea subsurface temperatures (subSST), intermediate water temperatures (IWT) and bottom water temperatures (BWT) (e.g. Nürnberg et al., 1996, 2000; Bryan & Marchitto, 2008; Regenberg et al., 2009; Elderfield et al., 2010; Spero et al., 2015).
4) **$\delta^{18}O$** as a proxy for temperature and salinity:
   The proportion of the lighter oxygen isotope ^{16}O to the heavier isotope ^{18}O in seawater is a function of seawater temperature, salinity and global ice volume (e.g. Shackleton, 1974). The ratio of ^{18}O to ^{16}O of seawater referenced to an international standard and expressed as $\delta^{18}O$ is basically reflected in the fossil foraminiferal $\delta^{18}O$ calcite tests and can be used to assess past seawater $\delta^{18}O$. In paleo-oceanography,

the foraminiferal $\delta^{18}O$ is commonly used as a proxy for past global ice volume changes (e.g. Chappell & Shackleton, 1986; Oppo et al., 2015). In combination with foraminiferal Mg/Ca based past seawater temperature reconstructions, derived from the same species, the ice-volume corrected $\delta^{18}O$ signal can be used to reliably approximate past changes in seawater salinity (e.g. Nürnberg et al., 1996; Schmidt et al., 2004; Elderfield et al., 2010).

5) **εNd** as a proxy for past water mass distribution changes:
Since the predominant supply of neodymium (Nd) to the open ocean is triggered by the weathering of continental rocks, the radiogenic composition of Nd (expressed as εNd) in different water masses mainly depends on the type of rock in the water mass formation region and hence can be used as a water mass tracer to reconstruct water mass source changes (e.g. Frank, 2002). While water masses that form in areas of young mantle derived rocks are typically characterised by more radiogenic signatures (e.g. Pacific waters), waters that form in areas surrounded by old continental rocks in contrast show more unradiogenic signatures (e.g. N-Atlantic waters) (e.g. Piepgras & Wasserburg, 1980, 1987). Waters that form by the mixing of N-Atlantic and Pacific waters, such as those originating in the SO, are characterised by medium radiogenic signatures (e.g. Stichel et al., 2012; Molina-Kescher et al., 2014). The seawater εNd signature can be reliably reconstructed from foraminiferal coatings and can be used to analyse past ocean circulation changes (e.g. Roberts et al., 2010).

Scientific Chapter 1: Rapid Deglacial Injection of Nutrients into the tropical Atlantic via Antarctic Intermediate Water

This scientific chapter consists of the paper entitled “Rapid Deglacial Injection of Nutrients into the tropical Atlantic via Antarctic Intermediate Water” as it was published in *Earth and Planetary Science Letters* (2017).

The authors are David-Willem Poggemann[a], Ed C. Hathorne[a], Dirk Nürnberg[a], Martin Frank[a], Imke Bruhn[a], Stefan Reißig[a], André Bahr[b].

[a]GEOMAR Helmholtz Centre for Ocean Research Kiel, D-24148 Kiel, Germany

[b]Heidelberg University, Institute of Earth Science, D-69120 Heidelberg, Germany

Earth and Planetary Science Letters 463 (2017) 118–126

Contents lists available at ScienceDirect

Earth and Planetary Science Letters

www.elsevier.com/locate/epsl

Rapid deglacial injection of nutrients into the tropical Atlantic via Antarctic Intermediate Water

David-Willem Poggemann [a,*], Ed C. Hathorne [a], Dirk Nürnberg [a], Martin Frank [a], Imke Bruhn [a], Stefan Reißig [a], André Bahr [b]

[a] GEOMAR Helmholtz Centre for Ocean Research Kiel, D-24148 Kiel, Germany
[b] Heidelberg University, Institute of Earth Science, D-69120 Heidelberg, Germany

ARTICLE INFO

Article history:
Received 24 March 2016
Received in revised form 16 January 2017
Accepted 25 January 2017
Available online xxxx
Editor: H. Stoll

Keywords:
Atlantic intermediate water circulation
Caribbean nutrient concentrations
Cd reconstruction
Atlantic Meridional Overturning circulation
Antarctic Intermediate Water
deglacial CO_2

ABSTRACT

As part of the return flow of the Atlantic overturning circulation, Antarctic Intermediate Water (AAIW) redistributes heat, salt, CO_2 and nutrients from the Southern Ocean to the tropical Atlantic and thus plays a key role in ocean–atmosphere exchange. It feeds (sub)tropical upwelling linking high and low latitude ocean biogeochemistry but the dynamics of AAIW during the last deglaciation remain poorly constrained. We present new multi-decadal benthic foraminiferal Cd/Ca and stable carbon isotope ($\delta^{13}C$) records from tropical W-Atlantic sediment cores indicating abrupt deglacial nutrient enrichment of AAIW as a consequence of enhanced deglacial Southern Ocean upwelling intensity. This is the first clear evidence from the intermediate depth tropical W-Atlantic that the deglacial reconnection of shallow and deep Atlantic overturning cells effectively altered the AAIW nutrient budget and its geochemical signature. The rapid nutrient injection via AAIW likely fed temporary low latitude productivity, thereby dampening the deglacial rise of atmospheric CO_2.

1. Introduction

The Atlantic Meridional Overturning Circulation (AMOC) today is driven by the deep water formation in the N-Atlantic (e.g. Talley, 2013) and underwent considerable changes during the transition from the Last Glacial Maximum (LGM) to the Holocene (McManus et al., 2004; Gherardi et al., 2009; Böhm et al., 2015). During abrupt deglacial climate cooling periods, namely the Heinrich Stadial 1 (HS1, 18–14.6 ka, thousand years) and the Younger Dryas (YD, 12.8–11.5 ka), a severe weakening or even collapse of the AMOC occurred. As a consequence, the temperature contrast between the hemispheres decreased, the Southern Ocean (SO) warmed and sea ice retreated (Toggweiler and Lea, 2010). Amplified by the synchronous strengthening and southward shift of the trade winds and the westerly wind belt, upwelling of nutrient-rich intermediate to deep water masses in the E-Atlantic and in the SO resumed after these cold periods (e.g. Broecker, 1998; Anderson et al., 2009; Bradtmiller et al., 2016). As the deep stratification in the SO, which likely characterised the LGM, collapsed (Burke and Robinson, 2012), outgassing from upwelling abyssal water released CO_2 to the atmosphere (e.g. Denton et al., 2010; Jaccard et al., 2016). A synchronous re-organisation of intermediate to deep Atlantic ocean water mass exchange likely enhanced these processes: The apparently weakened or even ceased formation of southward flowing shoaled North Atlantic Deep Water (NADW), termed Glacial North Atlantic Intermediate Water (GNAIW), influenced the oceanic circulation Atlantic-wide and likely contributed to the enhanced upwelling and release of CO_2 in the SO (e.g. Broecker, 1998; Burke and Robinson, 2012). Other studies have suggested changes in NADW formation as a major driving factor for the deglacial atmospheric CO_2 increase (e.g. Hain et al., 2014; Lund et al., 2015). In addition, the southward shift of the westerly wind belt led to a decrease in dust supply and therefore lower iron fertilisation of surface waters in the SO (Jaccard et al., 2016).

The implications of these deglacial atmospheric and oceanographic perturbations during HS1 and/or the YD for Atlantic intermediate water circulation, in particular for AAIW and GNAIW, are contentious. A weakened southward flow of northern sourced waters has been hypothesised to have resulted in an extended northward expansion of AAIW into the NW-Atlantic (e.g. Pahnke et al., 2008; Hendry et al., 2012) or even further north (Rickaby and Elderfield, 2005). In contrast, other studies have either suggested a continuous or even enhanced advection of northern sourced wa-

* Corresponding author.
E-mail address: dpoggemann@geomar.de (D.-W. Poggemann).

http://dx.doi.org/10.1016/j.epsl.2017.01.030
0012-821X/

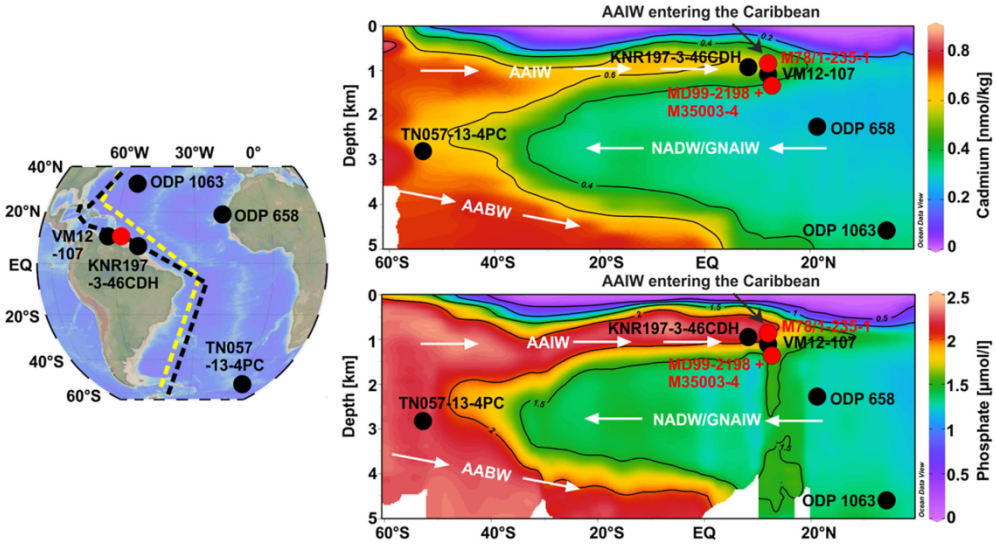

Fig. 1. Location of study sites, cadmium and phosphate concentration of different Atlantic water masses: *Left:* Bathymetric chart of the Atlantic Ocean with locations of the sediment cores studied here (red dot, identifiers in the right side profiles). Reference records of previous studies are depicted by black dots (Böhm et al., 2015; McManus et al., 2004 (ODP 1063); Meckler et al., 2013 (ODP 658); Xie et al., 2014 (VM12-107); Huang et al., 2014 (KNR197-3-46CDH); Anderson et al., 2009 (TN057-13-4PC)). Dashed lines show cadmium and phosphate sections (yellow = Cd; black = P). *Right:* S–N-trending cadmium- (top, data from GEOTRACES; Mawji et al., 2015) and phosphate-profile (bottom, data from WOA; Boyer et al., 2013) with locations of proxy records, placed at the according water depths. Major Atlantic water masses can be differentiated by their phosphate and cadmium concentrations (AAIW = Antarctic Intermediate Water; NADW = North Atlantic Deepwater; GNAIW = Glacial North Atlantic Intermediate Water; AABW = Antarctic Bottom Water). Figures were created using Ocean Data View (Schlitzer, 2015). (For interpretation of the references to colour in this figure legend, the reader is referred to the web version of this article.)

ters at intermediate depth (Came et al., 2003, 2008; Xie et al., 2012) that may even have resulted in the absence of AAIW during these periods (Huang et al., 2014; Howe et al., 2016). Recent data also indicate that northern sourced waters continuously influenced mid-depth waters in the SW-Atlantic and that the AMOC may not have collapsed completely (e.g. Lund et al., 2015). At the same time a postulated short-term breakdown of SO stratification may have led to increased AAIW ventilation during northern hemisphere cooling events (Burke and Robinson, 2012).

To reconstruct past changes in intermediate and deep Atlantic circulation patterns benthic foraminiferal Cd/Ca has been used routinely as a proxy for seawater cadmium concentrations. Seawater cadmium concentrations (Cd_w) are closely correlated with phosphate concentrations. Prior work has demonstrated that benthic foraminifera incorporate Cd as a function of Cd_w. Hence, the Cd content of fossil calcitic tests reflects the distinct nutrient concentrations of bottom water masses in the past (Boyle, 1988, 1992). Various studies have demonstrated the reliability of benthic foraminiferal Cd/Ca ratios to reconstruct deep and intermediate water masses in the past (e.g. Came et al., 2003; Rickaby and Elderfield, 2005; Came et al., 2008; Bryan and Marchitto, 2010).

Our study reconstructs the deglacial intermediate water mass changes in the tropical W-Atlantic based on a unique sediment core from Tobago Basin presently bathed by the tip of the AAIW tongue (M78/1-235-1, 852 m) (Fig. 1). We also studied adjacent but deeper core MD99-2198 located at the modern lower boundary of AAIW. Complemented by published Cd/Ca data of core M35003 (Zahn and Stüber, 2002; same location and depth as MD99-2198), the composite Cd/Ca dataset from ~1300 m adds information on past changes in the vertical extent of AAIW (Fig. 1). Our benthic foraminiferal Cd/Ca (endobenthic species *Uvigerina spp.*) are complemented by $\delta^{13}C$ time series (epibenthic species *Cibicidoides pachyderma*) and allow intermediate nutrient inventory and circulation changes to be deciphered at unprecedented temporal resolution for the past ~24,000 years.

2. Material and methods

We analysed the sediment cores M78/1-235-1 (11°36.53′N, 60°57.86′W, 852 m) and MD99-2198 (12°05.51′N, 61°14.01′W, 1330 m) (Fig. 1), both from the Tobago Basin, to reconstruct the Cd_w and $\delta^{13}C$ signatures of past bottom waters for the time interval from ~24 ka BP to late Holocene. Today, sediment core M78/1-235-1 is bathed by AAIW located at a depth between ~600 and 1200 m in the S-Caribbean. Core MD99-2198 is located nearby but at greater depth at the transition zone between AAIW and NADW. Together, the proxy data obtained from these sediment cores should reveal vertical and frontal movements of AAIW and NADW/GNAIW. Sediment core MD99-2198 was sampled at 5 cm-intervals and at a slightly lower resolution during the Holocene. Core M78/1-235-1 was sampled at 2 cm-intervals. For the YD and HS1 intervals both cores were sampled at 1 cm-resolution to monitor rapid changes in Cd_w at the highest resolution possible. Samples were freeze-dried before wet sieving.

2.1. Age models

The age model for sediment core M78/1-235-1 was generated by linear interpolation between 9 Accelerator Mass Spectrometer AMS ^{14}C dates (see supplementary Table S1, Fig. S1), of which 4 dates are published (Hoffmann et al., 2014). AMS ^{14}C measurements were carried out at the Cologne AMS (Cologne, Germany) and Beta Analytic Limited (London, UK). Mixed layer dwelling *Globigerinoides ruber* and *Globigerinoides sacculifer* were used (with the exception of one sample where some *Orbulina universa* were included to ensure a sufficient sample mass) and calibrated with CALIB 7.1 using the MARINE13 reservoir age data set (Reimer et al., 2013). The average sedimentation rate is ~18 cm/kyr. For sediment

core MD99-2198 we used the established, previously published age model (Pahnke et al., 2008).

2.2. Cd/Ca measurements

A minimum of 10 tests of the endobenthic foraminiferal species *Uvigerina spp.* (315–400 µm size fraction), the most abundant benthic species in sediment cores M78/1-235-1 and MD99-2198, were cleaned with reductive and oxidative reagents following established techniques (Boyle and Rosenthal, 1996; Rosenthal et al., 1997). Several studies showed that the endobenthic species *Uvigerina spp.* can be used to reliably reconstruct Cd_w of ancient water masses (e.g. Boyle, 1988; Zahn and Stüber, 2002; Bryan and Marchitto, 2010). To improve the efficiency of the Cd/Ca analyses, a novel technique using an Elemental Scientific "seaFAST" pre-concentration system coupled to an Agilent 7500ce ICP-MS was adapted from a method for seawater trace metal analyses (Hathorne et al., 2012). This method is well suited for small sample sizes as all the Cd contained in the 2.5 ml sample loop and loaded onto the preconcentration column is measured during time resolved analysis of the elution peak. While the Cd and other trace metals are loaded onto the column the Ca matrix is removed allowing high Ca concentration solutions to be measured with minimal instrumental drift. Therefore, in a first step an aliquot of the dissolved sample was diluted, scandium added as an internal standard, and the Ca concentration determined using conventional nebulisation. Then for the Cd analyses, all samples were diluted to exact Ca-concentrations, which ranged from 10 to 100 ppm Ca depending on sample size. Indium was added to every sample at a concentration of 100 parts per trillion (ppt), to check for any drift or changes in preconcentration efficiency, and was routinely within 5% of the initial In intensity throughout the run. Similar column yields were obtained for Cd and In and the yield for Cd in sample matrix measured online was 94%. The column yield was reproducible and linear as evident from calibration curves obtained ($r^2 > 0.99$) over a range of Cd concentrations (1–40 ppt). Measuring ^{111}Cd no interferences were observed and detection limits (defined as 3.3 times the standard deviation of blank measurements) of around 0.6 ppt were obtained. All blanks, calibration standards and reference materials, with the same Ca concentration as the samples, were run through the preconcentration column exactly like the samples.

To assess accuracy and allow comparison with subsequent studies the Cd/Ca ratio of the limestone powder reference material ECRM-752 (Greaves et al., 2008; dissolved in weak nitric acid and centrifuged as recommended for Mg/Ca analyses) was measured ($n = 20$) and the mean during the course of this study found to be 562 ± 22 nmol/mol. This is in good agreement with the average values of two other laboratories (544 ± 18 nmol/mol and 574 ± 13 nmol/mol, respectively; Greaves et al., 2008). This Cd/Ca value is an order of magnitude higher than that found in our intermediate water depth samples so for routine quality control the ECRM-752 solution was diluted by a factor of 10 using a Ca single element solution to have the same Ca concentration as samples. The single element Ca solution was also run as a blank and found to contain no measurable Cd signal. The reproducibility is dependent on the sample size, with larger samples having better precision (e.g. 3% at 50 ppm Ca, 5.6% at 25 ppm Ca and 6.6% at 10 ppm Ca), but was always better than 15% (2σ). Three samples with sufficient material were used to perform replicate measurements. The average standard deviation of these replicates (8.91 nmol/mol, 2σ) equates to an uncertainty of the Cd_w data of 0.076 nmol/kg using the published depth dependent calibration of Boyle (1992). This estimate does not include uncertainties in the apparent partition coefficient (see Marchitto and Broecker, 2006, and Bryan and Marchitto, 2010 for a thorough discussion of this) but using a D_{Cd} of 1.3 for core M78/1-235-1 and of 1.46 for core MD99-2198 we obtain Cd_w values for the youngest Holocene samples that match modern Cd concentrations in the W-Atlantic (GEOTRACES; Mawji et al., 2015). Using a partition coefficient of 1.7 suggested by Bryan and Marchitto (2010), based on an assumed Cd:PO_4 relationship, leads to Cd_w values 0.15 nmol/kg lower than observed near the core sites.

2.3. Composite Cd_w-record for 1300 m water depth

In order to support previously published Cd_w-data from the modern transition zone between modern AAIW and NADW in the tropical W-Atlantic (Zahn and Stüber, 2002; core M35003), we produced a new higher resolution Cd_w record from the same location and water depth (core MD99-2198). The age model of the latter sediment core is based on AMS ^{14}C dates and optical tuning of $\delta^{13}C$ records of both cores (Pahnke et al., 2008). As both Cd_w records should have the same age intervals, we created a composite Cd_w-record by simple merging, which enables the elimination of high frequency noise (Fig. 2B).

2.4. $\delta^{13}C$ measurements

For $\delta^{13}C$ analyses we used 3–5 tests of the epibenthic species *Cibicidoides pachyderma* per sample. This benthic species is considered to record the seawater $\delta^{13}C$ signature most reliably (e.g. Duplessy et al., 1984; Zahn et al., 1986; Curry and Oppo, 2005; Marchitto and Broecker, 2006). The uncleaned samples were measured using a Thermo Fischer Scientific MAT 253, equipped with an automated CARBO Kiel IV carbon preparation device. Stable isotope measurements are referenced to the "NBS 19" (National Bureau of Standards) carbonate standard and the "Standard Bremen" (in-house standard). The results are reported against the VPDB scale (Vienne Pee Dee Belemnite). The analytical error was $\pm 0.05‰$ (2σ, $n = 16$) and the long-term reproducibility $\pm 0.035‰$ (2σ, $n = 172$), based on repeated standard measurements.

2.5. Data outliers

Within the high resolution data a small number of single data points appear unrealistically high compared with the surrounding data (Fig. 2). Therefore a Grubb's test was performed and one Cd_w and two $\delta^{13}C$ data points from core M78/1-235-1 and three Cd_w data points published from core M35003 (Zahn and Stüber, 2002) were rejected as outliers.

3. Results and discussion

Both the deeper (~1300 m) and the shallower (~850 m) intermediate depth Cd_w records, exhibit similarly low values during the LGM and document a general increase to higher values during HS1 and towards the early Holocene (Fig. 2B). The deglacial rise in Cd_w from ~0.3 nmol/kg to ~0.7 nmol/kg in the 850 m record is markedly stronger than at 1300 m, for which the increase is ~0.2 nmol/kg. While at the deeper core location Cd_w remained essentially constant since ~16 ka BP (~0.4–0.6 nmol/kg), we observe significant variations at 850 m depth. Three pronounced Cd_w maxima occur in the AAIW tongue ($>\sim 1.0$ nmol/kg) at the end of HS1 (~15.1 ka), during (~12.4–11.5 ka BP) and shortly after the YD (~11–10 ka BP), separated by lowered values during the Antarctic Cold Reversal (ACR). During the Holocene, Cd_w gradually declined from ~0.8 nmol/kg to 0.6 nmol/kg. This W-Atlantic Cd_w pattern from ~850 m water depth is in striking synchronicity with upwelling reconstructions from the SO (Anderson et al., 2009; Burke and Robinson, 2012), where AAIW is formed (Fig. 3), and suggests a close link between changes in the SO and W-Atlantic.

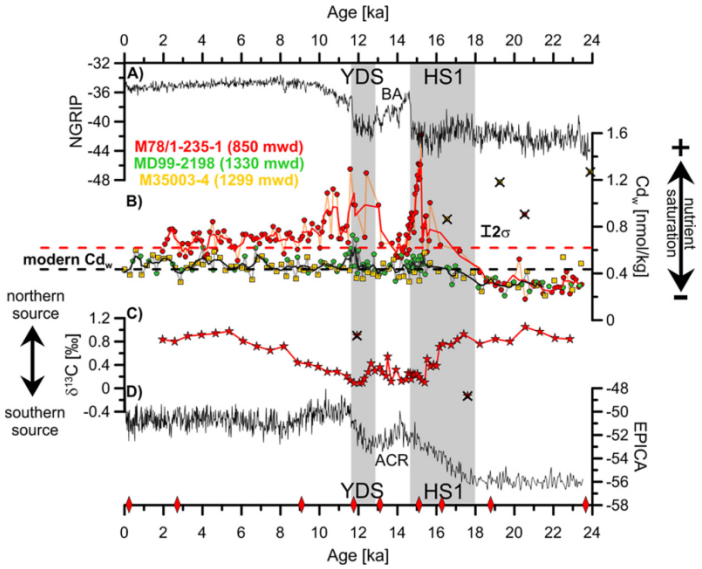

Fig. 2. Results and data treated as flyers. **A**) Oxygen isotope record of the NGRIP ice core (NGRIP Dating Group, 2006) as reference for the northern hemisphere climate signal. **B**) Cd_w of sediment core M78/1-235-1 (850 m; red, this study) and composite Cd_w record (black) from ~1300 m (composed of sediment cores MD99-2198 (1330 m; green, this study) and M35003 (1299 m; yellow; Zahn and Stüber, 2002)) denoting nutrient saturation at intermediate water depth and beneath. Thick lines represent 3-point running averages. All Cd_w reconstructed from Cd/Ca-ratios of endobenthic species *Uvigerina spp.* Dashed lines indicate approximated modern Cd-concentrations at the appropriate depth (Mawji et al., 2015). The uncertainty based on replicate measurements is indicated (2σ). **C**) Stable carbon isotopes ($\delta^{13}C$) of core M78/1-235-1 (this study). **D**) Oxygen isotope record of the EPICA Dome C (Stenni et al., 2006) as reference for the southern hemisphere climate signal. Crossed data points were treated as flyers due to failed Grubb's test. HS1 = Heinrich Stadial 1; YD = Younger Dryas Stadial; BA = Bølling-Allerød, ACR = Antarctic Cold Reversal; Red crosses along the lower age-axis indicate ^{14}C age control points for core M78/1-235-1. (For interpretation of the references to colour in this figure legend, the reader is referred to the web version of this article.)

Northern sourced water masses are generally characterised by low nutrient concentrations and therefore by low Cd_w signatures, whereas southern sourced water masses have high nutrient concentrations and therefore high Cd_w (e.g. Came et al., 2003; Rickaby and Elderfield, 2005; Marchitto and Broecker, 2006). Hence, the general Cd_w increases at both, deep and shallow intermediate depth can either be explained by enhanced transport of AAIW to 11°N and/or the nutrient content of AAIW itself increased. The overall rise in Cd_w at ~850 m could thus reflect a general change from a GNAIW dominated state during the LGM to an AAIW dominated state during HS1, which has persisted ever since, potentially accompanied by rapid increases of nutrient levels of AAIW itself at the end of HS1, during and shortly after the YD. The general marked increase of Cd_w from ~0.3 to ~0.7 nmol/kg at ~850 m accompanied by minor changes at ~1300 m clearly documents that the tongue of AAIW expanded northwards starting at ~17 ka BP but was accompanied by minor changes in its vertical extent. The discrepancy between the intermediate and the deeper Cd_w-record contradicts a recent hypothesis of Meckler et al. (2013) that related enhanced opal production in the subtropical E-Atlantic during HS1 and YD to increased nutrient supply via the Atlantic-wide shoaling of Antarctic Bottom Water (AABW) even reaching intermediate water depths (Fig. 3C). An upward shift of AABW, however, cannot explain both, our shallower and deeper Cd_w-signatures. While our shallower depth Cd_w-record from 850 m water depth shows distinctive, abrupt changes in the nutrient distribution, the record from the deeper site only points to minor changes in the nutrient inventory implying that additional nutrients did not originate from below 1300 m. An Atlantic-wide upward incursion of nutrients from abyssal waters should have caused strong nutrient enrichment at the deeper site as well. Bradtmiller et al. (2016), indeed, point out that enhanced wind-driven upwelling of nutrient-rich waters took place in the E-Atlantic due to the postulated strengthening and southward shift of trade winds during times of abrupt cooling events in the northern hemisphere. Consistent with Si isotope distribution patterns from several Atlantic sediment cores (Hendry et al., 2016), increased nutrient supply via intermediate water masses feeding into the thermocline is a viable explanation for the observed opal changes in the E-Atlantic (Meckler et al., 2013).

The new data presented here may not only reveal changes in the advection but also in the nutrient content of AAIW. The low values during the LGM point to nutrient poor glacial AAIW, possibly amplified due to the admixture of GNAIW. GNAIW in fact expanded far across the equator into the southern hemisphere (Marchitto and Broecker, 2006). The increase in Cd_w during HS1 observed in both our cores thus likely reflects an overall change to higher nutrient levels of AAIW. The offset between both Cd_w records is rather related to their positions with respect to the centre of AAIW (M78/1-235-1, 850 m) and the transition zone between AAIW and northern sourced water masses below (MD99-2198, 1300 m). The latter core therefore most likely was strongly influenced by underlying northern sourced waters.

To differentiate between both the advection and the nutrient content scenarios, and to further constrain changes in water mass properties at ~850 m in the tropical W-Atlantic, we consider the $\delta^{13}C$ signature of the epibenthic species *C. pachyderma*. The temporal pattern of $\delta^{13}C$ in the intermediate depth core M78/1-235-1 is in broad agreement with the Cd_w record (Fig. 2C). High $\delta^{13}C$ values of >0.7‰ prevailed during the LGM prior to ~16 ka BP and during the Holocene since ~8 ka BP. Distinct $\delta^{13}C$ minima of ~0–0.2‰ occurred during the end of HS1 and during the YD, synchronous with the Cd_w maxima, interrupted by elevated values during the ACR. These $\delta^{13}C$ minima are a common feature of (sub)tropical intermediate depth $\delta^{13}C$ reconstructions (e.g. Curry and Oppo, 2005; Romahn et al., 2014) and are considered to reflect upwelling

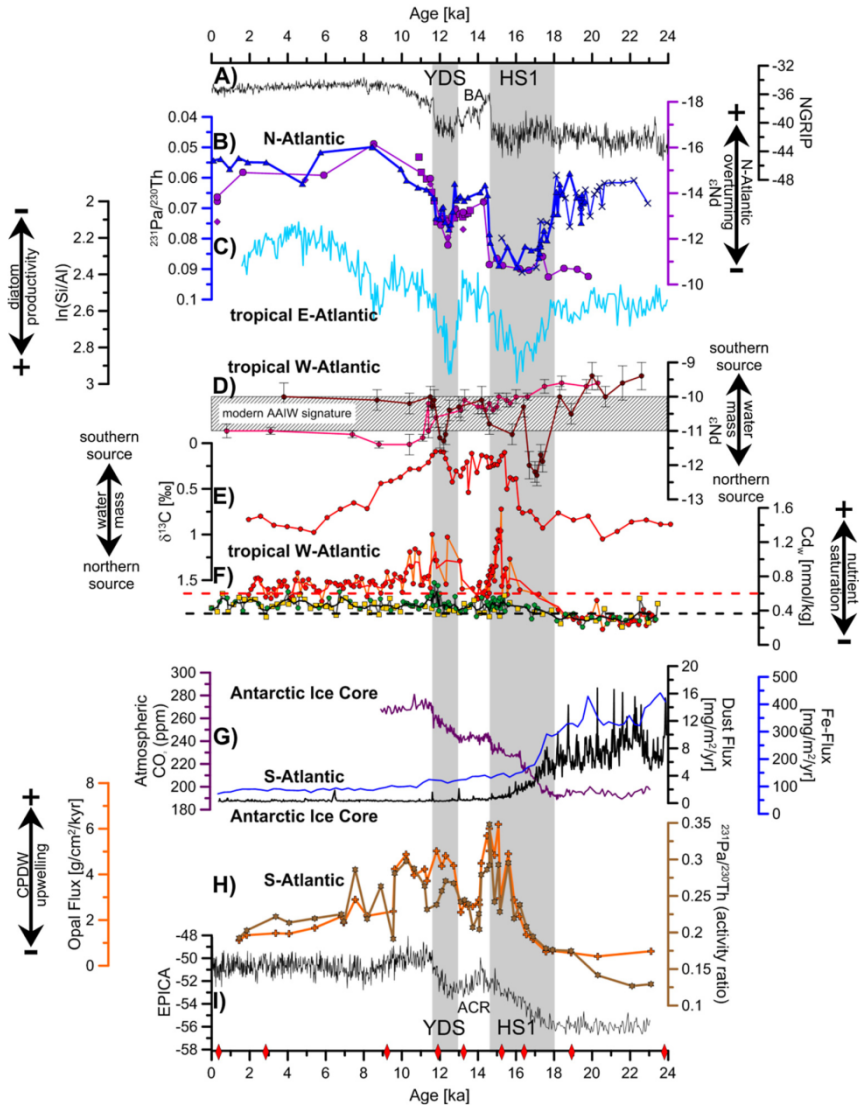

Fig. 3. Intermediate water mass evolution of the tropical E- and W-Atlantic compared to N- and S-Atlantic circulation records for the last glacial termination. **A**) Oxygen isotope record of the Greenland NGRIP ice core (NGRIP Dating Group, 2006) as reference reflecting the northern hemisphere climate signal. **B**) Pa/Th (blue) and εNd (purple) records of N-Atlantic sediment core ODP Site 1063 (Böhm et al., 2015 and references therein) indicating N-Atlantic overturning strength. **C**) Ln(Si/Al) (light blue) of tropical E-Atlantic sediment core ODP Site 658 (Meckler et al., 2013) showing changes in diatom productivity. **D**) εNd reconstructions from the Bonaire Basin (pink, Xie et al., 2014, 1079 m) and the Demarara Rise, off Brazil (brown, Huang et al., 2014, 947 m). Shaded area indicates modern εNd signature of AAIW in the tropical W-Atlantic (Osborne et al., 2014). **E**) Stable carbon isotopes (δ^{13}C, red) of core M78/1-235-1 (this study). **F**) Cd_w of sediment core M78/1-235-1 (850 m; red, this study) and composite Cd_w record (black) from ~1300 m (composed of sediment cores MD99-2198 (1330 m; green, this study) and M35003 (1299 m; yellow, Zahn and Stüber, 2002)) denoting nutrient saturation at intermediate water depth. Thick lines represent 3-point running averages. All Cd_w reconstructed from Cd/Ca-ratios of endobenthic species *Uvigerina spp.* Dashed lines indicate approximated modern Cd-concentrations at the appropriate depth (Mawji et al., 2015). **G**) Atmospheric CO_2 evolution, reconstructed from Antarctic ice core analyses (purple, Marcott et al., 2014), dust flux (black, Lambert et al., 2012) and Fe flux in the SO (blue, Martínez-García et al., 2011). **H**) Opal flux (orange) and Pa/Th (brown) records of S-Atlantic sediment core TN057-13 showing upwelling changes of nutrient-rich CPDW (Anderson et al., 2009). **I**) Oxygen isotope record of the Antarctica EPICA Dome C (Stenni et al., 2006) as reference reflecting the southern hemisphere climate signal. HS1 = Heinrich Stadial 1; YD = Younger Dryas Stadial; BA = Bølling-Allerød; ACR = Antarctic Cold Reversal; Red diamonds along the lower age-axis indicate ^{14}C age control points for core M78/1-235-1. (For interpretation of the references to colour in this figure legend, the reader is referred to the web version of this article.)

of deep, old and δ^{13}C depleted Circumpolar Deepwater (CPDW) in the SO, of which the isotope signal was then transferred to low latitudes such as our intermediate depth core location via AAIW (e.g. Pena et al., 2013). The contribution of GNAIW with its significantly heavier δ^{13}C signature of 1.5‰ (Curry and Oppo, 2005) can therefore be ruled out at the depth of our core location. Thornalley et al. (2010) observed similar negative excursions in the northern N-Atlantic and interpreted these as a shift from southern sourced waters mixing with GNAIW to southern sourced waters mixing with northern high latitude brine waters. This mechanism is unlikely to have caused the HS1 and YD δ^{13}C signatures presented here. The regional setting differs significantly from the one in the northern N-Atlantic (Fig. 1) as the northern sourced water masses in the intermediate tropical W-Atlantic

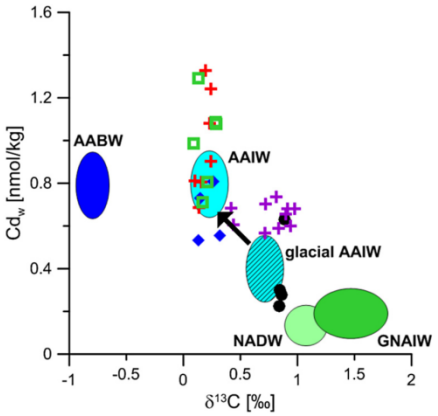

Fig. 4. Evolution of intermediate water depth nutrient levels as reflected by combined Cd_w and $\delta^{13}C$ signatures. Modern and suggested glacial water mass signatures indicated by ellipses (Curry and Oppo, 2005; Marchitto and Broecker, 2006; Mawji et al., 2015). Time series data separated for distinct time intervals: black dots = Last Glacial Maximum; red crosses = Heinrich Stadial 1; open green squares = Younger Dryas Stadial; blue diamonds = Bølling-Allerød; purple crosses = Holocene; AABW = Antarctic Bottom Water; AAIW = Antarctic Intermediate Water; NADW = North Atlantic Deep Water; GNAIW = Glacial North Atlantic Intermediate Water; Black arrow indicates postulated shift in AAIW signature. (For interpretation of the references to colour in this figure legend, the reader is referred to the web version of this article.)

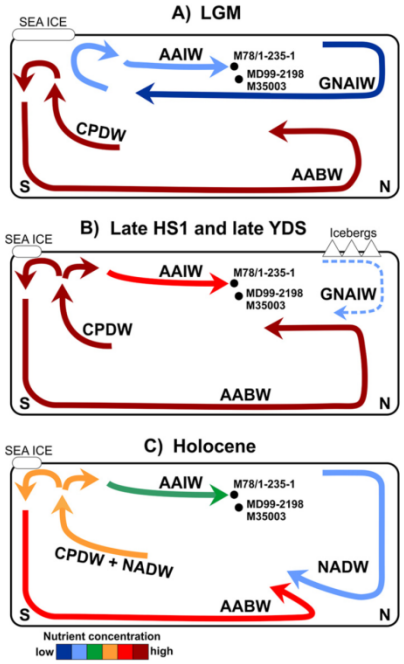

Fig. 5. Schematic illustration of different Atlantic overturning modes complemented from the Cd_w and $\delta^{13}C$ reconstructions (following Talley, 2013 and Ferrari et al., 2014). Water masses and flow are indicated by arrows. Colour-coding implies nutrient concentrations (see legend). Locations of proxy records from this study are indicated by black dots. **A**) Last Glacial Maximum: The AMOC is characterised by clearly separated overturning cells. In the shallow cell, AAIW is mainly fed by nutrient depleted, shallow GNAIW resulting in low Cd_w and high $\delta^{13}C$ signatures at intermediate depths in the tropical W-Atlantic. As Antarctic sea ice cover is largely expanded, upwelling of nutrient-rich CPDW and according air–sea-exchange is hampered. CPDW sinks to the abyss and forms AABW in the deep cell. **B**) Late Heinrich Stadial 1 and shortly after the Younger Dryas Stadial: Due to warming in the southern hemisphere large scale Antarctic sea-ice retreated fostered the shallow upwelling of CPDW north of the ice edge, feeding both AABW and AAIW. The formation of GNAIW in contrast was suppressed. AAIW therefore was characterised by high nutrient conditions and low $\delta^{13}C$, as reflected by the new data. **C**) Holocene: The modern AMOC is characterised by the strengthened formation of oxygenated NADW, ventilating the deep Atlantic. Modern AAIW is thereby fed by a mixture of CPDW and NADW, causing mediocre benthic Cd_w. Relatively positive benthic $\delta^{13}C$ values imply a considerable contribution from northern sources.

are characterised by high $\delta^{13}C$ signatures (Curry and Oppo, 2005; Marchitto and Broecker, 2006). The intermediate depth $\delta^{13}C$ minima observed here more likely originated from subantarctic surface waters, where AAIW is formed (e.g. Spero and Lea, 2002; Romahn et al., 2014). The change in $\delta^{13}C$ observed at our location therefore points to a shift in the AAIW source waters from GNAIW during the LGM to CPDW at the end of HS1 and during the YD.

The Cd_w and $\delta^{13}C$ reconstructions presented here allow the contrasting views on the northward advection of AAIW during the YD and HS1 to be reconciled. Our data imply that AAIW continuously reached the tropical W-Atlantic during the last 24 ka although its nutrient composition and $\delta^{13}C$ signature varied significantly as a consequence of SO circulation changes (Figs. 3, 4).

The prevalence of GNAIW or CPDW sourced AAIW is also consistent with nearby foraminifera/fish debris Nd isotope data from intermediate water depths (Fig. 3D; Huang et al., 2014 (KNR197-3-46CDH from 947 m); Xie et al., 2014 (VM12-107 from 1079 m)). These two intermediate depth ε Nd records conflict in detail but the data mostly fall within the range of -10 to -11εNd typical for modern AAIW in the tropical W-Atlantic (Huang et al., 2014; Osborne et al., 2014). Therefore, although the decrease in εNd from a GNAIW like signature of -9.7 (Gutjahr et al., 2008) in the LGM to -11.4 in the early Holocene can be explained by a change from GNAIW to NADW (Xie et al., 2014), these changes could also be explained by variability of εNd within AAIW. A change in the εNd signature of AAIW is consistent with a change of source waters feeding AAIW. With GNAIW as the main source for AAIW during the LGM and a combination of NADW and CPDW today as suggested from proxy data and modelling by Talley (2013) and Ferrari et al. (2014), this change in source waters would have altered the AAIW εNd signature accordingly. The offsets between the two εNd records (Huang et al., 2014; Xie et al., 2014) are likely the result of their different locations within different parts of the AAIW tongue. Furthermore exchange processes with the sediments may have caused sharp excursions to unradiogenic εNd values given that the detrital sediments in the region have values of ~ -13 (Weiss et al., 1985; Howe et al., 2016). Recently published data from the Brazil Margin further confirmed suggestions of Xie et al. (2014) that the reliability of different techniques to extract the seawater εNd near ocean margins needs to be tested and confirmed for each location (Howe et al., 2016). Sedimentary exchange process may thus be an important cause of the divergence of εNd time series from the W-Atlantic (Pahnke et al., 2008; Xie et al., 2012, 2014; Huang et al., 2014).

The timing of our Cd_w and $\delta^{13}C$ excursions at the end of HS1 and YD and the comparison of the records from ~850 m depth to Pa/Th and Nd isotope data from the deep N-Atlantic (Fig. 3B; Böhm et al., 2015) and to biogenic opal flux and Pa/Th data from the SO (Fig. 3H; Anderson et al., 2009) supports SO upwelling changes as the main driver of the nutrient content of low latitude AAIW.

It has been hypothesised that during the LGM, the Atlantic circulation was separated into two overturning cells (Ferrari et al., 2014). A shallow cell was driven by the formation of relatively shallow GNAIW in the N-Atlantic, which flowed southwards and fed glacial AAIW in the S-Atlantic given that the nutrient-rich CPDW did not upwell to the surface where AAIW is formed, at that time. The deep cell instead, was characterised by northward flowing AABW, which filled the Atlantic basin at depth and re-

circulated at shallower depths (e.g. Sigman et al., 2010; Ferrari et al., 2014). Due to the extended Antarctic sea ice cover, the deep overturning cell was isolated from the atmosphere and therefore carbon and nutrients were stored in the abyss (e.g. Stephens and Keeling, 2000; Gersonde et al., 2005) (Fig. 5A). A distinct boundary between both cells (e.g. Marchitto and Broecker, 2006; Lund et al., 2015) and a modified distribution of deep water properties likely prevailed (e.g. Lynch-Stieglitz et al., 2007). The modern overturning circulation in contrast, is controlled by the formation of NADW in the N-Atlantic, which flows southwards, mixes with CPDW and both contribute to the formation of AAIW in the SO (Talley, 2013) (Fig. 5C).

For the last deglaciation, we propose a circulation pattern deviating from the above-mentioned overturning cells. The southern hemisphere experienced two warmer periods during the deglaciation separated by the ACR (e.g. Blunier et al., 1997; Stenni et al., 2006; Denton et al., 2010) (Fig. 3I). These warm intervals coincided with the HS1 and the YD intervals, during which the northern hemisphere experienced abrupt cooling and a weakening or even a collapse of the AMOC (Fig. 3B; McManus et al., 2004; Böhm et al., 2015). The corresponding slowdown of northward heat transport led to the warming of the southern hemisphere (Crowley, 1992; Toggweiler and Lea, 2010) and consequently the westerly wind belt shifted southward (e.g. Denton et al., 2010). Anderson et al. (2009) suggested that the shift of the Westerlies caused a strengthening of the upwelling of nutrient-rich CPDW leading to higher productivity (Fig. 3H) and CO_2 release in the SO during HS1 and YD (e.g. Burke and Robinson, 2012; Jaccard et al., 2016). These mechanisms are likely to have been augmented by changes in the role of northern component waters and their southward expansion for the deglacial CO_2 rise (e.g. Hain et al., 2014; Chen et al., 2015; Lund et al., 2015).

The striking synchronicity of our 850 m intermediate depth Cd_w and $\delta^{13}C$ records to S-Atlantic biogenic opal flux supports the notion that upwelling CPDW has driven the nutrient inventory of AAIW on deglacial millennial timescales.

We argue that the deglacial change in nutrient inventory at intermediate depths reflects the varying admixture of sources to AAIW and hence, provides evidence for the reconnection of the shallow and the deep Atlantic overturning cells (Figs. 4 and 5). During the LGM, when both overturning cells were separated from each other, the contribution of low nutrient GNAIW to AAIW formation (Ferrari et al., 2014) is evident in low Cd_w values at ~850 m in the tropical W-Atlantic. In contrast, the Cd_w maxima at the end of HS1, during and shortly after the YD suggest a complete cessation of GNAIW contributions in favour of high nutrient CPDW, feeding SO productivity and AAIW (Fig. 5B). The sharp drop in Cd_w at the beginning of the BA may indicate a link to a postulated short-term "overshooting event" characterised by enhanced AMOC strength that lasted only a few hundreds of years (Chen et al., 2015). There is evidence, that the YD climatic rebound was necessary to complete the last termination by raising atmospheric CO_2, which fostered interglacial warm conditions (Denton et al., 2010). During the post YD warming, the Atlantic overturning strengthened and deepened to its modern state (Ferrari et al., 2014). A second postulated short-term AMOC strengthening event (Chen et al., 2015) may have caused the distinct negative Cd_w excursion at the beginning of the Holocene. The ultimate Holocene reconnection of both overturning cells is consistent with our intermediate depth Cd_w values documenting modern contributions of both, nutrient-rich CPDW and nutrient depleted NADW. Today, nutrient levels at intermediate water depths in the equatorial W-Atlantic are higher than during the LGM, but significantly lower than at times when AAIW did not receive any NADW contribution (during late HS1, during and shortly after the YD).

Our study suggests that the tropical W-Atlantic nutrient inventory of AAIW was mainly controlled by SO sea ice extent, upwelling of deeper water masses in the SO and related atmospheric processes rather than by deep water formation processes in the N-Atlantic. Of particular importance for the nutrient levels of AAIW, were periods of intense upwelling of CPDW in the SO causing pronounced increases in primary productivity during HS1 and the YD (Anderson et al., 2009). We speculate that during deglacial periods of prevailing increased Cd_w, the complete utilisation of nutrients in the "high-nutrient, low-chlorophyll" SO was hampered by low iron fluxes and the lack of metabolizable iron (e.g. Lambert et al., 2012; Martínez-García et al., 2011, 2014). The reduced nutrient utilisation in the SO would have allowed a large portion of unused nutrients to be transported northward via AAIW causing prominent intermediate-depth Cd_w maxima in the tropical W-Atlantic.

Increased low and high latitude Atlantic primary productivity, fostered by the nutrient injection via AAIW, likely enhanced the biological pump and thus is a possible cause of the deglacial atmosphere CO_2 plateau at the end of HS1 (Marcott et al., 2014) (Fig. 3G). Increased diatom productivity during HS1 in the N-Atlantic may reflect the high nutrient supply during this time (Gil et al., 2010; Hendry et al., 2016). Enhanced silicic acid supply to the NE-Atlantic during northern hemisphere cooling events further implies a weakened stratification (Hendry et al., 2016). Further support for the postulated short-term AAIW fertilisation by old nutrient-rich deep waters and the subsequent transfer to the tropical W-Atlantic comes from cold water coral $\Delta^{14}C$ off Brazil and in the western N-Atlantic, pointing to higher ventilation ages and thus, the presence of southern sourced waters during HS1 and YD (Robinson et al., 2005; Mangini et al., 2010). Proxy data from the Drake Passage indicate that the Southern Ocean ventilation increased during these times (Burke and Robinson, 2012), which through AAIW, had far reaching effects on the biological pump globally.

4. Conclusions

High resolution reconstructions of intermediate water Cd_w concentrations and $\delta^{13}C$ suggest that AAIW continuously reached the tropical N-Atlantic during the entire last 24 ka and underwent only minor shifts in northward expansion. At the end of HS1, as well as during and shortly after the YD the AAIW was enriched in Cd_w indicating a change of source water masses feeding AAIW from low nutrient GNAIW to high nutrient CPDW. The striking resemblance of our Cd_w reconstructions from ~850 m depth to upwelling reconstructions from the Atlantic sector of the SO and postulated short-term AMOC strengthening during the BA and at the beginning of the Holocene demonstrate that the SO effectively shaped the N-Atlantic nutrient inventory. In contrast, our Cd_w results from nearby but deeper intermediate water depth location (~1300 m) preclude a recent theory arguing for Atlantic wide shoaling of AABW. The increased AAIW nutrient content at intermediate depth likely enhanced N-Atlantic productivity and hence led to a dampening of the deglacial global atmospheric CO_2 increase. The new AAIW Cd_w and $\delta^{13}C$ data demonstrate the importance of deglacial ocean circulation reorganisations for global marine biogeochemistry and climate.

Acknowledgements

This research was funded by the Deutsche Forschungsgemeinschaft (DFG) via the "Cluster of Excellence – The Future Ocean" Kiel; Project number CP1142. We are thankful for the detailed and constructive comments of two anonymous reviewers which substantially improved this manuscript.

Appendix A. Online content

Cd_w and $\delta^{13}C$ data are available online at the Data Publisher for Earth and Environmental Science, PANGEA: www.pangea.de.

Supporting information associated with this article can be found in the online version at http://dx.doi.org/10.1016/j.epsl.2017.01.030.

References

Anderson, R.F., et al., 2009. Wind-driven upwelling in the Southern ocean and the deglacial rise in atmospheric CO_2. Science 323 (5920), 1443–1448.

Blunier, T., et al., 1997. Timing of the Antarctic Cold Reversal and the atmospheric CO_2 increase with respect to the Younger Dryas event. Geophys. Res. Lett. 24 (21), 2683–2686.

Böhm, E., et al., 2015. Strong and deep Atlantic meridional overturning circulation during the last glacial cycle. Nature 517 (7532), 73–76.

Boyer, T.P., et al., 2013. World Ocean Database 2013. In: Levitus, S., Mishonov, A. (Eds.), NOAA Atlas NESDIS 72. Silver Spring, MD. 209 pp. http://doi.org/10.7289/V5NZ85MT.

Boyle, E.A., 1988. Cadmium: chemical tracer of deepwater paleoceanography. Paleoceanography 3 (4), 471–489.

Boyle, E.A., 1992. Cadmium and $\delta^{13}C$ paleochemical ocean distributions during the stage 2 glacial maximum. Annu. Rev. Earth Planet. Sci. Lett. 20, 245–287.

Boyle, E.A., Rosenthal, Y., 1996. Chemical hydrography of the South Atlantic during the last glacial maximum: Cd vs. $\delta^{13}C$. In: The South Atlantic. Springer, Berlin, Heidelberg, pp. 423–443.

Bradtmiller, L.I., et al., 2016. Changes in biological productivity along the northwest African margin over the past 20,000 years. Paleoceanography 31 (1), 185–202.

Broecker, W.S., 1998. Paleocean circulation during the Last Deglaciation: a bipolar seesaw? Paleoceanography 13 (2), 119–121.

Bryan, S.P., Marchitto, T.M., 2010. Testing the utility of paleonutrient proxies Cd/Ca and Zn/Ca in benthic foraminifera from thermocline waters. Geochem. Geophys. Geosyst. 11 (1).

Burke, A., Robinson, L.F., 2012. The Southern Ocean's role in carbon exchange during the last deglaciation. Science 335 (6068), 557–561.

Came, R.E., Oppo, D.W., Curry, W.B., 2003. Atlantic Ocean circulation during the Younger Dryas: insights from a new Cd/Ca record from the western subtropical South Atlantic. Paleoceanography 18 (4).

Came, R.E., et al., 2008. Deglacial variability in the surface return flow of the Atlantic meridional overturning circulation. Paleoceanography 23 (1).

Chen, T., et al., 2015. Synchronous centennial abrupt events in the ocean and atmosphere during the last deglaciation. Science 349 (6255), 1537–1541.

Crowley, T.J., 1992. North Atlantic deep water cools the southern hemisphere. Paleoceanography 7 (4), 489–497.

Curry, W.B., Oppo, D.W., 2005. Glacial water mass geometry and the distribution of $\delta^{13}C$ of ΣCO_2 in the western Atlantic Ocean. Paleoceanography 20, PA1017. http://dx.doi.org/10.1029/2004PA001021.

Denton, G.H., et al., 2010. The last glacial termination. Science 328 (5986), 1652–1656. http://dx.doi.org/10.1126/science.1184119.

Duplessy, J.-C., et al., 1984. ^{13}C record of benthic foraminifera in the last interglacial ocean: implications for the carbon cycle and the global deep water circulation. Quat. Res. 21 (2), 225–243.

Ferrari, R., et al., 2014. Antarctic sea ice control on ocean circulation in present and glacial climates. Proc. Natl. Acad. Sci. USA 111 (24), 8753–8758. http://dx.doi.org/10.1073/pnas.1323922111.

Gersonde, R., et al., 2005. Sea-surface temperature and sea ice distribution of the Southern Ocean at the EPILOG Last Glacial Maximum—a circum-Antarctic view based on siliceous microfossil records. Quat. Sci. Rev. 24 (7), 869–896.

Gherardi, et al., 2009. Glacial–interglacial circulation changes inferred from $^{231}Pa/^{230}Th$ sedimentary record in the North Atlantic region. Paleoceanography 24, PA2204. http://dx.doi.org/10.1029/2008PA001696.

Gil, I.M., Keigwin, L.D., Abrantes, F., 2010. Comparison of diatom records of the Heinrich Event 1 in the Western North Atlantic. IOP Conf. Ser.: Earth Environ. Sci. http://dx.doi.org/10.1088/1755-1315/9/1/012008.

Greaves, M., et al., 2008. Interlaboratory comparison study of calibration standards for foraminiferal Mg/Ca thermometry. Geochem. Geophys. Geosyst. 9 (8).

Gutjahr, M., et al., 2008. Tracing the Nd isotope evolution of North Atlantic deep and intermediate waters in the Western North Atlantic since the Last Glacial Maximum from Blake Ridge sediments. Earth Planet. Sci. Lett. 266 (1), 61–77.

Hain, M.P., Sigman, D.M., Haug, G.H., 2014. Distinct roles of the Southern Ocean and North Atlantic in the deglacial atmospheric radiocarbon decline. Earth Planet. Sci. Lett. 394, 198–208.

Hathorne, E.C., et al., 2012. Online preconcentration ICP-MS analysis of rare earth elements in seawater. Geochem. Geophys. Geosyst. 13 (1), Q01020. http://dx.doi.org/10.1029/2011GC003907.

Hendry, K.R., et al., 2012. Abrupt changes in high-latitude nutrient supply to the Atlantic during the last glacial cycle. Geology 40 (2), 123–126.

Hendry, K.R., et al., 2016. Deglacial diatom production in the tropical North Atlantic driven by enhanced silicic acid supply. Earth Planet. Sci. Lett. 438, 122–129.

Hoffmann, J., et al., 2014. Disentangling abrupt deglacial hydrological changes in northern South America: insolation versus oceanic forcing. Geology 42 (7), 579–582.

Howe, J.N.W., et al., 2016. Antarctic intermediate water circulation in the South Atlantic over the past 25,000 years. Paleoceanography 31, 1302–1314.

Huang, K.-F., Oppo, D.W., Curry, W.B., 2014. Decreased influence of Antarctic intermediate water in the tropical Atlantic during North Atlantic cold events. Earth Planet. Sci. Lett. 389, 200–208.

Jaccard, S.L., et al., 2016. Covariation of deep Southern Ocean oxygenation and atmospheric CO_2 through the last ice age. Nature 530, 207–210.

Lambert, F., et al., 2012. Centennial mineral dust variability in high-resolution ice core data from Dome C, Antarctica. Clim. Past 8 (2), 609–623.

Lund, D.C., et al., 2015. Southwest Atlantic water mass evolution during the last deglaciation. Paleoceanography 30, 477–494.

Lynch-Stieglitz, J., et al., 2007. Atlantic meridional overturning circulation during the last glacial maximum. Science 316, 66–69.

Mangini, A., et al., 2010. Deep sea corals off Brazil verify a poorly ventilated Southern Pacific Ocean during H2, H1 and the Younger Dryas. Earth Planet. Sci. Lett. 293 (3–4), 269–276.

Marchitto, T.M., Broecker, W.S., 2006. Deep water mass geometry in the glacial Atlantic Ocean: a review of constraints from the paleonutrient proxy Cd/Ca. Geochem. Geophys. Geosyst. 7 (12).

Marcott, S.A., et al., 2014. Centennial-scale changes in the global carbon cycle during the last deglaciation. Nature 514 (7524), 616–619.

Martínez-García, A., et al., 2011. Southern Ocean dust-climate coupling over the past four million years. Nature 476 (7360), 312–315.

Martínez-García, A., et al., 2014. Iron fertilization of the Subantarctic Ocean during the last ice age. Science 343 (6177), 1347–1350.

Mawji, E., et al., 2015. The GEOTRACES Intermediate Data Product 2014. Mar. Chem. http://dx.doi.org/10.1016/j.marchem.2015.04.005.

McManus, J.F., et al., 2004. Collapse and rapid resumption of Atlantic meridional circulation linked to deglacial climate changes. Nature 428 (6985), 834–837.

Meckler, A.N., et al., 2013. Deglacial pulses of deep-ocean silicate into the subtropical North Atlantic Ocean. Nature 495 (7442), 495–498.

NGRIP Dating Group, 2006. Greenland Ice Core Chronology 2005, (GICC05). IGBP PAGES/World Data Center for Paleoclimatology. Data Contribution Series # 2006-118. NOAA/NCDC Paleoclimatology Program, Boulder CO, USA.

Osborne, A.H., et al., 2014. Neodymium isotopes and concentrations in Caribbean seawater: tracing water mass mixing and continental input in a semi-enclosed ocean basin. Earth Planet. Sci. Lett. 406, 174–186.

Pahnke, K., Goldstein, S.L., Hemming, S.R., 2008. Abrupt changes in Antarctic Intermediate Water circulation over the past 25,000 years. Nat. Geosci. 1 (12), 870–874.

Pena, L., et al., 2013. Rapid changes in meridional advection of Southern Ocean intermediate waters to the tropical Pacific during the last 30 kyr. Earth Planet. Sci. Lett. 368, 20–32.

Reimer, P.J., et al., 2013. IntCal13 and Marine13 radiocarbon age calibration curves 0–50,000 years cal BP. Radiocarbon 55 (4).

Rickaby, R.E.M., Elderfield, H., 2005. Evidence from the high-latitude North Atlantic for variations in Antarctic Intermediate water flow during the last deglaciation. Geochem. Geophys. Geosyst. 6 (5).

Robinson, L.F., et al., 2005. Radiocarbon variability in the western North Atlantic during the last deglaciation. Science 310 (5753), 1469–1473.

Romahn, S., Mackensen, A., Groeneveld, J., 2014. Deglacial intermediate water reorganization: new evidence from the Indian Ocean. Clim. Past 10 (1), 293–303.

Rosenthal, Y., Boyle, E., Labeyrie, L., 1997. Last glacial maximum paleochemistry and deepwater circulation in the Southern Ocean: evidence from foraminiferal cadmium. Paleoceanography 12 (6), 787–796.

Schlitzer, R., 2015. Ocean Data View. http://odv.awi.de.

Sigman, D.M., Hain, M.P., Haug, G.H., 2010. The polar ocean and glacial cycles in atmospheric CO_2 concentration. Nature 466, 47–55.

Spero, H.J., Lea, D.W., 2002. The cause of carbon isotope minimum events on glacial terminations. Science 296 (5567), 522–525.

Stenni, B., et al., 2006. EPICA Dome C Stable Isotope Data to 44.8 KYr BP. IGBP PAGES/World Data Center for Paleoclimatology Data Contribution Series # 2006-112. NOAA/NCDC Paleoclimatology Program, Boulder CO, USA.

Stephens, B.B., Keeling, R.F., 2000. The influence of Antarctic sea ice on glacial–interglacial CO_2 variations. Nature 404 (6774), 171–174.

Talley, L.D., 2013. Closure of the global overturning circulation through the Indian, Pacific, and Southern Oceans: schematics and transports. Oceanography 26 (1), 80–97. http://dx.doi.org/10.5670/oceanog.2013.07.

Thornalley, D.J.R., Elderfield, H., McCave, I.N., 2010. Intermediate and deep water paleoceanography of the northern North Atlantic over the past 21,000 years. Paleoceanography 25 (1).

Toggweiler, J.R., Lea, D.W., 2010. Temperature differences between the hemispheres and ice age climate variability. Paleoceanography 25, PA2212. http://dx.doi.org/10.1029/2009PA001758.

Weiss, R.F., et al., 1985. Atmospheric chlorofluoromethanes in the deep equatorial Atlantic. Nature 314, 608–610.
Xie, R.C., Marcantonio, F., Schmidt, M.W., 2012. Deglacial variability of Antarctic Intermediate Water penetration into the North Atlantic from authigenic neodymium isotope ratios. Paleoceanography 27, PA3221.
Xie, R.C., Marcantonio, F., Schmidt, M.W., 2014. Reconstruction of intermediate water circulation in the tropical North Atlantic during the past 22,000 years. Geochim. Cosmochim. Acta 140 (0), 455–467.
Zahn, R., Stüber, A., 2002. Suborbital intermediate water variability inferred from paired benthic foraminiferal Cd/Ca and $\delta^{13}C$ in the tropical West Atlantic and linking with North Atlantic climates. Earth Planet. Sci. Lett. 200, 191–205.
Zahn, R., Winn, K., Sarthein, M., 1986. Benthic foraminiferal $\delta^{13}C$ and accumulation rates of organic carbon: Uvigerina peregrina group and Cibicidoides wuellerstorfi. Paleoceanography 1, 27–42.

Scientific Chapter 2: Deglacial heat deprivation from the atmosphere in the Southern Ocean via Antarctic Intermediate Water

This scientific chapter consists of the manuscript entitled “Deglacial heat deprivation from the atmosphere in the Southern Ocean via Antarctic Intermediate Water” as it is prepared for submission to *Nature Communications*.

The authors are David-Willem Poggemann[a], Dirk Nürnberg[a], Willi Rath[a], Ed C. Hathorne[a], Martin Frank[a], Stefan Reißig[a], André Bahr[b].

[a]GEOMAR Helmholtz Centre for Ocean Research Kiel, D-24148 Kiel, Germany

[b]Heidelberg University, Institute of Earth Science, D-69120 Heidelberg, Germany

Deglacial heat deprivation from the atmosphere in the Southern Ocean via Antarctic Intermediate Water

David-Willem Poggemann[a,*], Dirk Nürnberg[a] , Willi Rath[a], Ed C. Hathorne[a], Martin Frank[a], Stefan Reißig[a], André Bahr[b]

[a]GEOMAR Helmholtz Centre for Ocean Research Kiel, D-24148 Kiel, Germany

[b]Heidelberg University, Institute of Earth Science, D-69120 Heidelberg, Germany

*Corresponding author: GEOMAR Helmholtz Centre for Ocean Research Kiel, D-24148 Kiel, Germany. Tel.: 0049 431 6002309. E-mail address: dpoggemann@geomar.de.

2.1 Highlights

- First Mg/Ca-based temperature reconstruction of intermediate waters in the W-Atlantic
- Deglacial heat uptake by the Southern Ocean and rapid northward distribution via Atlantic Intermediate Water
- Warmed Antarctic Intermediate Water might have dampened deglacial southern hemisphere warming
- Delayed heat transfer into intermediate water via the Southern Ocean due to AMOC variability

2.2 Abstract

The discrepancy between the apparent recent cessation in global warming and the disagreement of model predictions for the 21st century climate evolution is subject of ongoing debate. Many modelling studies point to the pivotal role of heat transfer from the atmosphere into the intermediate and deep Southern Ocean (SO) and the subsequent transfer of ocean heat to low latitudes via intermediate and deep water circulation. The long-term perspective on millennial timescales provides further insight into these processes.

We reconstruct benthic foraminiferal Mg/Ca-based intermediate water temperatures (IWT) and planktonic foraminiferal εNd from sediment cores located at the northern tip of modern Antarctic Intermediate Water (AAIW) in the tropical W-Atlantic (850 and 1018 m water depth). Congruent to recent notions, our results suggest efficient and rapid deglacial transfer of ocean heat from the surface Southern Ocean, which accumulated during Atlantic Meridional Overturning (AMOC) perturbations, to intermediate-depths. The subsequent transmission to the tropical W-Atlantic via AAIW supposedly responded delayed by ~ 1000 years but similarly rapid and pronounced in shape and amplitude to the deglacial changes in N-Atlantic deep water formation. We validated our hypothesis of southern-sourced ocean heat injection into

the intermediate tropical W-Atlantic by a simple test calculation of the static stability of the Atlantic's water column under the postulated deglacial conditions. We speculate that the ocean heat deprivation via AAIW dampened southern hemisphere warming during the deglaciation and was intimately linked to the major deglacial perturbations of the AMOC. We further postulate that a weakened or even collapsed AMOC therefore directly triggered the IWT in the tropical W-Atlantic with a detour via the Southern Ocean. Our results likely support previous studies, suggesting a response time of ~ 1 ka in the SO warming due to collapsed N-Atlantic deep water formation.

2.3 Introduction

Despite continuously increasing atmospheric greenhouse gases, the intensified radiative forcing and related global warming, the cessation of global surface air warming since the beginning of the 21st century affords explanation (e.g. Lee et al., 2015 and references therein). While Marotzke & Forster (2015) claim a random modelling problem artificially causing this hiatus in global warming, there is also supporting evidence that the transfer of ocean heat from the surface SO and its subsequent storage at deeper ocean levels may have caused this hiatus in global atmospheric warming (Meehl et al., 2011; Chen & Tung, 2014). In this respect, studies on the past ocean heat dispersal taken place under natural forcing conditions may provide further insight into the processes shaping present-day climate modifications and may help to assess future climate predictions. The last deglaciation and its pronounced cold events, the Heinrich Stadial 1 (HS1, 18 – 14.6 ka; Barker et al., 2009) and the Younger Dryas Stadial (YD, 12.8 – 11.5 ka; Barker et al., 2009), may serve as an example for rapid climate change. These climatic rebound events were characterised by distinct cooling of the northern hemisphere (e.g. NGRIP Dating Group, 2006) but synchronous SO warming (e.g. Stenni et al., 2006), while the AMOC experienced pronounced perturbations. Today, the overturning in the Atlantic is mainly driven by the formation of North Atlantic Deep Water (NADW) in the N-Atlantic, which receives contributions from AAIW and warm and saline tropical waters (e.g. Talley, 1996, 2013). During the Last Glacial Maximum (LGM), in contrast, the AMOC was likely split into two separate overturning cells (e.g. Ferrari et al., 2014). During the transition from the LGM to the Holocene, when the AMOC experienced major weakening (YD) or even collapsed (HS1) (e.g. McManus et al., 2004; Böhm et al., 2015), these overturning cells reconnected (Poggemann et al., 2017). Due to these AMOC decelerations and the related reduction in northward heat transport, modelling and proxy data suggested ocean heat accumulation in the tropical Atlantic and in the SO (e.g. Vellinga & Wood, 2002; Toggweiler & Lea, 2010; Schmidt et al., 2012). SO sea surface temperature (SST) reconstructions for the last deglaciation verified major warming during northern hemisphere cold events pointing to a seesaw mechanism between the high-latitude ocean areas (e.g. Kaiser et al., 2005; Calvo et al., 2007; Lamy et al., 2007; Stenni et al., 2011; Landais et al., 2015). Synchronous upwelling of old, nutrient-rich, and carbon-enriched water masses in the SO and the concomitant release of CO_2 to the atmosphere accompanied northern hemisphere cold events (e.g. Anderson et al., 2009; Burke & Robinson, 2012). These processes might have triggered ventilation and nutrient enrichment of AAIW (Burke & Robinson, 2012; Poggemann et al., 2017).

Despite the absence of suitable sediment records and the lack of direct temperature reconstructions from intermediate water depths, previous studies argued for the transmission of the SO surface temperature signature via intermediate waters into the (sub-)tropics (e.g. Rühlemann et al., 2004; Kiefer et al., 2006; Naidu & Govil, 2010; Romahn et al., 2014). In particular during deglacial AMOC perturbations, atmospheric changes in temperature and wind strength might have affected the water mass composition of AAIW and therefore its geochemical signatures which then would have been transferred from the polar regions to the tropics (e.g. Lynch-Stieglitz et al., 1994; Ninnemann & Charles, 1997; Spero & Lea, 2002; Bostock et al., 2004). However, direct evidence from intermediate waters for the postulated warming is unfortunately missing and the processes linking high to low latitude intermediate temperature evolution remain unclear. We here present the first high resolution deglacial AAIW temperature reconstruction in the tropical W-Atlantic based on benthic foraminiferal Mg/Ca. Combined with reconstructed intermediate water Nd isotope (εNd) signatures obtained from uncleaned mixed planktonic foraminifera, we are able to quantify past AAIW variations and to relate them to changes in Atlantic water mass mixing and circulation. We test our results for their physical plausibility with respect to the static stability of the Atlantic water column using a simple calculation of the postulated changes in water mass density.

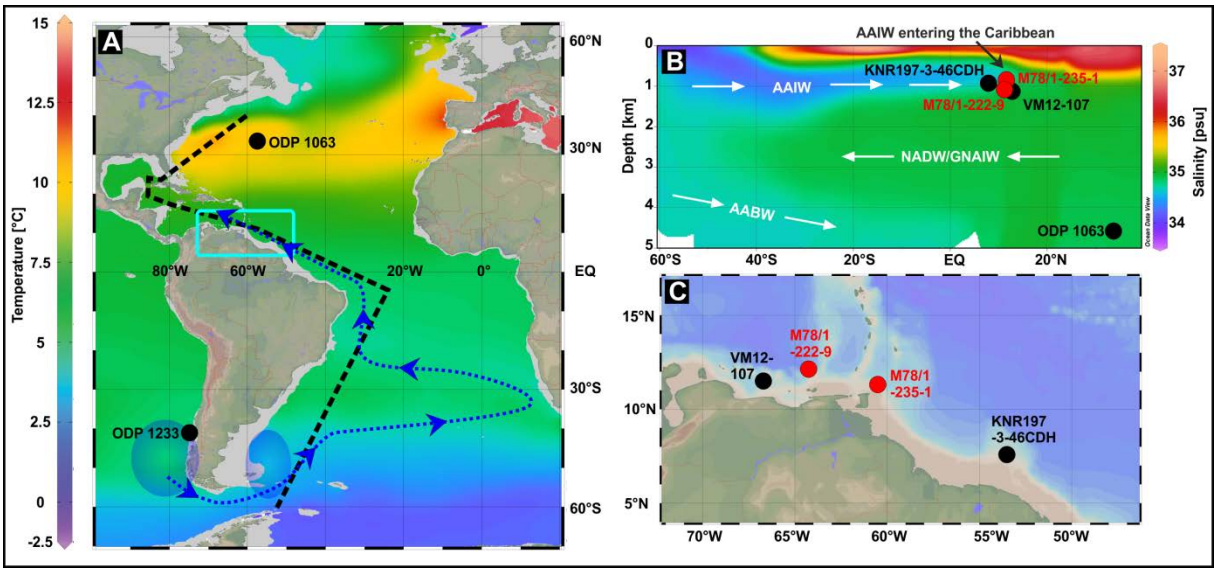

Figure 2.1: Overview of intermediate water masses in the Atlantic Ocean showing core locations studied here (red) and reference sites (black). **A)** Annual IWT distribution in the Atlantic at 850 m water depth (data from World Ocean Atlas, WOA2013; Boyer et al., 2013). The major pathway of AAIW from the SO into the tropical W-Atlantic is marked by the blue dashed line. The study area is indicated by the light blue square enlarged in C. Black dashed line marks salinity section displayed in B. **B)** Vertical salinity profile (data from WOA2013; Boyer et al., 2013; see A)) with locations of proxy records placed at the corresponding water depths (red = this study; black = reference records). Major deep and intermediate water masses are indicated, differentiated by their salinities (AAIW = Antarctic Intermediate Water; NADW = North Atlantic Deep Water; GNAIW = Glacial North Atlantic Intermediate Water; AABW = Antarctic Bottom Water). **C)** Bathymetric chart of the tropical W-Atlantic with locations of the sediment cores (red = this study; black = reference records). Figures were created using Ocean Data View (Schlitzer, 2015).

2.4 Materials and Methods

The Mg/Ca-ratio of benthic foraminiferal tests has been established as proxy for paleo bottom temperature reconstructions (e.g. Bryan & Marchitto, 2008; Elderfield et al., 2010). We analysed Mg/Ca of the endobenthic foraminiferal species *Uvigerina spp.* selected from sediment core M78/1-235-1 (11°36.53'N, 60°57.86'W; termed 235 in the following). The core was retrieved from the Tobago Basin (SE-Caribbean) from 852 m water depth, which is within the core of modern AAIW (Fig. 2.1). *Uvigerina spp*. is not influenced by carbonate ion effects at intermediate water depth, which makes $Mg/Ca_{Uvigerina}$ a suitable proxy to estimate past changes in IWT (Elderfield et al., 2010; Elmore et al., 2015). We use the established age model of sediment core M78/1-235-1 (Poggemann et al., 2017), which was generated by linear interpolation between 9 AMS^{14}C datings.

We further determined the εNd signatures of uncleaned mixed planktonic foraminifera to reconstruct changes in the mixing of the prevailing intermediate water masses. Previous studies have proven that authigenic coatings of unclean planktonic foraminiferal tests reliably record past bottom water εNd signatures (e.g. Roberts et al., 2010; Piotrowski et al., 2012; Huang et al., 2014). Due to the lack of sample material in sediment core 235, the εNd signatures were measured on adjacent sediment core M78/1-222-9 (12°1.49'N, 64°28.50'W, 1018 m; termed 222 in the following). Core 222 was retrieved from the southern Caribbean Sea north of Blanquilla Island and located at the lower boundary of modern AAIW (Fig. 2.1). The age model for sediment core 222 is based on linear interpolation between 4 AMS^{14}C datings and oxygen isotope stratigraphy (see supplement S2). Due to the low abundances of benthic foraminifera in sediment core 222, we were not able to accomplish Mg/Ca-based bottom water reconstructions on these samples.

All sediment samples were freeze dried, wet sieved and fractionated. For Mg/Ca-ratios, ~ 30 benthic foraminiferal tests of *Uvigerina spp*. from the 315 – 400 µm size fraction were selected. For εNd analyses, > 45 mg of mixed planktonic foraminiferal shells from the > 250 µm size fraction were picked. The foraminiferal tests were gently crushed between glass plates and rinsed with ethanol and MilliQ water to remove the clay minerals in an ultrasonic bath before measurements.

Table2.1: Calibrated AMS^{14}C datings for sediment core M78/1-222-9 using Calib 7.1 and Marine13 databases

Depth (cm)	Measured Radiocarbon Age (BP)	+/- (BP)	Median Age (ka BP)
3.5	130	30	0.13
113.5	10810	40	12.36
163.5	21020	100	24.87
178.5	22820	120	26.76

Mg/Ca analyses

For Mg/Ca analyses, the foraminiferal samples were cleaned oxidatively and reductively following established protocols (Lea et al., 2003) and measured on an ICP-OES and ICP-MS at GEOMAR Helmholtz Centre for Ocean Research Kiel. Replicate measurements resulted

in a Mg/Ca uncertainty of 0.24 mmol/mol (2σ). For comparability the Mg/Ca-ratios were referenced to the ECRM-752 limestone powder standard (Greaves et al., 2008). For this study, the ECRM-752 mean was 3.80 ± 0.04 mmol/mol and hence in good agreement with published values. The calculated Mg/Ca-ratios were transformed to absolute temperatures using the established down-core calibration of Elderfield et al. (2010). Although reconstructed core-top IWT are slightly (~ 1 – 2°C) below modern IWT at the core location 235, this calibration provides the most reliable glacial-interglacial temperature reconstruction. Most likely due to the low temperatures at the analysed location of core 235 and the reconstructed deglacial high amplitude changes in IWT, other Mg/Ca-temperature calibrations for *Uvigerina spp.* provide unrealistic high temperature changes during the last deglaciation (see supplement S2 and discussion in Elderfield et al., 2010). Due to no evidence for sample contamination by clay minerals and diagenetic coatings, this effect on our reconstructed IWT can be generally ruled out (see supplement S2). A small number of single data points appeared unrealistically high/low compared with the surrounding data and hence a Grubb's test was performed. A total of 16 Mg/Ca data points were defined as outliers and removed from the 235-data record (see supplement S2).

Nd isotope measurements

For εNd analyses, the crushed planktonic foraminiferal samples were dissolved carefully in ~0.35 M acetic acid to avoid the leaching of possibly still adhering detrital material, then centrifuged and transferred into Teflon vials following the protocols of Roberts et al. (2010, 2012) and Piotrowski et al. (2012). Chemical cleaning and isolation of Nd from the sample solutions was performed applying standard methods (e.g. Barrat et al., 1996; Le Fèvre and Pin, 2005; Roberts et al., 2012; Osborne et al., 2014). The Nd isotope data were measured on a Nu Plasma Multi Collector ICP-MS at GEOMAR, Kiel. Some samples with low concentrations were measured on a Thermo Fischer Scientific Neptune MC-ICPMS at the University of Oldenburg. All εNd results were normalized to the established JNdi-1 standard with εNd = 0.512115 (Tanaka et al., 2000). The standard deviations (2σ, internal reproducibility) of repeated standard measurements ranged between 0.1 and 0.5 εNd units.

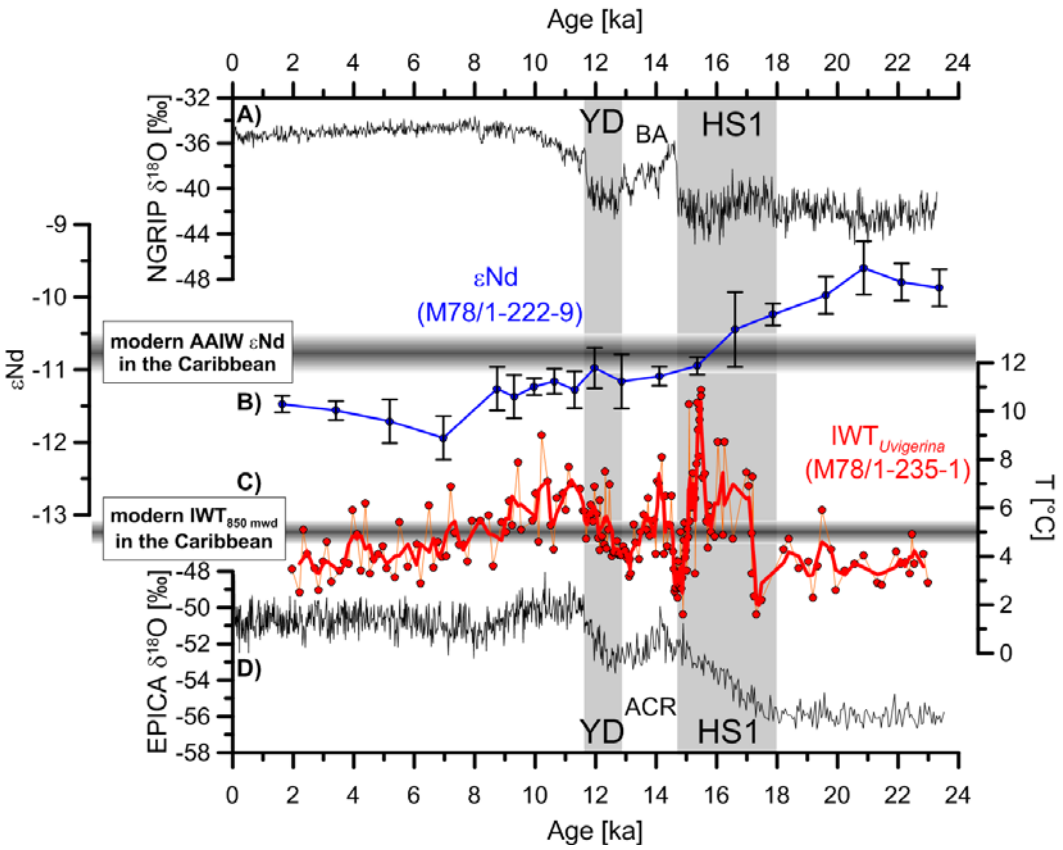

Figure 2.2: Intermediate water mass evolution in the tropical W-Atlantic during glacial/interglacial change. **A)** Oxygen isotope record of the Greenland NGRIP ice core (NGRIP Dating Group, 2006) as reference for northern hemisphere climate change. **B)** εNd signature of unclean planktonic foraminifera from Tobago basin (core 222; this study) reflecting intermediate water mass variability. The modern AAIW εNd signature from the respective water depth close to the core location is indicated by shading (Osborne et al., 2014). **C)** IWT record based on $Mg/Ca_{Uvigerina}$ of core 235 (this study). Red dots and the thin orange line represent the original data, while the thick red line represents the 3 point running average. Shading indicates modern IWT at 850 m water depth in the S-Caribbean (from WOA2013; Boyer et al., 2013). **D)** Oxygen isotope record of EPICA Dome C (Stenni et al., 2006) as reference for the southern hemisphere climate variability. HS1 = Heinrich Stadial 1; YD = Younger Dryas; BA = Bølling-Allerød; ACR = Antarctic Cold Reversal.

2.5 Results

During full glacial times (~ 24 - 18 ka BP), the IWT at the core location 235 is ~ 3.5 – 4.5°C, close to modern AAIW annual temperatures of 4.5 – 5.5°C (WOA2013; Boyer et al., 2013). During HS1 the IWT rapidly rise to ~ 7°C in the early HS1 (~ 17.5 - 17 ka BP), finally reaching ~ 11°C at the end of HS1 (~ 15.5 ka BP). Afterwards, a marked drop in IWT > 9°C is apparent, ending at ~ 15 ka BP at IWT of ~ 2°C close to the full glacial conditions (Fig. 2.2). IWT subsequently reach a maximum of ~ 8°C at ~ 14.5 ka BP, which is synchronous to the Antarctic Cold Reversal (ACR, ~14.5 – 12.8 ka BP, e.g. Anderson et al., 2009). This increase is followed by a rapid drop to modern-like values (~ 14 - 13 ka BP). The YD is characterised by gradually increasing IWT for ~ 3 - 4°C, reaching maximum values of 7 - 9°C

during the early Holocene (~ 10 - 11 ka BP). The remaining Holocene period is characterized by a gradual decline in IWT of overall ~4°C, reaching values slightly lower than the modern IWT at the core location (WOA2013, Boyer et al., 2013).

In order to further elaborate the intermediate water dynamics in the tropical W-Atlantic, we compared the core 235 IWT record to the εNd dataset of adjacent core 222. The reconstructed intermediate εNd pattern differs clearly from the IWT record (Fig. 2.2). The εNd data show a gradual and continuous decline from more radiogenic values of ~ 9.8 on average during full glacial times (~ 24 - 18 ka BP) to less radiogenic values of ~ -11.5 during the late Holocene (last ~ 4 kyr). During the deglaciation, in particular during the late HS1 to shortly after the YD when IWT reveals prominent variability, the εNd signal remains rather stable at ~ -11.

2.6 Discussion

The reconstructed IWT record exhibiting prominent warming phases during HS1, synchronous to the ACR, and during the YD into the early Holocene argues for efficient heat transfer into the intermediate tropical W-Atlantic. These temperature peaks may be explained by two possible scenarios: a) Replacement of nutrient rich AAIW or strongly enhanced mixing with nutrient depleted northern sourced waters at the corresponding depth. b) A major warming of AAIW itself.

The first suggested process implies that cold nutrient-rich AAIW might have been replaced by, or at least experienced major admixture of a warmer and nutrient-depleted water mass during short deglacial time intervals. In this scenario AAIW might have been supplanted by northern sourced water masses or from above. Previous studies already argued for the reduced northward advection of AAIW and the replacement by northern sourced water masses during HS1 and the YD (Came et al., 2008; Xie et al., 2012). Other studies, in contrast, either suggested an increased northward advection of AAIW during these periods of time (Zahn & Stüber, 2002; Pahnke et al., 2008) or only minor changes in its distribution (Huang et al., 2014; Howe et al., 2016). The replacement of AAIW by or a major admixture of northern sourced water masses from overlying water depth would also be reflected by pronounced changes in other proxies (e.g. in εNd, nutrient and $\delta^{13}C$ reconstructions). Previously published $\delta^{13}C$ and Cd_w reconstructions obtained from the same sediment material clearly argue for enhanced nutrient supply to the S-Caribbean at intermediate water depth during late HS1, as well as during and shortly after the YD (Poggemann et al., 2017). Thus a replacement of AAIW or enhanced mixing of nutrient rich AAIW with nutrient depleted northern sourced waters is not consistent with the available data. Several studies indicated an expansion of the subtropical gyre and therefore a warming trend in sea surface and subsurface temperatures in the tropical W-Atlantic during the last deglaciation with rapidly increasing temperatures during HS1 and the YD (e.g. Schmidt et al., 2012; Parker et al., 2015). Nonetheless, a vertical heat transfer of 2 – 6°C into intermediate depth waters from overlying water masses is likewise unlikely. Such a process cannot have occurred without major water mass mixing and would thus be reflected in a distinct alteration of other water mass proxy data like Cd_w and εNd, which has not been observed. The direct comparison of our reconstructed IWT to subsurface temperatures (subSST) from a nearby sediment core (Schmidt et al., 2012) further indicates no significant correlation between the signals and

therefore does not point to a major thermal exchange between subsurface and intermediate water masses (Fig. 2.3C).

An alternative and more likely scenario involves a significant change in AAIW properties in the formation areas of AAIW in the Southern Ocean and the subsequent northward transport of the modulated AAIW signature into the tropical W-Atlantic. Our previously published Cd_w and $\delta^{13}C$ data support this theory (Poggemann et al., 2017).

The εNd reconstruction accomplished on tropical W-Atlantic core 222 (Fig. 2.2) allows distinction between the admixed water masses and therefore to support or disprove the postulated mechanisms. Today, the εNd signature for NADW is -13.5 as a consequence of weathering input of old continental material surrounding the N-Atlantic, in particular the Labrador Sea (Piepgras & Wasserburg, 1987). In contrast, Pacific subsurface water masses are characterized by more radiogenic signatures of - 2 to – 4 preformed by young volcanic rocks surrounding the Pacific (Piepgras & Wasserburg, 1980; Piepgras & Jacobsen, 1988). In the Southern Ocean, the formation area of AAIW, water masses are a mixture of Pacific and Atlantic water masses and are therefore, characterized by intermediate εNd signatures of - 6.2 to - 9.2 (Jeandel, 1993). Along its northward dispersal in the Atlantic, the modern primary AAIW εNd signature of ~ - 8.4 (Stichel et al., 2012, Molina-Kescher et al., 2014) is modified by both water mass mixing (Jeandel, 1993) and, to some extent, through external inputs (e.g. remobilization of sedimentary Nd), which results in a less radiogenic signature of ~ - 10.5 to - 11 in the tropical W-Atlantic (Huang et al., 2014; Osborne et al., 2014). In contrast to modern NADW, the supposed εNd signature of Glacial North Atlantic Intermediate Water (GNAIW), which replaced NADW during glacial times (Marchitto & Broecker, 2006), is still debated (van de Flierdt et al., 2006; Foster et al., 2007; van de Flierdt et al., 2016) but may have been as radiogenic as - 10 (Gutjahr et al., 2008).

In the light of this, our new εNd results afford a modified interpretation of previous εNd reconstructions from the Bonaire Basin (Xie et al., 2014). These were interpreted in terms of a gradual change from GNAIW during the LGM to NADW during the Holocene with no contribution of AAIW. This published εNd record is slightly more radiogenic during most of the analysed time interval, compared to the record presented here. This difference can most likely be explained by the location of the core in the Bonaire Basin, which is likely affected by weathering inputs from highly radiogenic volcanic rocks that altered the water mass signature is this area (Pearce et al., 2013; Osborne et al., 2014). Having this in mind and combined with the evidence from previously published Cd_w and $\delta^{13}C$ reconstructions from sediment core M78/1-235-1 (Poggemann et al., 2017), we interpret the εNd record as a gradual change in the εNd signature of AAIW rather than a result from water mass mixing.

Nutrient and ventilation reconstructions from the tropical W-Atlantic imply a change in the composition of water masses forming AAIW due to SO upwelling changes (Poggemann et al., 2017). Given the potential higher similarity of the εNd signatures of GNAIW and Circumpolar Deep Water (CPDW) during the last glacial (Gutjahr et al., 2008) in addition to the alteration of the AAIW εNd signature on its pathway into the N-Atlantic, the εNd results presented here and those from nearby Bonaire Basin (Xie et al., 2014) support this hypothesis. Both εNd reconstructions are from similar water depths (1018 and 1079 m) at the modern transition zone between AAIW and NADW. The glacial values of about – 9.7 in both records are consistent with the postulated theory of GNAIW being the main source water mass for AAIW during full glacial times (e.g. Ferrari et al., 2014; Poggemann et al., 2017) and a possible direct admixture of GNAIW from beneath. During HS1 and in the YD when N-

Atlantic deep water formation collapsed / weakened, the upwelling of nutrient rich deep CPDW in the Southern Ocean was enhanced (Anderson et al., 2009) and the AAIW was mainly fed by this water mass (Poggemann et al., 2017). Both εNd records therefore show close to modern AAIW values during times of rapid northern hemisphere cold periods (~ -10.4 - -11). During the Holocene, when AAIW was fed by both source water masses, CPDW and NADW, the enhanced contribution of NADW would explain the less radiogenic values during the Holocene (~ - 11 to - 12). Our published Cd_w and $\delta^{13}C$ data (Poggemann et al., 2017) confirm such a shift from GNAIW being the major contributor feeding into the AAIW during the LGM to Circumpolar Deep Water (CPDW) and upper NADW being the main source waters during the Holocene, in agreement with Ferrari et al., (2014).

In contrast to the εNd records, the observed rapid high amplitude temperature changes do not seem to be a consequence of AAIW source water alterations. The IWT record instead likely reflects major AMOC perturbations during times of rapid cooling events in the northern hemisphere (Fig. 2.3B) (McManus et al., 2004; Böhm et al., 2015) associated with the resulting southern hemisphere temperature increases (Fig. 2.3E) (e.g. Kaiser et al., 2005; Stenni et al., 2006; Lamy et al., 2007). This close similarity between our reconstructed IWT from the tropical W-Atlantic and AMOC strength reconstructions on one hand and to southern hemisphere temperature pattern on the other hand points to Southern Ocean SST evolution linking N-Atlantic AMOC perturbations and the advection of this signal into the equatorial Atlantic via AAIW.

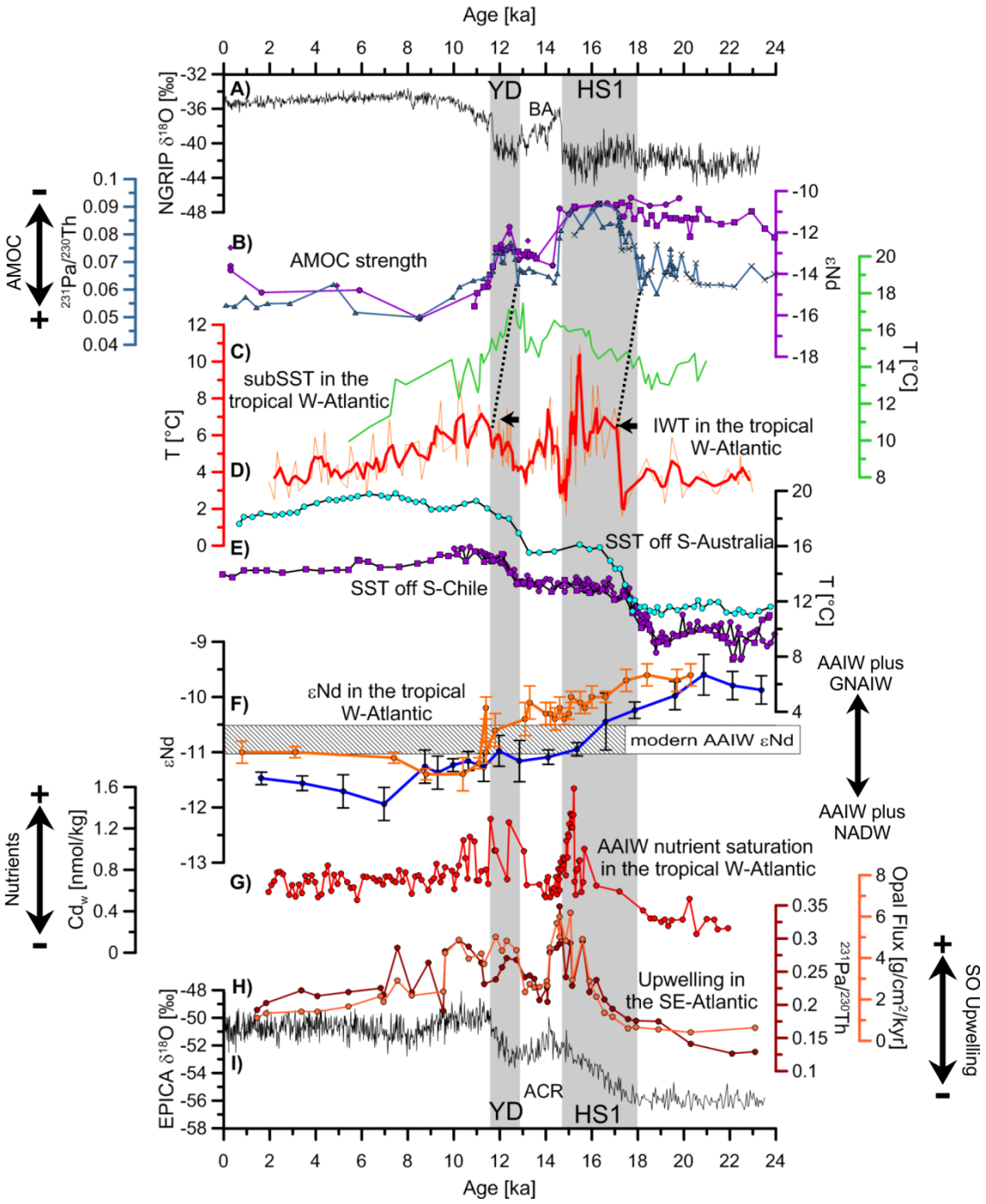

Figure 2.3: N-Atlantic, tropical W-Atlantic and Southern Ocean proxy records crucial for the interpretation of Atlantic intermediate water dynamics. **A)** Oxygen isotope record of the Greenland NGRIP ice core (NGRIP Dating Group, 2006) representing northern hemisphere climate changes. **B)** N-Atlantic overturning strength reconstructed from Pa/Th (blue) and εNd data (purple) of N-Atlantic ODP Site 1063 (Böhm et al., 2015 and references therein). **C)** Planktonic foraminiferal Mg/Ca based subsurface temperature reconstructions obtained from S-Caribbean core VM12-107 (green, Schmidt et al., 2012) **D)** Mg/Ca*Uvigerina*-based IWT record of core 235 (this study, orange = original data, red = 3-point running average). Dashed lines connecting B) and D) and black arrows indicate the postulated ~ 1ka response time of W-Atlantic IWT to N-Atlantic AMOC perturbations as suggested by Stocker & Johnsen (2003). **E)** Alkenone-based SST reconstructions from the SE-Pacific (purple, ODP Site 1233, Kaiser et al., 2005 (squares), Lamy et al., 2007 (dots)) and from offshore S-Australia (cyan, core MD03-2611,

Calvo et al., 2007). **F)** Intermediate water εNd records from the S-Caribbean obtained from sediment cores VM12-107 (orange, 1079 m water depth, Xie et al., 2014) and M78/1-222-9 (blue, 1018 m, this study). Shading indicates the modern AAIW εNd signature from the respective water depth close to the core locations (Osborne et al., 2014). **G)** Temporal change in AAIW nutrient inventory (Cd_w) for the tropical W-Atlantic core 235 based on benthic Cd/Ca ratios (red, Poggemann et al., 2017).**H)** Record of nutrient-rich CPDW upwelling in the SE-Atlantic based on opal flux (orange) and $^{231}Pa/^{230}Th$ ratios (brown) of S-Atlantic core TN057-13 (Anderson et al., 2009). **I)** Stable Oxygen isotope reference record from Antarctica EPICA Dome C (Stenni et al., 2006) reflecting southern hemisphere climate changes. HS1 = Heinrich Stadial 1; YD = Younger Dryas; BA = Bølling-Allerød; ACR = Antarctic Cold Reversal;

Heat accumulation in the southern Hemisphere due to AMOC perturbations triggered AAIW warming?

At present-day, the surface-limb of the AMOC effectively transports oceanic heat across hemispheres into the N-Atlantic, thereby cooling the southern hemisphere (e.g. Crowley, 1992). During the deglaciation, major warming events in the southern hemisphere occurred during times of rapid northern hemisphere cooling, in particular during HS1 and YD, validating the seesaw pattern in ocean temperatures between the hemispheres (e.g. Broecker, 1998; Kaiser et al., 2005; Calvo et al., 2007; Lamy et al., 2007; Stenni et al., 2011; Landais et al., 2015). Therefore, the observed intervals of heat accumulation in the southern hemisphere might have been caused by a weakened or collapsed AMOC (e.g. Denton et al., 2010). Due to the heat storage capacity of the SO, a ceased AMOC is suggested to result in SO warming with a response time of ~ 1000 years (Stocker & Johnson, 2003; Hansen et al., 2016). Accordingly, the observed weakening/collapse of deep water formation in the N-Atlantic (McManus et al., 2004; Böhm et al., 2015) would lead to reduced heat transfer from the southern hemisphere into the N-Atlantic and therefore increase SST in the Southern Ocean.

The most prominent features of the tropical W-Atlantic core 235 are rapid centennial-scale and large-amplitude (~4°C) IWT changes during the deglaciation. The shape of the reconstructed deglacial IWT record strikingly echoes N-Atlantic AMOC strength reconstructions (Böhm et al. 2015 and references therein) with a lag of up to ~ 1000 years, depending on the correction of the age model (see supplement). This lagged IWT response in the tropical W-Atlantic to N-Atlantic AMOC perturbations therefore is likely a result of the signal detour via the SO. The surface SO likely warmed, therefore storing the heat, from where it was subducted due to the formation of AAIW and subsequently transported into the N-Atlantic. Based on the published age model of Poggemann et al. (2017), the IWT response to AMOC perturbations correlates convincingly well with the response time of ~ 1000 years suggested by Stocker & Johnson (2003). It is evident between the beginning of HS1 and the associated breakdown of the AMOC (Fig. 2.3B) and the reaction in the reconstructed IWT record (Fig. 2.3D; indicated by dashed lines). The delayed response of IWT to AMOC perturbations explains the Holocene IWT maximum, which basically is a reflection of the AMOC slowdown during the YD. Similarly, IWT warming during the B/A is the postponed signal of AMOC collapse during HS1. This delay is absent, when using an age model that is corrected using the standard reservoir age of 400 years (Calib 7.10; IntCal13; Reimer et al., 2013).

But why did tropical W-Atlantic IWT react on AMOC perturbations, postponed by hundreds of years but notably at the same rapidity of change? We argue that oceanic heat accumulated in the SO during AMOC perturbations was subsequently subducted towards intermediate water depths at AAIW formation sites. A major northward dispersal of SO signals via intermediate water masses was in fact suggested before (e.g. Bostock et al., 2004; Rühlemann et al., 2004; Romahn et al., 2014). This has been supported by recently published benthic foraminiferal Cd_w data from intermediate depth core 235, indicating that the nutrient inventory of AAIW was preformed in the SO and reached the tropical W-Atlantic synchronously to major AMOC reorganisations during postulated SO upwelling events (Anderson et al., 2009) at the end of HS1 and the YD (Poggemann et al., 2017). In contrast to the nutrient signal, which was a result of changes in deep water upwelling in the SO, the IWT record presented here, reconstructed at the same core location and the same foraminiferal species, argues for a direct atmospheric – oceanic link between rapid northern hemisphere cooling events and the temperature evolution in the tropical W-Atlantic at intermediate water depth. The detour via the heat accumulation in the SO therefore explains the ~ 1000 year lag between the AMOC strength and the here presented IWT. There is indeed evidence for SO surface warming during AMOC perturbations (e.g. Stocker, 1998; Toggweiler & Lea, 2010; Stenni et al., 2011; Landais et al., 2015), which is considered as requirement for IWT warming in the tropical W-Atlantic. Alkenone-based SST data from off S-Australia and off S-Chile reveal distinct warming of ~ 4°C during HS1 and ~ 3°C during the YD (Calvo et al., 2007; Lamy et al., 2007; Fig 2.3E). Consistent with these SO SST data, other proxy data from Patagonian mountain glaciers indicate a temperature increase of ~ 6°C during HS1 and another ~ 3°C during the YD (e.g. Denton et al., 2010 and references therein).

Today, AAIW that is present in the tropical W-Atlantic at core location 235 is formed off S-Chile in the SE-Pacific and off S-Argentina in the SW-Atlantic north of the Antarctic Circumpolar Current (Fig. 2.1A) (e.g. Taft 1963; Talley 1996; Boebel et al., 1999; Bostock et al., 2010). We propose that increased SO surface warmth was directly transferred to intermediate depths and transported northward via the AAIW as direct response to major AMOC perturbations and the subsequent heat accumulation in the southern hemisphere. We note that in spite of the observed time-lag between AMOC perturbations and IWT response only minor heat loss occurred along the pathway of AAIW into the tropical W-Atlantic.

The heat deprivation from the surface SO by AAIW at times of prominent AMOC slowdowns or even collapses should have caused a dampening of southern hemisphere atmospheric warming. We speculate that the absorption of oceanic heat by AAIW and the adjacent distribution to the (sub-)tropical Atlantic might even have affected Antarctic sea ice expansion. In particular, the long phase of storage of SO heat by AAIW during the early Holocene (~ 11 – 7 ka) and its subsequent cooling might have reduced the intensity of the early Holocene warm period in the southern hemisphere. We further argue that the observed southern hemisphere warming trends during HS1 and the YD would have been even more pronounced if SO heat deprivation via AAIW would have been absent.

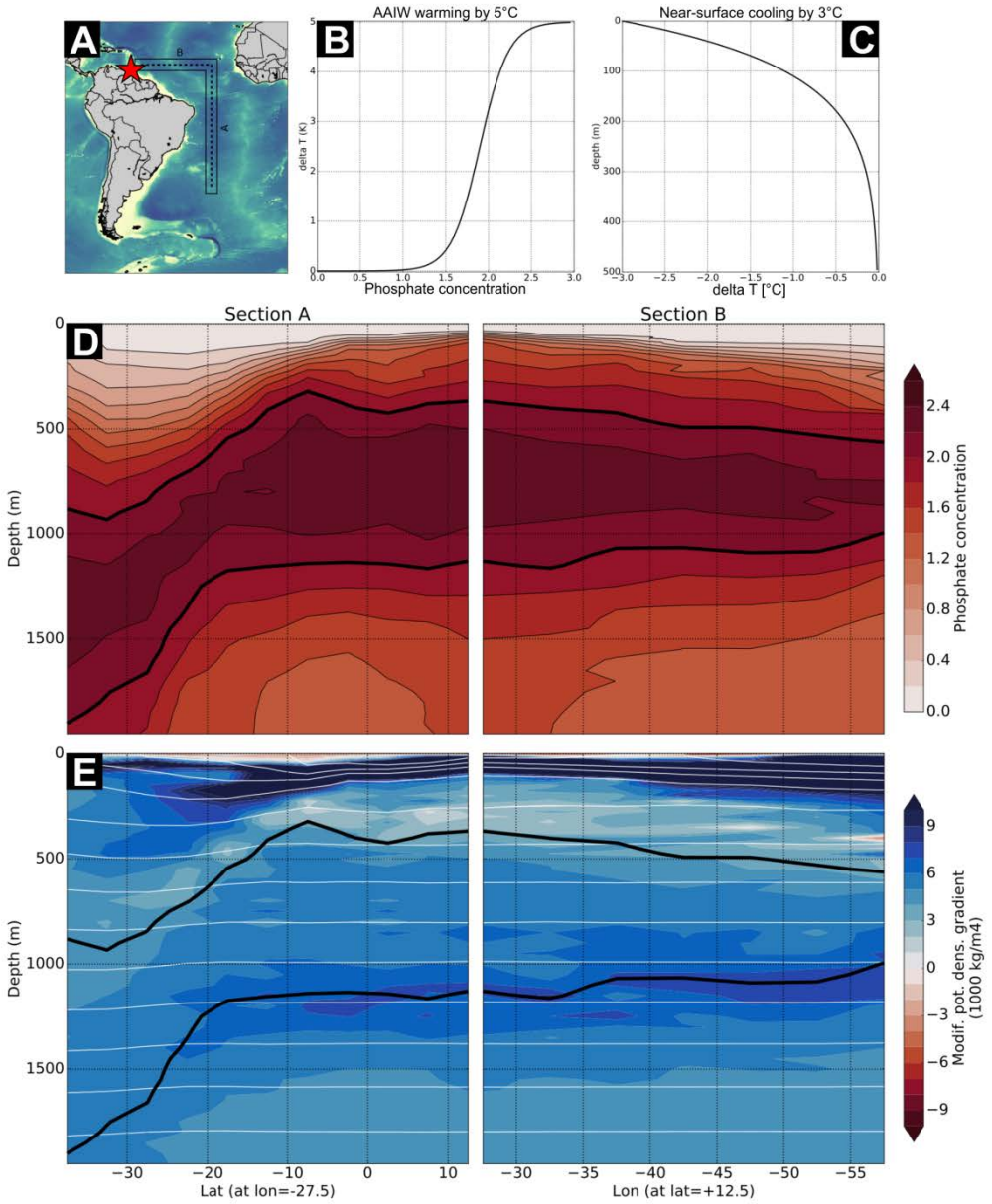

Figure 2.4: Static stability test calculations at modulated IWT and SST conditions and resulting vertical density gradient. **A**) Model calculations were done along two sections A and B with the area covered by the climatological grid, and position of M78/1-235-1 indicated by the star. **B**) The IWT increase was moderated by phosphate concentration. **C**) Decreased sea surface temperature pattern as postulated for the LGM. **D**) Modern phosphate concentration along sections A and B (WOA2013; Boyer et al., 2013). Thick contour lines indicate a phosphate concentration of 2 µmol/l. **E**) Modulated vertical gradient of locally referenced potential density ($1000 kg/m^4$) along sections A and B. Negative values indicate static instability.

2.7 Static stability check for warmed AAIW conditions

To check the plausibility of the postulated warming of AAIW in the tropical W-Atlantic during times of AMOC perturbations, we tested if 4 - 6°C warmer AAIW and the modified vertical temperature and density profiles would contradict to the water column stability. We used the static stability as determined by the vertical (positive downward) gradient of locally

referenced potential density as an indication for water column stability or instability. A positive vertical gradient (denser waters below less dense waters) points to a stable water column, while a negative vertical gradient (less dense waters below denser waters) indicates an unstable, non-lasting configuration**.**

In our calculation we modified modern AAIW temperatures by raising for 5°C, congruent to our deglacial IWT estimate in the tropical W-Atlantic. Further, a ~ 3°C SST decline within the uppermost 100 m of the tropical W-Atlantic during the LGM was taken into consideration (e.g., Rühlemann et al., 1999; Schmidt et al., 2012), in order to simulate water column stability under an extreme, although unrealistic, small density gradient between surface and intermediate ocean.

We used observed temperature and salinity fields from the World Ocean Atlas (WOA2013, Boyer et al., 2013) along two sections at 27.5°W (N-S-oriented) and at 12.5°N (W-E-oriented; Fig. 2.4A),. To selectively warm AAIW, we used phosphate concentrations from the same climatological product and defined AAIW by phosphate concentrations above 2 µmol/l, corresponding to 500-1200 m water depth (Fig. 2.4D) (e.g., Piola & Georgi, 1982; Marchitto & Broecker, 2006; Mawji et al., 2015; Poggemann et al., 2017). We then modified the climatological temperature from WOA2013 using a transition function, which smoothly increases from ΔT = 0°C at ~ 0 µmol/l phosphate to ΔT = 5°C at ~2 µmol/l phosphate (Fig. 2.4B). To mimic the near-surface cooling during the LGM, we added a cooling profile focused on the upper ocean using an exponential profile with ΔT = -3°C at the surface and a vertical e-folding scale of 100 m (Fig. 2.4C). Both modifications were applied at the same time.

The calculated static stability under warmed AAIW and cooled near-surface conditions (Fig. 2.4E) implies statically unstable conditions in the near-surface ocean, which are due to the cooling profile superimposed on the vertically homogenous hydrography of the mixed layer. Above the core of the warmed AAIW, the modified temperature profile yields reduced static stability as is evident from the reduction of the vertical gradient of locally reference potential density which is, however, never inverted. Consequently, we found that a selective increase of deglacial AAIW temperatures by 5°C is compatible with the modern water mass structure in the Atlantic and in the studied region.

2.8 Conclusions

Our high resolution benthic foraminiferal Mg/Ca based IWT reconstructions from the tropical W-Atlantic indicate a pronounced warming of AAIW in the S-Caribbean during northern hemisphere abrupt climate cooling events supposedly postponed by ~ 1000 years, as hypothesised by Stocker & Johnson (2003). Combined with our εNd reconstructions, upwelling- and SST-reconstructions from the SO (Kaiser et al., 2005; Calvo et al., 2007; Lamy et al., 2007; Anderson et al., 2009) and AMOC strength reconstructions from the N-Atlantic (McManus et al., 2004; Böhm et al., 2015), the data indicate a pronounced deglacial heat deprivation from the atmosphere in the SO during the formation of AAIW and subsequent transfer to the equatorial Atlantic. During HS1 and the YD, when the AMOC supposedly weakened or even collapsed, heat consequently accumulated in the southern hemisphere and warmed AAIW. We therefore argue, that rapid northern hemisphere cooling events during the last deglaciation directly triggered the AAIW heat budged in the tropical W-Atlantic with a detour via the surface SO.

Together these results indicate a major heat uptake of AAIW during northern hemisphere rapid cooling events and a following northward distribution at intermediate depth level. We speculate that deglacial AAIW heat uptake dampened SO warming and may therefore have been a crucial player in the climate seesaw mechanisms of the two hemispheres.

2.9 Acknowledgements

This research was funded by the Deutsche Forschungsgemeinschaft (DFG) via the “Cluster of Excellence – The Future Ocean” Kiel. Mg/Ca measurements were acquired at the GEOMAR Helmholtz Centre for Ocean Research Kiel. We would like to thank Katharina Pahnke (University of Oldenburg, Germany) for providing measurement time for the Nd isotope measurements.

2.10 References

Anderson et al.: "Wind-driven upwelling in the Southern Ocean and the deglacial rise in atmospheric CO_2." *Science* 323.5920 (2009): 1443-1448.

Barker et al.: "Interhemispheric Atlantic seesaw response during the last deglaciation." *Nature* 457.7233 (2009): 1097-1102.

Barrat et al.: “Determination of rare earth elements in sixteen silicate reference samples by ICP-MS after Tm addition and ion exchange separation.” *Geostandards Newsletter* (1996), 20(1), 133-139.

Boebel et al.: "The intermediate depth circulation of the western South Atlantic." *Geophysical Research Letters* 26.21 (1999): 3329-3332.

Böhm et al.: "Strong and deep Atlantic meridional overturning circulation during the last glacial cycle." *Nature* 517.7532 (2015): 73-76.

Bostock et al.: "Carbon isotope evidence for changes in Antarctic Intermediate Water circulation and ocean ventilation in the southwest Pacific during the last deglaciation." *Paleoceanography* 19.4 (2004).

Bostock et al.: "Characterising the intermediate depth waters of the Pacific Ocean using δ 13 C and other geochemical tracers." *Deep Sea Research Part I: Oceanographic Research Papers* 57.7 (2010): 847-859.

Boyer et al., 2013: World Ocean Database 2013, NOAA Atlas NESDIS 72, S. Levitus, Ed., A. Mishonov, Technical Ed.; Silver Spring, MD, 209 pp.,

Burke, Robinson: "The Southern Ocean’s role in carbon exchange during the last deglaciation." *Science* 335.6068 (2012): 557-561.

Bryan, Marchitto: "Mg/Ca–temperature proxy in benthic foraminifera: New calibrations from the Florida Straits and a hypothesis regarding Mg/Li." *Paleoceanography* 23.2 (2008).

Broecker: "Paleocean circulation during the last deglaciation: a bipolar seesaw?." *Paleoceanography* 13.2 (1998): 119-121.

Calvo et al.: "Antarctic deglacial pattern in a 30 kyr record of sea surface temperature offshore South Australia." *Geophysical Research Letters* 34.13 (2007).

Came et al.: "Deglacial variability in the surface return flow of the Atlantic meridional overturning circulation." *Paleoceanography* 23.1 (2008).

Chen, Tung: "Varying planetary heat sink led to global-warming slowdown and acceleration." *Science* 345.6199 (2014): 897-903.

Crowley: "North Atlantic deep water cools the Southern Hemisphere." *Paleoceanography* 7.4 (1992): 489-497.

Denton et al.: "The last glacial termination." *Science* 328.5986 (2010): 1652-1656.

Divine et al.: "Holocene Antarctic climate variability from ice and marine sediment cores: Insights on ocean–atmosphere interaction." *Quaternary Science Reviews* 29.1 (2010): 303-312.

Elderfield et al.: "A record of bottom water temperature and seawater δ 18 O for the Southern Ocean over the past 440kyr based on Mg/Ca of benthic foraminiferal Uvigerina spp." *Quaternary Science Reviews* 29.1 (2010): 160-169.

Elmore et al.: "Antarctic Intermediate Water properties since 400 ka recorded in infaunal (*Uvigerina peregrina*) and epifaunal (*Planulina wuellerstorfi*) benthic foraminifera." *Earth and Planetary Science Letters* 428 (2015): 193-203.

Ferrari et al.: "Antarctic sea ice control on ocean circulation in present and glacial climates." *Proceedings of the National Academy of Sciences* 111.24 (2014): 8753-8758.

Foster et al.: "No change in the neodymium isotope composition of deep water exported from the North Atlantic on glacial-interglacial time scales." *Geology* 35.1 (2007): 37-40.

Greaves et al.: "Interlaboratory comparison study of calibration standards for foraminiferal Mg/Ca thermometry." *Geochemistry, Geophysics, Geosystems* 9.8 (2008).

Gutjahr et al.: "Tracing the Nd isotope evolution of North Atlantic deep and intermediate waters in the Western North Atlantic since the Last Glacial Maximum from Blake Ridge sediments." *Earth and Planetary Science Letters* 266.1 (2008): 61-77.

Hansen et al.: "Ice melt, sea level rise and superstorms: Evidence from paleoclimate data, climate modelling, and modern observations that 2 C global warming could be dangerous." *Atmospheric Chemistry and Physics* 16.6 (2016): 3761-3812.

Howe et al.: "Antarctic intermediate water circulation in the South Atlantic over the past 25,000 years." *Paleoceanography* 31.10 (2016): 1302-1314.

Huang, Oppo, Curry: "Decreased influence of Antarctic intermediate water in the tropical Atlantic during North Atlantic cold events." *Earth and Planetary Science Letters* 389 (2014): 200-208.

Jeandel: "Concentration and isotopic composition of Nd in the South Atlantic Ocean." *Earth and Planetary Science Letters* 117.3 (1993): 581-591.

Kaiser et al.: "A 70-kyr sea surface temperature record off southern Chile (Ocean Drilling Program Site 1233)." *Paleoceanography* 20.4 (2005).

Kiefer et al.: "Antarctic control on tropical Indian Ocean sea surface temperature and hydrography." *Geophysical Research Letters* 33.24 (2006).

Lamy et al.: "Modulation of the bipolar seesaw in the Southeast Pacific during Termination 1." *Earth and Planetary Science Letters* 259.3 (2007): 400-413.

Landais et al.: "A review of the bipolar see–saw from synchronized and high resolution ice core water stable isotope records from Greenland and East Antarctica." *Quaternary Science Reviews* 114 (2015): 18-32.

Lea et al.: "Synchroneity of tropical and high-latitude Atlantic temperatures over the last glacial termination." *Science* 301.5638 (2003): 1361-1364.

Lee et al.: "Pacific origin of the abrupt increase in Indian Ocean heat content during the warming hiatus." *Nature Geoscience* 8.6 (2015): 445-449.

Le Fèvre, Pin: “A straightforward separation scheme for concomitant Lu-Hf and Sm-Nd isotope ratio and isotope dilution analysis”, *Analytica Chimica Acta*, 543(1-2), 209-221 (2005).

Lynch-Stieglitz et al.: "Glacial-interglacial history of Antarctic Intermediate Water: relative strengths of Antarctic versus Indian Ocean sources." *Paleoceanography* 9.1 (1994): 7-29.

Marchitto, Broecker: "Deep water mass geometry in the glacial Atlantic Ocean: A review of constraints from the paleonutrient proxy Cd/Ca." *Geochemistry, Geophysics, Geosystems* 7.12 (2006).

Marotzke, Forster: "Forcing, feedback and internal variability in global temperature trends." *Nature* 517.7536 (2015): 565-570.

Mawji, et al.: The GEOTRACES Intermediate Data Product 2014, Mar. Chem. (2015), http://dx.doi.org/10.1016/j.marchem.2015.04.005.

McManus et al.: "Collapse and rapid resumption of Atlantic meridional circulation linked to deglacial climate changes." *Nature* 428.6985 (2004): 834-837.

Meehl et al.: "Model-based evidence of deep-ocean heat uptake during surface-temperature hiatus periods." *Nature Climate Change* 1.7 (2011): 360-364.

Molina-Kescher et al.: "South Pacific dissolved Nd isotope compositions and rare earth element distributions: water mass mixing versus biogeochemical cycling." *Geochimica et Cosmochimica Acta* 127 (2014): 171-189.

Naidu, Govil: "New evidence on the sequence of deglacial warming in the tropical Indian Ocean." *Journal of Quaternary Science* 25.7 (2010): 1138-1143.

Ninnemann, Charles: "Regional differences in Quaternary Subantarctic nutrient cycling: Link to intermediate and deep water ventilation." *Paleoceanography* 12.4 (1997): 560-567.

NGRIP Dating Group, 2006. Greenland Ice Core Chronology 2005 (GICC05). IGBP PAGES/World Data Center for Paleoclimatology. Data Contribution Series # 2006-118. NOAA/NCDC *Paleoclimatology Program*, Boulder CO, USA.

Osborne et al.: "Neodymium isotopes and concentrations in Caribbean seawater: Tracing water mass mixing and continental input in a semi-enclosed ocean basin." *Earth and Planetary Science Letters* 406 (2014): 174-186.

Pahnke et al.: "Abrupt changes in Antarctic Intermediate Water circulation over the past 25,000 years." *Nature Geoscience* 1.12 (2008): 870-874.

Parker et al.: "Tropical North Atlantic subsurface warming events as a fingerprint for AMOC variability during Marine Isotope Stage 3." *Paleoceanography* 30.11 (2015): 1425-1436.

Pearce et al.: "The effect of particulate dissolution on the neodymium (Nd) isotope and Rare Earth Element (REE) composition of seawater." *Earth and Planetary Science Letters* 369 (2013): 138-147.

Piepgras, Wasserburg: "Neodymium isotopic variations in seawater." *Earth and Planetary Science Letters* 50.1 (1980): 128-138.

Piepgras, Wasserburg: "Rare earth element transport in the western North Atlantic inferred from Nd isotopic observations." *Geochimica et Cosmochimica Acta* 51.5 (1987): 1257-1271.

Piepgras, Jacobsen: "The isotopic composition of neodymium in the North Pacific." *Geochimica et Cosmochimica Acta* 52.6 (1988): 1373-1381.

Piola, Georgi: "Circumpolar properties of Antarctic intermediate water and Subantarctic Mode Water." *Deep Sea Research Part A. Oceanographic Research Papers* 29.6 (1982): 687-711.

Piotrowski et al.: "Reconstructing deglacial North and South Atlantic deep water sourcing using foraminiferal Nd isotopes." *Earth and Planetary Science Letters* 357 (2012): 289-297.

Poggemann et al.: "Rapid deglacial injection of nutrients into the tropical Atlantic via Antarctic Intermediate Water." *Earth and Planetary Science Letters* 463 (2017): 118-126.

Roberts et al.: "Synchronous deglacial overturning and water mass source changes." *Science* 327.5961 (2010): 75-78.

Roberts et al.: "Rare earth element association with foraminifera." *Geochimica et Cosmochimica Acta* 94 (2012): 57-71.

Reimer et al.: “IntCal13 and Marine13 Radiocarbon Age Calibration Curves 0–50,000 Years cal BP.” *Radiocarbon*; (2013) 55 (4).

Romahn et al.: "Deglacial intermediate water reorganization: new evidence from the Indian Ocean." *Climate of the Past* 10.1 (2014): 293-303.

Rühlemann, et al.: "Warming of the tropical Atlantic Ocean and slowdown of thermohaline circulation during the last deglaciation." *Nature* 402.6761 (1999): 511-514.

Rühlemann et al.: "Intermediate depth warming in the tropical Atlantic related to weakened thermohaline circulation: Combining paleoclimate data and modelling results for the last deglaciation." *Paleoceanography* 19.1 (2004).

Schlitzer, R., 2015. Ocean Data View, http://odv.awi.de.

Schmidt et al.: "Impact of abrupt deglacial climate change on tropical Atlantic subsurface temperatures." *Proceedings of the National Academy of Sciences* 109.36 (2012): 14348-14352.

Spero, Lea: "The cause of carbon isotope minimum events on glacial terminations." *Science* 296.5567 (2002): 522-525.

Stenni et al., 2006. EPICA Dome C Stable Isotope Data to 44.8 Kyr BP. IGBP PAGES/World Data Center for Paleoclimatology Data Contribution Series # 2006-112. NOAA/NCDC *Paleoclimatology Program*, Boulder CO, USA.

Stenni et al: "Expression of the bipolar see-saw in Antarctic climate records during the last deglaciation." *Nature Geoscience* 4.1 (2011): 46-49.

Stichel et al. "The hafnium and neodymium isotope composition of seawater in the Atlantic sector of the Southern Ocean." *Earth and Planetary Science Letters* 317 (2012): 282-294.

Stocker: "The seesaw effect." *Science* 282.5386 (1998): 61-62.

Stocker, Johnsen: "A minimum thermodynamic model for the bipolar seesaw." *Paleoceanography* 18.4 (2003).

Taft: "Distribution of salinity and dissolved oxygen on surfaces of uniform potential specific volume in the South Atlantic, South Pacific, and Indian Oceans." *Journal of Marine Research* 21.2 (1963): 129-141.

Talley: "Antarctic intermediate water in the South Atlantic." The South Atlantic. Springer Berlin Heidelberg, 1996. 219-238.

Talley: "Closure of the global overturning circulation through the Indian, Pacific, and Southern Oceans: Schematics and transports." *Oceanography* 26.1 (2013): 80-97.

Tanaka et al.: "JNdi-1: a neodymium isotopic reference in consistency with LaJolla neodymium." *Chemical Geology* 168.3 (2000): 279-281.

Toggweiler, Lea: "Temperature differences between the hemispheres and ice age climate variability." *Paleoceanography* 25.2 (2010).

van de Flierdt et al.: "Temporal stability of the neodymium isotope signature of the Holocene to glacial North Atlantic." *Paleoceanography* 21.4 (2006).

van de Flierdt et al.: "Neodymium in the oceans: a global database, a regional comparison and implications for palaeoceanographic research." *Phil. Trans. R. Soc.* A 374.2081 (2016): 20150293.

Vellinga, Wood: "Global climatic impacts of a collapse of the Atlantic thermohaline circulation." *Climatic change* 54.3 (2002): 251-267.

Xie et al.: "Deglacial variability of Antarctic Intermediate Water penetration into the North Atlantic from authigenic neodymium isotope ratios." *Paleoceanography* 27.3 (2012).

Xie et al.: "Reconstruction of intermediate water circulation in the tropical North Atlantic during the past 22,000 years." *Geochimica et Cosmochimica Acta* 140 (2014): 455-467.

Zahn, Stüber: "Suborbital intermediate water variability inferred from paired benthic foraminiferal Cd/Ca and $\delta^{13}C$ in the tropical West Atlantic and linking with North Atlantic climates." *Earth and Planetary Science Letters* 200.1 (2002): 191-205.

Appendix: Supplementary material S2

Cd_w and $\delta^{13}C$ data are available online at the Data Publisher for Earth and Environmental Science, PANGEA: www.pangea.de.

Scientific Chapter 3: Antarctic Intermediate Water effectively cooled the Gulf of Mexico during rapid deglacial northern hemisphere cooling events

This scientific chapter consists of the manuscript entitled “Antarctic Intermediate Water effectively cooled the Gulf of Mexico during rapid deglacial northern hemisphere cooling events” as it is prepared for submission to *Paleoceanography*.

The authors are David-Willem Poggemann[a], Dirk Nürnberg[a], Ed C. Hathorne[a], Martin Frank[a], Stefan Reißig[a],

[a]GEOMAR Helmholtz Centre for Ocean Research Kiel, D-24148 Kiel, Germany

Antarctic Intermediate Water effectively cooled the Gulf of Mexico during rapid deglacial northern hemisphere cooling events

David-Willem Poggemann[a,*], Dirk Nürnberg[a] , Ed C. Hathorne[a], Martin Frank[a], Stefan Reißig[a],

[a]GEOMAR Helmholtz Centre for Ocean Research Kiel, D-24148 Kiel, Germany

*Corresponding author: GEOMAR Helmholtz Centre for Ocean Research Kiel, D-24148 Kiel, Germany. Tel.: 0049 431 6002309. E-mail address: dpoggemann@geomar.de.

3.1 Highlights

- Nutrient supply via Antarctic Intermediate Water into the Gulf of Mexico
- Antarctic Intermediate Water cooled the Gulf of Mexico during HS1 and the YD
- Distinct differences in the hydrographic evolution on intermediate water depth between the Gulf of Mexico and the Florida Straits

3.2 Abstract:

Due to its position related to the Atlantic Meridional Overturning Circulation, the Gulf of Mexico and the Caribbean are of essential interest for (paleo-) oceanographic studies. Warm and saline surface and subsurface waters from these basins form the Gulfstream, therefore contributing ocean heat, moist, and salt to the N-Atlantic. On intermediate to deep depth level, nutrient-depleted North Atlantic Deepwater is flowing southwards, entering the Caribbean and the Gulf of Mexico. It is capped by nutrient-rich Antarctic Intermediate Water flowing northward from the Southern Ocean into the Caribbean and further into the Gulf of Mexico.

In this study we present combined benthic foraminiferal based nutrient (Cd_w) and Intermediate Water Temperature reconstructions from the Campeche Bank in the Gulf of Mexico. We compared our results to similar proxy data from the S-Caribbean and from the Florida Straits to determine the evolution of intermediate water mass exchange between these basins during the last deglaciation. Our results indicate that Antarctic Intermediate Water effectively cooled the Gulf of Mexico (GoM) at intermediate water depth during rapid northern hemisphere cooling events. In contrast it was likely absent in the GoM during the Last Glacial Maximum – comparable to the modern situation. Additionally, the nutrient supply via Antarctic Intermediate Water into the Gulf was enhanced during these times. On the contrary, our data comparison points to a distinct different hydrographic evolution at intermediate water depth in the Florida Straits.

3.3 Introduction:

The global oceanic conveyor belt transports different water masses into the several ocean basins and therefore redistributes heat, salt, CO_2 and nutrients over the globe. Within this sensitive system, the Atlantic Meridional Overturning Circulation (AMOC) is a major impetus factor and therefore plays a key role in the global climate system. It is driven by northward flowing saline and warm waters from the tropical W-Atlantic to the northern N-Atlantic and the resulting formation of southward flowing North Atlantic Deep Water (NADW) (e.g. Talley 1996; 2013). This southward flow of NADW is compensated by northward flowing Antarctic Water masses, Antarctic Intermediate Water (AAIW) and Antarctic Bottom Water (AABW). During the Last Glacial Maximum (LGM) Glacial North Atlantic Intermediate Water (GNAIW), the glacial substitute of NADW, spread far into the southern equatorial Atlantic at shallower depth (Marchitto & Broecker, 2006). Abrupt climate cooling events during the last deglacial period, the Heinrich Stadial 1 (HS1, 18 – 14.6 ka; Barker et al., 2009) and the Younger Dryas (YD, 12.8 – 11.5 ka; Barker et al., 2009), caused major perturbations of the AMOC (e.g. McManus et al., 2004; Böhm et al., 2015). These rapid cooling events were characterised by major deceleration or even stalling of the deep water formation in the N-Atlantic. According to recent studies, this slowdown or even collapse in the northward transport of ocean surface heat led to a heat accumulation in the tropics and in the Southern Ocean (SO), therefore implementing a seesaw effect between the polar regions (e.g. Barker et al., 2009; Schmidt et al., 2012; Landais et al., 2015). New results from the S-Caribbean indicate a major heat uptake from the surface SO and the subsequent northward distribution at intermediate water depth by AAIW (Poggemann, 2017 – Ph.D.-Thesis, Scientific Chapter 2). In contrast to the atmospheric – surface oceanic processes, the impacts of northern hemisphere cooling events on the intermediate to deep ocean circulation reorganisation occurred later, at the ends of HS1 and the YD. Due to the absence of N-Atlantic deep water formation, extremely nutrient rich Circumpolar Deep Water (CPDW), which was cut off from the upper ocean before, welled up in the Southern Ocean (Anderson et al., 2009). Antarctic Intermediate Water, during the LGM mainly fed by shallow and nutrient depleted GNAIW, experienced extreme nutrient enrichments during the YD and the HS1, since it was fed by CPDW only (Poggemann et al., 2017).

The Caribbean and the Gulf of Mexico (GoM) act as key regions for the AMOC, since warm and saline surface waters from these basins are transported into the N-Atlantic via the Gulf Stream, where they cool and sink into the abyss to form NADW (e.g. Talley 1996; 2013). Therefore climatic changes in these basins would affect northward flowing water masses directly and hence, the deep water mass formation in the N-Atlantic (e.g. Wen et al., 2010; Schmidt et al., 2012). On the intermediate depth level, the Caribbean and the GoM are influenced by both, AAIW and NADW (Fig 3.1) (e.g. Weiss et al., 1985; Rivas et al., 2005; Osborne et al., 2014). Therefore, the Caribbean and the GoM are well suited to monitor changes in AMOC strength and intermediate water mass changes sensitively and the oceanic processes in these basins are of essential importance for (paleo-) oceanographic research. However, the oceanographic evolution in the Caribbean and the GoM at intermediate water depth and especially the water mass exchange between both basins on longer time scales is insufficiently investigated.

Here we present a benthic foraminiferal based nutrient and temperature reconstructions from intermediate water depth to analyse intermediate water mass exchange between these basins. We analysed a sediment core from the Campeche Bank in the western GoM and

used Mg/Ca based Intermediate Water Temperature (IWT) reconstructions and Cd/Ca as a proxy for nutrient saturation. Together with previously published data sets from the S-Caribbean (Poggemann et al., 2017; Poggemann, 2017 – Ph.D.-Thesis, Scientific Chapter 2) and from the Florida Straits (Came et al., 2008) we compared the intermediate water mass distribution across the Caribbean and the GoM. We find, that AAIW not only transported high amounts of nutrients into the GoM during HS1 and the YD, it further effectively cooled the GoM at intermediate water depth during these times of rapid northern hemisphere cooling events. On the contrary AAIW was absent from the GoM during the LGM and in the Holocene, comparable to the modern situation. The distinct divergence between the Cd_w record from the GoM and published data from Came et al., (2008) points to a different hydrographic setting in the Florida Straits. The results presented here may help to understand the evolution of the intermediate water masses in these Basins for the past 24 ka under changing climatic impacts.

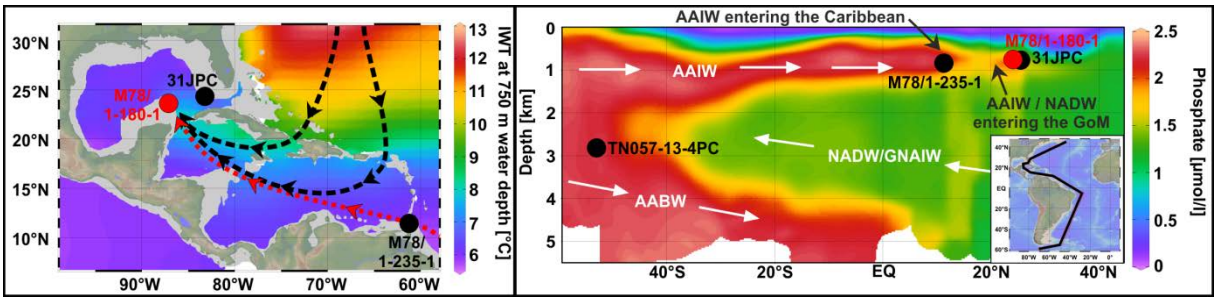

Figure 3.1: Overview of intermediate water masses entering the Caribbean and the Gulf of Mexico. **Left**: Modern annual average IWT distribution at 750 m water depth (colour shading) indicating major pathways of intermediate water mass into the Caribbean and the Gulf of Mexico (black arrows: NADW; red arrows: AAIW). Study site (red dot) and major reference sites (black dots) are marked. **Right**: S-N trending profile across the Atlantic (depicted in inlet) indicating major water masses differentiated by their modern phosphate concentrations (colour shading). Water masses, study site and reference sites are marked by arrows and dots, respectively. IWT = Intermediate Water Temperature; AAIW = Antarctic Intermediate Water; NADW = North Atlantic Deepwater; GNAIW = Glacial North Atlantic Intermediate Water; AABW = Antarctic Bottom Water. Figures were created using Ocean Data View (Schlitzer, 2015). Data for phosphate concentrations and modern annual average IWT were obtained from World Ocean Atlas (WOA2013; Boyer et al., 2013).

Caribbean and GoM oceanographic setting:

Today, the surface and subsurface hydrography in the Caribbean is mainly controlled by the Caribbean Current, which transports warm and saline waters into the GoM, where it extends into the Loop Current. After passing the Yucatan Channel between Cuba and Mexico, the Loop Current turns east and continues as the Gulf Stream. The most remarkable feature of the Loop Current is the associated eddy shedding (Oey, et al., 2005). These arising eddies can reach up to diameters of 200 – 350 km and a depth of 500 – 1000 m (Chang & Oey, 2010), therefore affecting surface, subsurface and intermediate water depth.

Due to the shallow sill depths of most of the passages surrounding the Caribbean, the only pathways for deep water exchange with the open Atlantic are the Windward Passage with a sill depth of ~ 1700 m and the Anegada-Jungfern Passage with a depth of ~ 1900 m (Johns et al., 2002). Therefore, the deep Caribbean below 1000 m is filled with upper NADW, which is characterized by high salinities and low nutrient content (Fig. 3.1) (e.g. Weiss et al., 1985; Rivas et al., 2005). The residence time of deep waters in the Caribbean is relatively high (~ 150 years) (Joyce et al., 1999). The deep Yucatan Channel (sill depth of ~ 2040 m) allows the NADW to flow from the Caribbean into the GoM, where the residence time is even higher (~ 250 years). Due to the shallow sill depth of the Florida Straits (~ 740 m), the deep water masses in the GoM only can leave this basin again via the Yucatan Channel into the Caribbean Basin, from where they exit into the Atlantic via the Windward and the Anegada-Jungfern Passages (Rivas et al., 2005; Sturges, 2005). NADW is capped by AAIW in the Caribbean, which is oxygen and salinity depleted and high in nutrients (Fig. 3.1) (Rivas et al., 2005). A small percentage of this water mass can be traced in the Yucatan Straits today, but vanishes in the Loop Current (Osborne et al., 2014). According to previous studies, AAIW admixes with overlying thermocline waters and flows northwards into the N-Atlantic, where it contributes to the formation of southward flowing deep waters (e.g. Talley, 2013; Ferrari et al., 2014). The subsurface above AAIW is mainly controlled by the Subtropical Gyre and dominated by Subtropical Underwater (e.g. Wüst, 1964; Johns et al., 2002).

3.4 Material & Methods

Sediment core M78/1-180-1 (termed 180 in the following), retrieved from the Campeche Bank in the GoM (23°49.63'N, 87°4.03'W; 695 m water depth), was sampled for every cm. All samples were freeze dried, wet sieved and fractionated using 63 µm, 125 µm, 250 µm, 315 µm, 355 µm and 400 µm sieves. The age model was created by linear interpolation between 5 AMS^{14}C datings, which were calibrated for the local reservoir age of 395 years (Marine13 data base) using Calib 7.1 and the MARINE13 reservoir age calibration curve (Reimer et al., 2013). In addition, the Cd_w record was visually referenced to the appropriate record of sediment core M78/1-235-1 (Poggemann et al., 2017) in the time span between 13.37 and 16.94 ka using AnalySeries 2.0.4.2. and two tie points were added to gain the best result (see supplement S3).

Mg/Ca and Cd/Ca measurements:

We used the epibenthic species *Cibicides lobatulus* for Mg/Ca and Cd/Ca measurements. This species is documented to trustfully record bottom water temperature and the published calibration was used to reconstruct the intermediate water temperatures (IWT) at our site (Quillmann et al., 2012). All samples were cleaned reductively and oxidatively following the established protocols of (Lea et al., 2003). All Cd/Ca samples where then prepared for measurement following the protocol published in Poggemann et al., 2017.

The Mg/Ca-ratios were measured for all samples on an Agilent 7500ce ICP-MS and an ICP-OES and all Cd/Ca samples were run using an Elemental Scientific “seaFAST” pre-concentration system coupled to the Agilent 7500ce ICP-MS. All samples were measured at GEOMAR Helmholtz Centre for Ocean Research Kiel.

All measurements were referenced to repeated standard measurements of the established standard ECRM 752 (Graeves et al., 2008), which was 3.75 ± 0.076 mmol/mol for Mg/Ca and 530 ± 21 nmol/mol for Cd/Ca respectively and therefore in good agreement with the published values. Samples with enough material were used to perform multiple measurements and the error was ± 6.6% for Mg/Ca and ± 1.8 % for Cd/Ca. All samples were checked for contamination diagenetic coatings and/or by clay minerals (see supplement S3).

IWT-gradient calculation:

To monitor the differences in the IWT evolution between the S-Caribbean and the GoM, we calculated the IWT-gradient between both basins. To gain the highest possible resolution, we calculated the IWT values for every cm of sediment core 180 by linear interpolation. We then subtracted the IWT signal of core 180 from the appropriate values of the IWT record of sediment core M78/1-235-1 from the S-Caribbean (Poggemann, 2017 – Ph.D.-Thesis, Scientific Chapter 2).

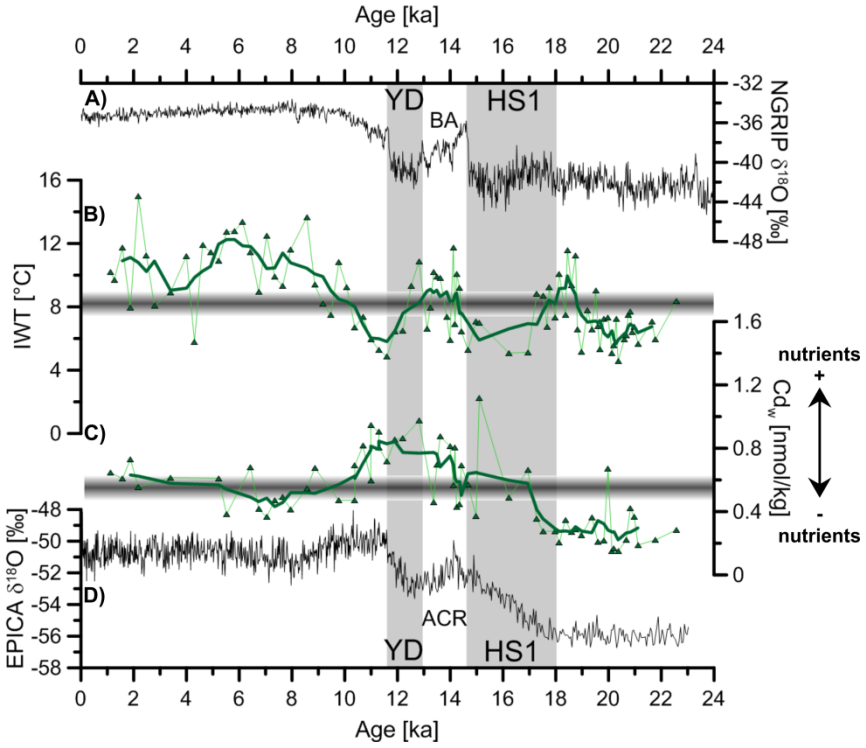

Figure 3.2: Benthic foraminiferal (*Cibicides lobatulus*) proxy records of sediment core M78/1-180-1 from the Campeche Bank. **A)** Greenland ice core oxygen isotope record as reference for the northern hemisphere climate signal (NGRIP Dating Group, 2006). **B)** Mg/Ca-based IWT record of core 180 reflecting distinct cooling episodes during HS1 and at the end of the YD / beginning of the Holocene and subsequent rapidly increasing temperatures in the early Holocene. Shaded bar indicates modern IWT at the Campeche Bank at ~ 700 m water depth (data obtained from WOA13, Boyer et al., 2013). **C)** Benthic foraminiferal Cd/Ca-based Cd_w reconstruction for core 180 pointing to major nutrient increases during HS1 and the YD at intermediate water depth. Shaded bar marks modern Cd_w at the Campeche Bank at ~ 700 m water depth bar (modern Cd_w estimated from modern seawater phosphate concentrations given in WOA13, Boyer et al., 2013). **D)** Antarctic ice core oxygen isotope record (EPICA Dome C) as

reference for the southern hemisphere climate signal (Stenni et al., 2006). IWT = Intermediate Water Temperature; HS1 = Heinrich Stadial 1; YD = Younger Dryas; BA = Bølling-Allerød; ACR = Antarctic Cold Reversal.

3.5 Results

The IWT at the Campeche Bank changed significantly during the past 24 ka several times (Fig. 3.2B). During the LGM, the data indicate IWT of about 6°C, before they rapidly increased for about 4°C shortly before the HS1 towards modern like values. During the HS1 and the YD, the IWT decreased to ~ 5°C again, while they rose to ~ 10°C during the Bølling-Allerød (BA) and even higher during the Holocene (~ 12°C). The youngest values indicate IWT of about 10°C which is slightly higher than the modern annual average at the Campeche Bank in 600 - 800 m water depth (~ 7.5 - 9°C) (Locarnini et al., 2013).

In the LGM, the Cd_w values of sediment core M78/1-180-1 are relatively low (~ 0.3 nmol/kg) (Fig. 3.2C). During the last deglaciation the Cd_w values increase during HS1 and YD towards high levels of around 0.9 nmol/kg, while the Holocene is characterized by moderate values (~ 0.5 – 0.7 nmol/kg). Due to the difficulties to find enough foraminiferal material for Cd/Ca measurements, the Cd_w data resolution during the HS1 is pretty low. Therefore, the single high Cd_w value (about 1.1 nmol/kg) at the end of HS1 may be the result of contamination and / or miss-measurement. But the comparison to previously published data from the S-Caribbean (Poggemann et al., 2017) indicates that this data point may be trustful as well (see discussion 3.6).

3.6 Discussion

Nutrient enriched Caribbean AAIW today is characterized by high Cd_w concentrations of ~ 0.6 nmol/kg (Mawji et al., 2015), while low Cd_w values of ~ 0.2 nmol/kg rather indicate the presence of nutrient depleted NADW, or of its glacial shallower flowing substitute GNAIW (e.g. Marchitto & Breocker, 2006).

The observed Cd_w pattern of sediment core 180 from the Campeche Bank roughly mirrors the general published Cd_w pattern of sediment core M78/1-235-1 (termed 235 in the following text) from the S-Caribbean (Fig. 3.3E) (Poggemann et al., 2017). The most prominent features of both cores are rapid nutrient increases during HS1 and the YD. The general pattern of core 180 is very similar to the Cd_w pattern of core 235. The absolute values in core 180 are slightly lower most of the analysed time, most likely due to enhanced admixture of nutrient depleted NADW / GNAIW, which majorly enters the Caribbean via the Anegada-Jungfern and the Windward Passages (Fig. 3.1) (Weiss et al., 1985; Johns et al., 2002; Rivas et al., 2005). The previously published Cd_w data from the S-Caribbean were interpreted in terms of a major source water change for AAIW in the southern Ocean (SO). While nutrient depleted GNAIW was most likely the major source water mass for AAIW during the LGM (Ferrari et al., 2014), it was supposedly fed by extremely nutrient enriched Circumpolar Deepwater (CPDW) exclusively during times of major AMOC perturbations (Poggemann et al., 2017). The reconstructed enhanced upwelling of nutrient rich CPDW in the SO at the end of HS1, during the YD and in the early Holocene (Fig. 3.3F) (Anderson et al., 2009) supposedly was the main trigger of AAIW nutrient enrichment at those times. AAIW therefore was characterised by very high Cd_w values at the end of HS1, during and shortly

after the YD as reconstructed for core 235. The high similarity between both Cd_w records, from the S-Caribbean and from the Campeche Bank in the GoM, therefore points to a direct nutrient transport at intermediate water depth into the GoM via AAIW at the end of HS1, during the YD and in the early Holocene. The single high Cd_w value during the HS1 in the 180 record might be a miss-measurement or an artefact, but the striking resemblance with the Cd_w record of core 235 points to a realistic value that only suffers from the low sample resolution at this time. Nonetheless, the generally lower Cd_w values at the Campeche Bank indicate a lower percentage of nutrient rich AAIW and a higher admixture of low-nutrient NADW / GNAIW. Most likely due to major reorganisations in the Atlantic overturning circulation after the YD, AAIW was fed by both, nutrient rich CPDW and nutrient depleted NADW (e.g. Talley, 1996, 2003; Ferrari et al., 2014). Both Cd_w records, from core 180 and from core 235, therefore indicate medium high values during the Holocene, close to modern values at the appropriate locations.

Contrary to the Cd_w records from the S-Caribbean and from the Campeche Bank, the published record of sediment core KNR166-231 JPC (termed 31JPC in the following text) from the Florida Straits indicates a distinguished different signal with generally lower values and minor increases during the BA and in the Holocene (Fig. 3.3C). This pattern was primarily interpreted to indicate enhanced northward expansion of AAIW during the BA and a decrease in the AAIW percentage during the YD (Came et al., 2008). During the late HS1, when the Cd_w records from the S-Caribbean and the Campeche Bank indicate the presence of nutrient enriched AAIW, the records from the Florida Straits indicate similar trends but with a lower amplitude. This indicates that only a minor amount of AAIW might have reached this location during this time. In contrast, the YD record from the Florida Straits indicates lower Cd_w values. This points to the absence of nutrient rich water masses. Previous studies suggested that the AMOC might have collapsed during the HS1, while it was weakened but still active during the YD (Fig. 3.3B) (e.g. McManus et al., 2004; Böhm et al., 2015). This might be the reason for the difference between the HS1 and the YD in the Cd_w record from the Florida Straits. While the AMOC collapsed during the HS1, the nutrient enriched AAIW penetrated not only into the GoM, but in a lower percentage and therefore highly diluted also into the Florida Straits. In contrast the AMOC was possibly not weak enough during the YD, to let AAIW reach the Florida Straits. Another possible explanation for the higher Cd_w values in the Florida Straits at the end of HS1 might be the contribution of nutrients via other water masses or processes. The relatively shallow sill depth of ~740 m in the Florida Straits prevents the deep water exchange with the open Atlantic and a strong contribution of nutrient depleted NADW / GNAIW therefore seems unlikely.

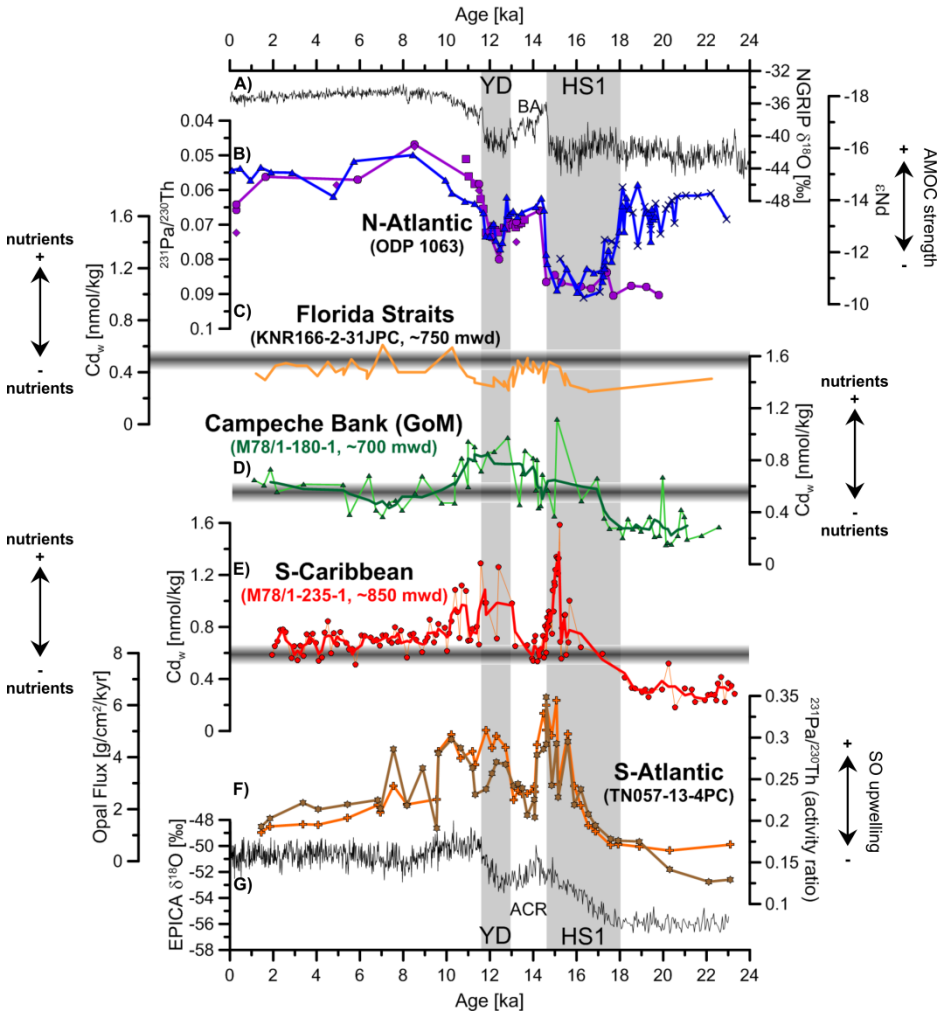

Figure 3.3: Cd_w data comparison for the S-Caribbean, the Gulf of Mexico and the Florida Straits related to N- and S-Atlantic overturning changes. **A)** Greenland ice core oxygen isotope record as reference for the northern hemisphere climate signal (NGRIP Dating Group, 2006). **B)** Changes in N-Atlantic deep water formation reconstructed from Pa/Th (blue) and εNd data (purple) of N-Atlantic ODP Site 1063 (Böhm et al., 2015 and references therein). **C)** Cd_w data from sediment core KNR166-2-31JPC (~ 750 m water depth) from the Florida Straits (Came et al., 2008). Shaded horizontal bar indicates modern Cd_w in the Florida Straits at ~ 750 m water depth (Cd_w estimated from phosphate concentration given in WOA13, Boyer et al., 2013). **D)** Cd_w record from the Campeche Bank (this study). Shaded horizontal bar indicates modern Cd_w at the Campeche Bank at ~ 700 m water depth (Cd_w estimated from phosphate concentration given in WOA13, Boyer et al., 2013). Bright green = original data; dark green line = 5-point running average. Note: The single high Cd_w value during the HS1 in the 180 record might be a miss-measurement or an artefact, but the striking resemblance with the Cd_w record of core 235 points to a realistic value that only suffers from the low sample resolution at this time. **E)** Published Cd_w data from sediment core M78/1-235-1 (~ 850 m water depth) from the S-Caribbean (Poggemann et al., 2017). Shaded bar indicates approximated modern Cd_w (Mawji et al., 2015). Orange line = original data; red line = 5-point running average. **F)** Southern Ocean upwelling reconstructions based on Pa/Th (brown) and opal flux (orange) from S-Atlantic core TN057-13 (Anderson et al., 2009). **G)** Antarctic ice core oxygen isotope record (EPICA Dome C) as reference for the southern hemisphere climate signal (Stenni et al., 2006). HS1 = Heinrich Stadial 1; YD = Younger Dryas; BA = Bølling-Allerød; ACR = Antarctic Cold Reversal.

In addition to the nutrient reconstructions from the Campeche Bank, we also reconstructed IWT based on benthic foraminiferal tests. In contrast to the S-Caribbean IWT record, the record from the GoM is characterized by strong temperature increases before HS1, during the BA and in the Holocene. Especially the very low temperatures of ~ 5°C during HS1 and the YD and the distinct IWT increase in the early Holocene for about 6°C are remarkable features of this record.

In a previous study, we were able to show, that the IWT in the S-Caribbean was supposedly a direct reaction to northern hemisphere AMOC perturbations in the HS1 and the YD with a detour via the Southern Ocean and a resulting response time of ~ 1 ka (Poggemann, 2017 – Ph.D.-Thesis, Scientific Chapter 2). This was in contrast to the Cd_w evolution, which was mainly triggered by upwelling changes of nutrient rich CPDW in the Southern Ocean (Poggemann et al., 2017). While the reconstructed Cd_w pattern of core 180 mostly mirrors the Cd_w pattern of core 235, the IWT seems to indicate an opposing or even anti-correlated trend at the first glance. When the IWT record of core 235 indicates warming trends during HS1 and in the YD and the early Holocene, the IWT record of core 180 in contrast indicates pronounced cooling periods (Fig. 3.4C). In the Holocene, when the S-Caribbean indicates slowly decreasing IWT, the Campeche Bank IWT record is characterised by a pronounced warming trend. In direct comparison, the IWT record of core 180 rather seems to mirror the reconstructed pattern for AMOC strength from the N-Atlantic (Fig. 3.4B) (Böhm et al., 2015 and references therein). To shed light on this discrepancy, we calculated the IWT-gradient between the S-Caribbean and the Campeche Bank in the GoM (Fig. 3.4D). The calculated record indicates that during HS1, in the YD and at the beginning of the Holocene both records were characterised by roughly the same IWT of about 6°C and the gradient therefore indicates only minor offsets. In contrast, the gradient indicates pronounced offsets during the LGM, the BA and especially in the Holocene, when the reconstructed record of core 180 indicates high IWT in comparison to low IWT in the S-Caribbean. We therefore argue that the AAIW might have cooled the IWT evolution in the GoM at times of major AAIW warming in the S-Caribbean. Even though the AAIW was characterised by strong warming by heat uptake from the surface Southern Ocean, it was still cold enough, to induce major cooling at intermediate water depth in the GoM.

During the LGM the surface GoM was cooler for about 6°C (e.g. Nürnberg et al., 2008; Ziegler et al., 2008; Nürnberg et al., 2015) and the Loop Current was characterized by higher transports through the Yucatan Channel and the Florida Straits, due to the southward shift of the Intertropical Convergence Zone, the lowered sea level and increased wind-driven transport in the N-Atlantic (e.g. Slowey & Curry, 1995; Mildner et al., 2013). In the same time, the shedding of eddies from the Loop Current most likely was diminished (Mildner et al., 2013). The number of eddies shedding from the Loop Current gradually increased during the last deglacial period. In the early Holocene, the through flow in the Yucatan Strait was slower, but the shedding of eddies fully established. Today eddies separate from the Loop current with a very unstable periodicity of 6 – 11 months (Sturges & Leben, 2000).

We speculate that this development might have triggered the major heat uptake of intermediate to deep water masses in the GoM in the Holocene. The long residence time of deep waters in the GoM in combination with vertical heat transport via eddies down to ~ 1000 m could therefore have led to the strong IWT increase we reconstructed in the early Holocene.

Nonetheless, this theory remains quite speculative and needs further investigation. Since the deep water from the GoM exit via the Yucatan Strait and later via Anegada Passage and Windward Passage, a heat uptake of these waters in the GoM would result in increased deep water temperature records in these passages synchronously. Intermediate to deep water temperature reconstructions from these passages would therefore help to further understand the Caribbean / GoM hydrographic evolution in the past and to estimate future changes.

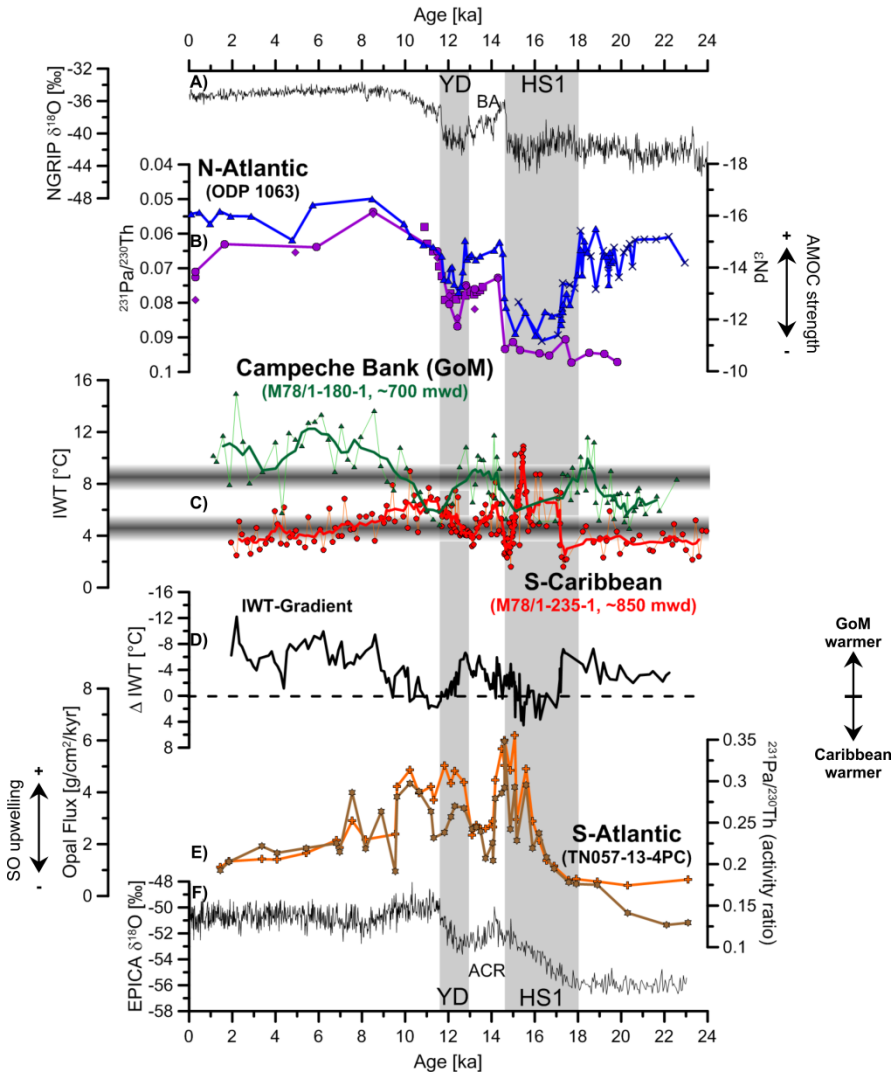

Figure 3.4: IWT comparison of the S-Caribbean and the Gulf of Mexico related to changes in N- and S-Atlantic overturning circulation. **A)** Greenland ice core oxygen isotope record as reference for the northern hemisphere climate signal (NGRIP Dating Group, 2006). **B)** AMOC strength reconstructed from Pa/Th (blue) and εNd data (purple) of N-Atlantic ODP Site 1063 (Böhm et al., 2015 and references therein). **C)** Green = IWT reconstruction for the Campeche Bank (core 180, this study). Red = IWT record from sediment core 235 from the S-Caribbean (Poggemann, 2017 – Ph.D.-Thesis, Scientific Chapter 2). Shaded horizontal bars indicate modern annual IWT at the study sites (WOA13, Boyer et al., 2013). **D)** Calculated IWT-gradient between the S-Caribbean (core 235) and the Gulf of Mexico (core 180) as deviation from zero (dashed line: S-Caribbean IWT equals Gulf of Mexico IWT). **E)** Southern Ocean upwelling change reconstructions based on Pa/Th (brown) and opal flux (orange) from S-Atlantic core TN057-13 (Anderson et al., 2009). **F)**

Antarctic ice core oxygen isotope record (EPICA Dome C) as reference for the southern hemisphere climate signal (Stenni et al., 2006). IWT = Intermediate Water Temperature; HS1 = Heinrich Stadial 1; YD = Younger Dryas; BA = Bølling-Allerød; ACR = Antarctic Cold Reversal.

3.7 Conclusion

Combined benthic foraminiferal based nutrient (Cd_w) and IWT reconstructions from the Campeche Bank in the Gulf of Mexico and the comparison to similar proxy records from the S-Caribbean and the Florida Straits imply that the evolution at intermediate water depths in the S-Caribbean and in the southern GoM were directly related via AAIW property changes. Abrupt deglacial nutrient enrichment of AAIW in response to Southern Ocean upwelling intensification first described from the S-Caribbean synchronously occurs in the Gulf of Mexico. Due to the different nutrient level we deduce that the Florida Straits are characterised by a different hydrographic regime, not affected by AAIW. Although AAIW was characterised by major heat uptake during HS1, in the YD and at the beginning of the Holocene in delayed response to AMOC perturbations and therefore, warmed the S-Caribbean at intermediate water depth, AAIW was still cool enough to cause major deglacial cooling in the overall warmer intermediate GoM. During the Holocene, when Loop Current strength and the related shedding of eddies fully established, the intermediate GoM warmed rapidly due to the downward mixing of surface and subsurface heat by eddies. This would further explain the similar but lower Cd_w values in the GoM compared to the S-Caribbean. Modern observation data show a northernmost extend of AAIW in the Yucatan Strait, but not further. Our data likewise indicate, that AAIW was absent during the Holocene and during the LGM.

3.8 Acknowledgements:

This research was funded by the Deutsche Forschungsgemeinschaft (DFG) via the “Cluster of Excellence – The Future Ocean” Kiel. Mg/Ca measurements were acquired at the GEOMAR Helmholtz Centre for Ocean Research Kiel.

3.9 References:

Anderson et al.: "Wind-driven upwelling in the Southern Ocean and the deglacial rise in atmospheric CO2." *Science* 323.5920 (2009): 1443-1448.

Barker et al.: "Interhemispheric Atlantic seesaw response during the last deglaciation." *Nature* 457.7233 (2009): 1097-1102.

Böhm et al.: "Strong and deep Atlantic meridional overturning circulation during the last glacial cycle." *Nature* 517.7532 (2015): 73-76.

Boyer et al: World Ocean Database 2013, NOAA Atlas NESDIS 72, S. Levitus, Ed., A. Mishonov, Technical Ed.; Silver Spring, MD, (2013) 209 pp.,

Came et al.: "Deglacial variability in the surface return flow of the Atlantic meridional overturning circulation." *Paleoceanography* 23.1 (2008).

Chang & Oey: "Why can wind delay the shedding of Loop Current eddies?" *Journal of Physical Oceanography* 40.11 (2010): 2481-2495.

Ferrari et al.: "Antarctic sea ice control on ocean circulation in present and glacial climates." *Proceedings of the National Academy of Sciences* 111.24 (2014): 8753-8758.

Greaves et al.: "Interlaboratory comparison study of calibration standards for foraminiferal Mg/Ca thermometry." *Geochemistry, Geophysics, Geosystems* 9.8 (2008).

Johns et al.: "On the Atlantic inflow to the Caribbean Sea." *Deep Sea Research Part I: Oceanographic Research Papers* 49.2 (2002): 211-243.

Joyce et al.: "Long-term hydrographic changes at 52 and 66 W in the North Atlantic Subtropical Gyre & Caribbean." *Deep Sea Research Part II: Topical Studies in Oceanography* 46.1 (1999): 245-278.

Landais et al.: "A review of the bipolar see–saw from synchronized and high resolution ice core water stable isotope records from Greenland and East Antarctica." *Quaternary Science Reviews* 114 (2015): 18-32.

Lea et al.: "Synchroneity of tropical and high-latitude Atlantic temperatures over the last glacial termination." *Science* 301.5638 (2003): 1361-1364.

Locarnini et al.: World Ocean Atlas 2013, Volume 1: Temperature. S. Levitus, Ed., A. Mishonov Technical Ed.; NOAA Atlas NESDIS 73 (2013), 40 pp.

Marchitto, Broecker: "Deep water mass geometry in the glacial Atlantic Ocean: A review of constraints from the paleonutrient proxy Cd/Ca." *Geochemistry, Geophysics, Geosystems* 7.12 (2006).

Mawji, et al.: The GEOTRACES Intermediate Data Product 2014, Mar. Chem. (2015), http://dx.doi.org/10.1016/j.marchem.2015.04.005.

McManus et al.: "Collapse and rapid resumption of Atlantic meridional circulation linked to deglacial climate changes." *Nature* 428.6985 (2004): 834-837.

Mildner et al.: "Revisiting the relationship between Loop Current rings and Florida Current transport variability." *Journal of Geophysical Research: Oceans* 118.12 (2013): 6648-6657.

NGRIP Dating Group, 2006. Greenland Ice Core Chronology 2005 (GICC05). IGBP PAGES/World Data Center for Paleoclimatology. Data Contribution Series # 2006-118. NOAA/NCDC Paleoclimatology Program, Boulder CO, USA.

Nürnberg et al.: "Interacting Loop Current variability and Mississippi River discharge over the past 400 kyr." *Earth and Planetary Science Letters* 272.1 (2008): 278-289.

Nürnberg et al.: "Loop current variability—Its relation to meridional overturning circulation and the impact of Mississippi discharge." Integrated Analysis of Interglacial Climate Dynamics (INTERDYNAMIC). Springer International Publishing, 2015. 55-62.

Oey et al.: "Loop Current, rings and related circulation in the Gulf of Mexico: A review of numerical models and future challenges." Circulation in the Gulf of Mexico: Observations and models (2005): 31-56.

Osborne et al.: "Neodymium isotopes and concentrations in Caribbean seawater: Tracing water mass mixing and continental input in a semi-enclosed ocean basin." *Earth and Planetary Science Letters* 406 (2014): 174-186.

Poggemann et al.: "Rapid deglacial injection of nutrients into the tropical Atlantic via Antarctic Intermediate Water." *Earth and Planetary Science Letters* 463 (2017): 118-126.

Poggemann: “Role of intermediate water variability in the Caribbean and Gulf of Mexico in deglacial climate change” Ph.D.-Thesis, Scientific Chapter 2; Christian-Albrechts-Universität Kiel.

Quillmann et al.: "Cooling and freshening at 8.2 ka on the NW Iceland Shelf recorded in paired δ 18 O and Mg/Ca measurements of the benthic foraminifer Cibicides lobatulus." *Quaternary Research* 78.3 (2012): 528-539.

Rivas et al.: "The ventilation of the deep Gulf of Mexico." *Journal of physical oceanography* 35.10 (2005): 1763-1781.

Reimer et al.: IntCal13 and Marine13 Radiocarbon Age Calibration Curves 0–50,000 Years cal BP. *Radiocarbon*; (2013) 55 (4).

Schmidt et al.: "Impact of abrupt deglacial climate change on tropical Atlantic subsurface temperatures." *Proceedings of the National Academy of Sciences* 109.36 (2012): 14348-14352.

Schlitzer, R., 2015. Ocean Data View, http://odv.awi.de.

Slowey, Curry: "Glacial-interglacial differences in circulation and carbon cycling within the upper western North Atlantic." *Paleoceanography* 10.4 (1995): 715-732.

Stenni et al., 2006. EPICA Dome C Stable Isotope Data to 44.8 Kyr BP. IGBP PAGES/World Data Center for Paleoclimatology Data Contribution Series # 2006-112. NOAA/NCDC Paleoclimatology Program, Boulder CO, USA.

Sturges: "Deep-Water Exchange Between the Atlantic, Caribbean, and Gulf of Mexico." *Circulation in the Gulf of Mexico: Observations and Models* (2005): 263-278.

Sturges, Leben: "Frequency of ring separations from the Loop Current in the Gulf of Mexico: A revised estimate." *Journal of Physical Oceanography* 30.7 (2000): 1814-1819.

Talley: "Antarctic intermediate water in the South Atlantic." The South Atlantic. Springer Berlin Heidelberg, 1996. 219-238.

Talley: "Closure of the global overturning circulation through the Indian, Pacific, and Southern Oceans: Schematics and transports." *Oceanography* 26.1 (2013): 80-97.

Weiss et al.: "Atmospheric chlorofluoromethanes in the deep equatorial Atlantic." *Nature* 314, (1985): 608-610.

Wen et al.: "Effect of Atlantic meridional overturning circulation changes on tropical Atlantic sea surface temperature variability: A 2½-layer reduced-gravity ocean model study." *Journal of Climate* 23.2 (2010): 312-332.

Wüst: “Stratification and Circulation in the Antillean–Caribbean Basins, Part 1, Spreading and Mixing of the Water Types with an Oceanographic Atlas”. *Columbia University Press* (1964), New York.

Ziegler et al.: "Persistent summer expansion of the Atlantic Warm Pool during glacial abrupt cold events." *Nature Geoscience* 1.9 (2008): 601-605.

Appendix: Supplementary material S3

General Synthesis & Outlook

The distinct changes in AMOC strength during the transition from the LGM into the Holocene, and particularly the rapid AMOC perturbations during northern hemisphere cooling events (HS1 and YD), triggered major atmospheric and oceanic re-organisations. This study targeted to reconstruct deglacial intermediate water alterations (dispersal, geochemical and thermal signatures) in the (sub-)tropical W-Atlantic in response to major overturning modifications in the N- and S-Atlantic. The results of this thesis suggest that the geochemical and thermal signatures of AAIW reacted to both, AMOC induced deep overturning fluctuations and thermal surface SO variations. Comparison of intermediate water property changes in the S-Caribbean with Cd_w and IWT reconstructions from the Gulf of Mexico further points to distinct variations in intermediate water mass exchange between these basins.

1) AMOC induced deep overturning fluctuations (Scientific Chapter 1):
   The reconstructed benthic foraminiferal Cd_w and $\delta^{13}C$ signals from intermediate water depth in the tropical W-Atlantic reflect a general change in the source water mass composition for AAIW due to AMOC-induced upwelling changes in the SO (Scientific Chapter 1). While AAIW was likely fed by nutrient depleted GNAIW exclusively in the upper Atlantic circulation cell during the LGM (e.g. Ferrari et al., 2014), it was characterised by a lowered nutrient saturation during full glacial conditions. Due to Antarctic sea ice northward extension and a deep stable stratification in the SO, nutrient-rich deep water masses (AABW and CPDW) were cut off from upwelling to the surface SO and therefore did not contribute to the formation of AAIW (e.g. Burke & Robinson, 2012; Ferrari et al, 2014). The missing contact to surface and subsurface waters in the SO likely caused a high nutrient accumulation in glacial AABW and CPDW. These water masses rather formed a deep overturning circulation cell in the glacial Atlantic, which was separated from the cell above. The low Cd_w values during the LGM, presented in Scientific Chapter 1, support the notion of nutrient-depleted glacial AAIW in the W-Atlantic.

   During HS1 and in the YD, the formation of deep water in the N-Atlantic weakened or even stalled (e.g. McManus et al., 2004; Böhm et al., 2015). In consequence the deep stratification in the SO collapsed and extremely nutrient enriched deep water welled up in the SO and fed into AAIW (e.g. Anderson et al., 2009; Burke & Robinson, 2012). The compelling synchronicity between the abrupt upwelling changes in the SO and the here presented rapidly increasing Cd_w values implies that AAIW was mainly fed by southern sourced waters at the end of HS1, during the YD in the early Holocene. AAIW therefore rapidly flushed the tropical W-Atlantic with nutrients for a limited time. This may have enhanced low latitude productivity and hence, might have dampened the atmospheric deglacial CO_2 rise. The $\delta^{13}C$ and Cd_w results, presented in Scientific Chapter 1, further point to low or no contribution of nutrient depleted northern sourced water masses to the AAIW formation during these times.

Subsequently to the AMOC perturbations during the YD and in the early Holocene, the Atlantic overturning cells finally reconnected to the modern overturning circulation pattern with nutrient depleted NADW and nutrient enriched CPDW as source water masses for AAIW. This gradual reconnection is indicated by the reconstructed gradually decreasing Cd_w values in the early Holocene and the subsequent stable medium high Cd_w level in the late Holocene.

In summary, the benthic foraminiferal based $\delta^{13}C$ and Cd_w reconstructions form the tropical W-Atlantic presented in Scientific Chapter 1 for the first time show, how the geochemical signature of AAIW varied due to major AMOC perturbations during the last deglaciation. The presented data indicate how the change in AAIW source water masses in response to the deglacial reconnection of the overturning cells in the Atlantic, effectively shaped the nutrient supply to the tropical W-Atlantic.

2) AMOC induced thermal surface SO variations (Scientific Chapter 2):
N-Atlantic deep water formation cessation triggered enhanced SO deep water upwelling during HS1, the YD, and in the early Holocene (e.g. Anderson et al., 2009). In response the nutrient budget and the $\delta^{13}C$ signature of AAIW in the tropical W-Atlantic changed significantly, delayed to AMOC perturbations by ~ 2.5 ka (Poggemann et al., 2017). In contrast, the benthic foraminiferal Mg/Ca based IWT reconstructions from the same site (Scientific Chapter 2) show that the thermal response of AAIW was likely faster compared to changes in SO deep water upwelling and delayed to AMOC perturbations by a maximum of ~ 1 ka. The presented IWT from the tropical W-Atlantic indicates a direct AMOC-induced heat transfer from the surface SO into the (sub-) tropical Atlantic via AAIW during HS1 and in the YD.

While both the glacial and the late Holocene IWT in the tropical W-Atlantic were comparable to modern IWT, the reconstructed AAIW temperature signal varied considerably during the last deglaciation (Scientific Chapter 2). Due to the AMOC cessation during HS1 and slowdown during the YD, the missing northward transport of surface ocean heat along with major atmospheric circulation changes likely caused considerable heat accumulation in the surface SO (e.g. Lamy et al., 2007; Toggweiler &Lea, 2010). As a result, a thermal see saw established between the hemispheres during the last deglaciation (e.g. Barker et al., 2009; Landais et al., 2015). The reconstructed IWT from the tropical W-Atlantic imply, that the ocean heat that accumulated in the surface SO was transferred to intermediate depths at regions of AAIW formation and was subsequently transported into the tropical W-Atlantic via AAIW. The data indicate that the northward transferal of the intermediate depth ocean heat anomaly was delayed by a maximum 1000 years with respect to the N-Atlantic AMOC perturbations, supporting the postulated SO heat storage response time to abrupt northern hemisphere cooling events of about 1000 years (Stocker & Johnson, 2003). The ocean heat export from the SO via AAIW might have dampened deglacial SO warming.

The planktonic foraminiferal based εNd reconstructions from the S-Caribbean (Scientific Chapter 2) further support the postulated deglacial change in AAIW source water masses and the notion, that AAIW permanently reached the S-Caribbean

throughout the past 24 ka (Poggemann et al., 2017). While glacial AAIW was fed by GNAIW exclusively, AAIW was mainly fed by CPDW during times of AMOC-perturbations and by a combination of both, NADW and CPDW in the Holocene (Ferrari et al., 2014; Poggemann et al., 2017). The εNd signature of AAIW therefore likely changed due to the change in AAIW source water masses. This gradual change is displayed by the presented gradually decreasing εNd in the S-Caribbean.

Scientific Chapter 2 presents the first high resolution Mg/Ca based IWT record from intermediate water mass. The data point to a direct heat transfer into the intermediate W-Atlantic via AAIW in response to deglacial AMOC cessations and the resulting heat accumulation in the surface SO. Based on the presented age model, the response time of AAIW temperature to abrupt northern hemisphere cooling events is delayed by a maximum of 1 ka, therefore supporting the postulated response time of Stocker & Johnson (2003). The εNd record further supports the notion that AAIW penetrated into the tropical W-Atlantic for the past 24 ka (Poggemann et al., 2017).

3) Intermediate water mass exchange between the S-Caribbean and the Gulf of Mexico: In addition to the geochemical and thermal changes of AAIW during times of weakened or even collapsed deep water formation in the N-Atlantic, the intermediate water mass exchange between the Caribbean and the Gulf of Mexico (GoM) clearly changed during the last deglaciation (Scientific Chapter 3). While AAIW was likely absent from the GoM during the LGM, it penetrated further north entering the GoM in response to AMOC perturbations during HS1 and in the YD. Comparison of reconstructed IWT and Cd_w from the Campeche Bank in the GoM with corresponding data sets from the S-Caribbean indicate that the rather warm AAIW effectively cooled the even warmer GoM at intermediate water depth synchronous to AMOC perturbations. The similarity between the GoM and the Caribbean Cd_w signals further points to enhanced nutrient supply to the GoM via AAIW at the end of HS1 and in the YD. Comparison of the GoM and Caribbean results with published Cd_w data sets from the Florida Straits (Came et al., 2008) indicates a distinctly different hydrographic setting in the Florida Straits. During the Holocene, when the shedding of Loop Current eddies in the GoM fully established in line with the rising sea level, the IWT at the Campeche Bank rose rapidly. The downward mixing of sea surface and subsurface temperature anomalies by GoM eddies might have triggered the Holocene rise in IWT.

Scientific Chapter 3 compares IWT and Cd_w reconstructions for the Campeche Bank in the Gulf of Mexico with corresponding published data sets from the S-Caribbean and the Florida Straits. The results show, that AAIW penetrated further north and effectively cooled the Gulf of Mexico at intermediate depth during northern hemisphere cooling events. In contrast it did not reach the Florida Straits.

By providing a suite of new and sophisticated proxy records at high temporal resolution for the last 24 ka from sediment core locations directly bathed in AAIW, this study provides valuable insight into processes shaping AAIW in the (sub-) tropical W-Atlantic during times of extreme climatic change. Although the results of this thesis need further appraisal, they nonetheless contribute to our understanding of current global warming processes and can be used to improve ocean and climate models.

Outlook:

The variability of AAIW formation in the SO during the last deglaciation is still insufficiently understood, mainly due to the lack of suitable core locations at intermediate depths. Likewise the intermediate water mass variability in the deep passages surrounding the GoM and the Caribbean remains unclear. Due to the morphology in the (sub-)tropical W-Atlantic the number of suitable locations in order to retrieve suitable sediment cores from intermediate water depth is sparse. Nonetheless, further reconstructions of water mass distribution would help our understanding of the hydrographic changes in these basins under a changing environment. Knowledge of the temporal dynamics of AAIW in the Atlantic in relation to intermediate water variability in the Pacific and Indian oceans is also lacking. Multi-proxy reconstructions of intermediate water variability from offshore western S-America would further constrain the effect of rapid AMOC perturbation on Pacific oceanography. Previous studies point to an Atlantic-Pacific ventilation see saw across the last deglacial period (Freeman et al., 2015). However, this theory needs further appraisal. Hence, Cd_w and IWT reconstructions from the tropical E-Pacific in comparison with the here presented results would improve our understanding of the Atlantic-Pacific intermediate water mass variability.

Additional references

Anderson et al.: "Wind-driven upwelling in the Southern Ocean and the deglacial rise in atmospheric CO2." *Science* 323.5920 (2009): 1443-1448.

Asmerom et al.: "Variable winter moisture in the southwestern United States linked to rapid glacial climate shifts." *Nature Geoscience* 3.2 (2010): 114-117.

Bard et al.: "Hydrological impact of Heinrich events in the subtropical northeast Atlantic." *Science* 289.5483 (2000): 1321-1324.

Barker et al.: "Interhemispheric Atlantic seesaw response during the last deglaciation." *Nature* 457.7233 (2009): 1097-1102.

Barker et al.: "Icebergs not the trigger for North Atlantic cold events." *Nature* 520.7547 (2015): 333-336.

Boebel et al.: "The intermediate depth circulation of the western South Atlantic." *Geophysical Research Letters* 26.21 (1999): 3329-3332.

Böhm et al.: "Strong and deep Atlantic meridional overturning circulation during the last glacial cycle." *Nature* 517.7532 (2015): 73-76.

Bostock et al.: "Characterising the intermediate depth waters of the Pacific Ocean using δ13C and other geochemical tracers." *Deep Sea Research Part I: Oceanographic Research Papers* 57.7 (2010): 847-859.

Boyer et al: World Ocean Database 2013, NOAA Atlas NESDIS 72, S. Levitus, Ed., A. Mishonov, Technical Ed.; Silver Spring, MD, (2013) 209 pp.,

Boyle, Keigwin: "Comparison of Atlantic and Pacific paleochemical records for the last 215,000 years: Changes in deep ocean circulation and chemical inventories." *Earth and Planetary Science Letters* 76.1-2 (1985): 135-150.

Buckley, Marshall: "Observations, inferences, and mechanisms of the Atlantic Meridional Overturning Circulation: A review." *Reviews of Geophysics* (2016).

Burke, Robinson: “The Southern Ocean’s role in carbon exchange during the last deglaciation.” *Science* (2012); 335.6068: 557-561.

Bradtmiller et al.: "Changes in biological productivity along the northwest African margin over the past 20,000 years." *Paleoceanography* 31.1 (2016): 185-202.

Bryan, Marchitto: "Mg/Ca–temperature proxy in benthic foraminifera: New calibrations from the Florida Straits and a hypothesis regarding Mg/Li." *Paleoceanography* 23.2 (2008).

Bryan, Marchitto: “Testing the utility of paleonutrient proxies Cd/Ca and Zn/Ca in benthic foraminifera from thermocline waters.” *Geochemistry, Geophysics, Geosystems* (2010) 11.1.

Calvo et al.: "Antarctic deglacial pattern in a 30 kyr record of sea surface temperature offshore South Australia." *Geophysical Research Letters* 34.13 (2007).

Came et al.: “Atlantic Ocean circulation during the Younger Dryas: Insights from a new Cd/Ca record from the western subtropical South Atlantic.” *Paleoceanography* (2003) 18.4.

Came et al.: "Deglacial variability in the surface return flow of the Atlantic meridional overturning circulation." *Paleoceanography* 23.1 (2008)

Chang, Oey: "Why can wind delay the shedding of Loop Current eddies?" *Journal of Physical Oceanography* 40.11 (2010): 2481-2495.

Chappell, Shackleton: "Oxygen isotopes and sea level." *Nature* 324, 137 - 140 (1986); doi:10.1038/324137a0.

Chiang, Bitz: "Influence of high latitude ice cover on the marine Intertropical Convergence Zone." *Climate Dynamics* 25.5 (2005): 477-496.

Curry, Oppo: “Glacial water mass geometry and the distribution of $\delta^{13}C$ of ΣCO_2 in the western Atlantic Ocean.” *Paleoceanography*, 20, (2005); PA1017, doi:10.1029/2004PA001021.

DeHaan, Sturges: "Deep cyclonic circulation in the Gulf of Mexico." *Journal of Physical Oceanography* 35.10 (2005): 1801-1812.

Denton et al.: "Interhemispheric linkage of paleoclimate during the last glaciation." Geografiska Annaler: Series A, *Physical Geography* 81.2 (1999): 107-153.

Denton et al.: "The role of seasonality in abrupt climate change." *Quaternary Science Reviews* 24.10 (2005): 1159-1182.

Denton et al.: “The Last Glacial Termination.” *Science* (2010) 328 (5986), 1652-1656. DOI:10.1126/science.1184119

Elderfield et al.: "A record of bottom water temperature and seawater $\delta^{18}O$ for the Southern Ocean over the past 440kyr based on Mg/Ca of benthic foraminiferal Uvigerina spp." *Quaternary Science Reviews* 29.1 (2010): 160-169.

Ferrari et al.: "Antarctic sea ice control on ocean circulation in present and glacial climates." *Proceedings of the National Academy of Sciences* 111.24 (2014): 8753-8758.

Flower et al.: "Phasing of deglacial warming and Laurentide Ice Sheet meltwater in the Gulf of Mexico." *Geology* 32.7 (2004): 597-600.

Frank: "Radiogenic isotopes: tracers of past ocean circulation and erosional input." *Reviews of geophysics*. 40.1 (2002)

Freeman et al.: "An Atlantic–Pacific ventilation seesaw across the last deglaciation." *Earth and Planetary Science Letters* 424 (2015): 237-244.

Griffiths et al.: "Increasing Australian–Indonesian monsoon rainfall linked to early Holocene sea-level rise." *Nature Geoscience* 2.9 (2009): 636-639.

Hanawa, Talley: "Mode waters." *International Geophysics Series* 77 (2001): 373-386.

Hartin et al.: "Formation rates of Subantarctic mode water and Antarctic intermediate water within the South Pacific." *Deep Sea Research Part I: Oceanographic Research Papers* 58.5 (2011): 524-534.

Hellweger, Gordon: "Tracing Amazon river water into the Caribbean Sea." *Journal of Marine Research* 60.4 (2002): 537-549.

Hendry et al.: Abrupt changes in high-latitude nutrient supply to the Atlantic during the last glacial cycle. *Geology* (2012) 40.2: 123-126.

Howe et al.: "Antarctic intermediate water circulation in the South Atlantic over the past 25,000 years." *Paleoceanography* 31.10 (2016): 1302-1314.

Huang, Oppo, Curry: "Decreased influence of Antarctic intermediate water in the tropical Atlantic during North Atlantic cold events." *Earth and Planetary Science Letters* 389 (2014): 200-208.

Jaccard et al.: “Covariation of deep Southern Ocean oxygenation and atmospheric CO2 through the last ice age.” *Nature* (2016), 530, 207-210.

Johns et al.: "On the Atlantic inflow to the Caribbean Sea." *Deep Sea Research Part I: Oceanographic Research Papers* 49.2 (2002): 211-243.

Joyce et al.: "Long-term hydrographic changes at 52 and 66 W in the North Atlantic Subtropical Gyre & Caribbean." *Deep Sea Research Part II: Topical Studies in Oceanography* 46.1 (1999): 245-278.

Kanzow et al.: "Seasonal variability of the Atlantic meridional overturning circulation at 26.5 N." *Journal of Climate* 23.21 (2010): 5678-5698.

Kroopnick: "The distribution of 13C of ΣCO2 in the world oceans." *Deep Sea Research Part A. Oceanographic Research Papers* 32.1 (1985): 57-84.

Kuhlbrodt et al.: "On the driving processes of the Atlantic meridional overturning circulation." *Reviews of Geophysics* 45.2 (2007).

Kujau et al.: "Mississippi River discharge over the last~ 560,000 years—Indications from X-ray fluorescence core-scanning." *Palaeogeography, Palaeoclimatology, Palaeoecology* 298.3 (2010): 311-318.

Lamy et al.: "Modulation of the bipolar seesaw in the Southeast Pacific during Termination 1." *Earth and Planetary Science Letters* 259.3 (2007): 400-413.

Landais et al.: "A review of the bipolar see–saw from synchronized and high resolution ice core water stable isotope records from Greenland and East Antarctica." *Quaternary Science Reviews* 114 (2015): 18-32.

Le Quéré et al.: "Global carbon budget 2016." Earth System Science Data 8.2 (2016): 605.

Liu et al.: "Transient simulation of last deglaciation with a new mechanism for Bølling-Allerød warming." *Science* 325.5938 (2009): 310-314.

Liu et al.: "Overlooked possibility of a collapsed Atlantic Meridional Overturning Circulation in warming climate." *Science Advances* 3.1 (2017): e1601666.

Lynch-Stieglitz et al.: "Atlantic meridional overturning circulation during the Last Glacial Maximum." *Science* 316.5821 (2007): 66-69.

Marchitto, Broecker: Deep water mass geometry in the glacial Atlantic Ocean: A review of constraints from the paleonutrient proxy Cd/Ca. *Geochemistry, Geophysics, Geosystems* (2006); 7(12).

Marcott et al.: Centennial-scale changes in the global carbon cycle during the last deglaciation. *Nature* (2014) 514.7524, 616-619.

Mawji, et al.: The GEOTRACES Intermediate Data Product 2014, Mar. Chem. (2015), http://dx.doi.org/10.1016/j.marchem.2015.04.005.

McManus et al.: "Collapse and rapid resumption of Atlantic meridional circulation linked to deglacial climate changes." *Nature* 428.6985 (2004): 834-837.

Merino: "Upwelling on the Yucatan Shelf: hydrographic evidence." *Journal of Marine Systems* 13.1-4 (1997): 101-121.

Metcalf: “Caribbean-Atlantic water exchange through the Anegada-Jungfern passage.” *Journal of Geophysical Research* (1976), 81(36), 6401–6409, doi:10.1029/JC081i036p06401.

Mildner et al.: "Revisiting the relationship between Loop Current rings and Florida Current transport variability." *Journal of Geophysical Research: Oceans* 118.12 (2013): 6648-6657.

Molina-Kescher et al.: "South Pacific dissolved Nd isotope compositions and rare earth element distributions: water mass mixing versus biogeochemical cycling." *Geochimica et Cosmochimica Acta* 127 (2014): 171-189.

Monnin et al.: "Atmospheric CO2 concentrations over the last glacial termination." *Science* 291.5501 (2001): 112-114.

Muller et al.: "Possible evidence for wet Heinrich phases in tropical NE Australia: the Lynch's Crater deposit." *Quaternary Science Reviews* 27.5 (2008): 468-475.

Müller-Karger et al.: "Pigment distribution in the Caribbean Sea: Observations from space." *Progress in Oceanography* 23.1 (1989): 23-64.

NGRIP Dating Group: Greenland Ice Core Chronology 2005 (GICC05). IGBP PAGES/World Data Center for Paleoclimatology (2006). Data Contribution Series # 2006-118. NOAA/NCDC Paleoclimatology Program, Boulder CO, USA.

Nürnberg et al.: "Assessing the reliability of magnesium in foraminiferal calcite as a proxy for water mass temperatures." *Geochimica et Cosmochimica Acta* 60.5 (1996): 803-814.

Nürnberg et al.: "Paleo-sea surface temperature calculations in the equatorial east Atlantic from Mg/Ca ratios in planktic foraminifera: A comparison to sea surface temperature estimates from U37K′, oxygen isotopes, and foraminiferal transfer function." *Paleoceanography* 15.1 (2000): 124-134.

Nürnberg et al.: "Interacting Loop Current variability and Mississippi River discharge over the past 400 kyr." *Earth and Planetary Science Letters* 272.1 (2008): 278-289.

Nürnberg et al.: "Loop current variability—Its relation to meridional overturning circulation and the impact of Mississippi discharge." Integrated Analysis of Interglacial Climate Dynamics (INTERDYNAMIC). Springer International Publishing, 2015. 55-62.

Oppo et al.: "What do benthic δ13C and δ18O data tell us about Atlantic circulation during Heinrich Stadial 1?." *Paleoceanography* 30.4 (2015): 353-368.

Osborne et al.: "Neodymium isotopes and concentrations in Caribbean seawater: Tracing water mass mixing and continental input in a semi-enclosed ocean basin." *Earth and Planetary Science Letters* 406 (2014): 174-186.

Pahnke et al.: "Abrupt changes in Antarctic Intermediate Water circulation over the past 25,000 years." *Nature Geoscience* 1.12 (2008): 870-874.

Pearman et al.: "Evidence of changing concentrations of atmospheric CO_2, N_2O and CH_4 from air bubbles in Antarctic ice." *Nature* 320, 248 - 250 (1986); doi:10.1038/320248a0.

Piepgras, Wasserburg: "Neodymium isotopic variations in seawater." *Earth and Planetary Science Letters* 50.1 (1980): 128-138.

Piepgras, Wasserburg: "Rare earth element transport in the western North Atlantic inferred from Nd isotopic observations." *Geochimica et Cosmochimica Acta* 51.5 (1987): 1257-1271.

Poggemann et al.: "Rapid deglacial injection of nutrients into the tropical Atlantic via Antarctic Intermediate Water." *Earth and Planetary Science Letters* 463 (2017): 118-126.

Rahmstorf: "Ocean circulation and climate during the past 120,000 years." *Nature* 419.6903 (2002): 207-214.

Regenberg et al.: "Calibrating Mg/Ca ratios of multiple planktonic foraminiferal species with δ 18 O-calcification temperatures: Paleothermometry for the upper water column." *Earth and Planetary Science Letters* 278.3 (2009): 324-336.

Rivas et al.: "The ventilation of the deep Gulf of Mexico." *Journal of physical oceanography* 35.10 (2005): 1763-1781.

Roberts et al.: "Synchronous deglacial overturning and water mass source changes." *Science* 327.5961 (2010): 75-78.

Sabine et al.: "The oceanic sink for anthropogenic CO2." *Science* 305.5682 (2004): 367-371.

Saenko et al.: "On the link between the two modes of the ocean thermohaline circulation and the formation of global-scale water masses." *Journal of Climate* 16.17 (2003): 2797-2801.

Schlitzer, R., 2015. Ocean Data View, http://odv.awi.de.

Schmidt et al.: "Links between salinity variation in the Caribbean and North Atlantic thermohaline circulation." *Nature* 428.6979 (2004): 160-163.

Sikes et al.: "Southern Ocean seasonal temperature and Subtropical Front movement on the South Tasman Rise in the late Quaternary." *Paleoceanography* 24.2 (2009).

Shackleton: "Attainment of isotopic equilibrium between ocean water and the benthonic foraminifera genus Uvigerina: isotopic changes in the ocean during the last glacial." (1974).

Sloyan et al.: "Antarctic Intermediate Water and Subantarctic Mode Water formation in the southeast Pacific: The role of turbulent mixing." *Journal of physical oceanography* 40.7 (2010): 1558-1574.

Spero et al.: "Timing and mechanism for intratest Mg/Ca variability in a living planktic foraminifer." *Earth and Planetary Science Letters* 409 (2015): 32-42.

Stenni et al.: EPICA Dome C Stable Isotope Data to 44.8 Kyr BP. IGBP PAGES/World Data Center for Paleoclimatology Data Contribution Series # 2006-112. NOAA/NCDC Paleoclimatology Program (2006), Boulder CO, USA.

Stenni et al: "Expression of the bipolar see-saw in Antarctic climate records during the last deglaciation." *Nature Geoscience* 4.1 (2011): 46-49.

Stichel et al. "The hafnium and neodymium isotope composition of seawater in the Atlantic sector of the Southern Ocean." *Earth and Planetary Science Letters* 317 (2012): 282-294.

Stocker, Johnsen: "A minimum thermodynamic model for the bipolar seesaw." *Paleoceanography* 18.4 (2003).

Stocker et al.: "Climate change 2013: the physical science basis. *Intergovernmental panel on climate change, working group I contribution to the IPCC fifth assessment report* (AR5)." New York (2013).

Strelin, Denton: Proceedings of the XVI Congreso Geologico Argentino, Asociación Geológica Argentina, La Plata, Argentina, 20 to 23 September 2005, article 269.

Stuiver, Grootes: "GISP2 oxygen isotope ratios." *Quaternary Research* 53.3 (2000): 277-284.

Sturges: “Deep-water exchange between the Atlantic, Caribbean, and Gulf of Mexico.” In: Circulation in the Gulf of Mexico: Observations and Models. American Geophysical Union (2005), Washington, DC, pp.263–278.

Taft: "Distribution of salinity and dissolved oxygen on surfaces of uniform potential specific volume in the South Atlantic, South Pacific, and Indian Oceans." *Journal of Marine Research* 21.2 (1963): 129-141.

Talley: "Antarctic intermediate water in the South Atlantic." The South Atlantic. Springer Berlin Heidelberg, (1996). 219-238.

Talley: "Shallow, intermediate, and deep overturning components of the global heat budget." *Journal of Physical oceanography* 33.3 (2003): 530-560.

Talley: "Closure of the global overturning circulation through the Indian, Pacific, and Southern Oceans: Schematics and transports." *Oceanography* 26.1 (2013): 80-97.

Toggweiler, Lea: “Temperature differences between the hemispheres and ice age climate variability.” *Paleoceanography*, 25 (2010), PA2212, doi:10.1029/2009PA001758.

Toucanne et al.: "Timing of massive ‘Fleuve Manche’discharges over the last 350kyr: insights into the European ice-sheet oscillations and the European drainage network from MIS 10 to 2." *Quaternary Science Reviews* 28.13 (2009): 1238-1256.

Wang et al.: "A high-resolution absolute-dated late Pleistocene monsoon record from Hulu Cave, China." *Science* 294.5550 (2001): 2345-2348.

Wang et al.: "Wet periods in northeastern Brazil over the past 210 kyr linked to distant climate anomalies." *Nature* 432.7018 (2004): 740-743.

Wawrik, Paul: "Phytoplankton community structure and productivity along the axis of the Mississippi River plume in oligotrophic Gulf of Mexico waters." *Aquatic Microbial Ecology* 35.2 (2004): 185-196.

Weaver et al.: "Stability of the Atlantic meridional overturning circulation: A model intercomparison." *Geophysical Research Letters* 39.20 (2012).

Wüst: “Stratification and Circulation in the Antillean–Caribbean Basins, Part 1, Spreading and Mixing of the Water Types with an Oceanographic Atlas”. Columbia University Press (1964), New York.

Xie et al.: "Deglacial variability of Antarctic Intermediate Water penetration into the North Atlantic from authigenic neodymium isotope ratios." *Paleoceanography* 27.3 (2012).

Xie et al.: "Reconstruction of intermediate water circulation in the tropical North Atlantic during the past 22,000 years." *Geochimica et Cosmochimica Acta* 140 (2014): 455-467.

Yu et al.: "Similar rates of modern and last-glacial ocean thermohaline circulation inferred from radiochemical data." *Nature* 379.6567 (1996): 689.

Yuan et al.: "Timing, duration, and transitions of the last interglacial Asian monsoon." *Science* 304.5670 (2004): 575-578.

Zickfeld et al.: "Centuries of thermal sea-level rise due to anthropogenic emissions of short-lived greenhouse gases." *Proceedings of the National Academy of Sciences* (2017): 201612066.

Acknowledgements

First of all I would like to thank Dirk, Ed and Martin for their guidance throughout this long journey. Whenever I got stuck during this time, you supported me with your advice, a lot of helpful discussions and of course with your scientific experience. Ed, you helped me to run through all the geochemical analyses and the work in the lab. I bet I asked a lot of stupid questions in the beginning (and maybe I still do it). Dirk, your comments and ideas on my manuscripts were really helpful and improved my scientific writing and interpretations. Without you pushing me on and on to compare my data to more of the other available published results, I may have not come to the same conclusions. Martin, many thanks to you for always having an look from above on my project. It was always very supportive to have your general evaluation comments.

Stefan and Jacek, I would like to thank both of you for having such a great time in the office, for being great colleagues and fantastic friends. It was always fun to chat with you about our work, to talk a lot of bullshit all the day and to enjoy a lot of tea and coffee together. Jacek, we had a great time on our Manihiki-cruise and together with Anne, we had a few very nice days in New Zealand. Your recommendations in the beginning of my work helped a lot to get everything started successfully. Stefan, I will really miss all the bullshitting and mocking with you. It was always fun to share an office with you, to have you as an associate in my project and I really hope we will stay in contact.

Anne, I would like to thank you for your comments on my Germanised English, for your advice and guidance in the lab and for having a good friend in you.

Nadine, Marlies, Nicklas, Imke, Max, without your support, I would not have been able to accomplish such a big data set. Having you as student helpers and technicians, I was able to base my manuscripts on a big load of high-resolution proxy analyses. Nadine, you have always been the helpful Mum of our working group and without you, we all would get stuck immediately.

Many thanks of course to the close paleo-oceanography people in corridor 8C + D. It was much fun to sit in the science lounge with you, drink a lot of tea and coffee, go for lunch or just enjoying some ice cream at the water. It was always a great atmosphere with you.

The most important “thank you” is for you, Katrin, Pablo and Floris, my family! You are the greatest gift I received. You gave me strength and motivation to go on and without your support and love I would not have accomplished this work. I love you!

Curriculum Vitae

David-Willem Poggemann
Jahnstraße 14
D-24116 Kiel, Germany

Phone: +49 (0)431 600 2309
E-Mail: dpoggemann@geomar.de

Place and date of birth	1983-12-22 Siegen, Germany
Nationality	German

Academia

2006 – 2012	Christian-Albrechts-University of Kiel „Geology/Paleontology“, Certificate: Diploma
2012 - 2017	Ph.D.-student at GEOMAR Helmholtz Centre for Ocean Research Kiel, Germany

Publications and scientific contributions

Poggemann, D.-W.; Hathorne, E. C.; Nürnberg, D.; Frank, M.; Bruhn, I.; Reißig, S.; Bahr, A.: „Rapid deglacial injection of nutrients into the tropical Atlantic via Antarctic Intermediate Water.” *Earth and Planetary Science Letters*, *463*, 118-126 (2017).

Reißig, S.; Nürnberg, D.; Bahr, A.; Hoffmann, J.; Poggemann, D.-W.: “Subtropical W-Atlantic subsurface warming during deglacial times of reduced Atlantic Meridional Overturning Circulation” [Poster] In: 12th International Conference on Paleoceanography (ICP12), 28.08.-02.09.2016, Utrecht, The Netherlands. (2016)

Reißig, S.; Nürnberg, D.; Poggemann, D.-W.; Hoffmann, J.; Brunke, L.; Clarke, T.: “Millenial-scale Surface and Subsurface Dynamics in the Caribbean Sea from Last Glacial Maximum to Holocene” [Poster] In: AGU Fall Meeting 2016, 12.-16.12.2016, San Francisco, USA. (2016)

Poggemann, D.-W.; Nürnberg, D.; Hathorne, E. C.; Bruhn, I.; Reißig, S.; Frank, M.: “Variability in Intermediate Water Mass Geometry in the Tropical W-Atlantic from LGM to Holocene” [Poster] In: AGU Fall Meeting 2014, 15.-19.12.2014, San Francisco, USA. (2014)

Tiedemann, R.; Lamy, F.; Molina-Kescher, M.; Tapia Arroyo, R.; Poggemann, D.-W.; Nürnberg, D.; SO213 Cruise participants: “FS Sonne Fahrtbericht / Cruise Report SO213 - SOPATRA: South Pacific Paleoceanographic Transects Geodynamic and Climatic Variability in Space and Time, Leg 1: Valparaiso/Chile - Valparaiso/Chile, 27.12.2010 - 12.01.2011 and Leg 2: Valparaiso/Chile - Wellington/New Zealand, 12.01.2011 - 07.03.2011”, 111 pp. (2014), DOI 10.2312/cr_so213.

Poggemann, D.-W.; Hathorne, E.; Nürnberg, D.; Bruhn, I.; Frank, M.; Hoffmann, J.: “Role of intermediate water variability in the Caribbean and Gulf of Mexico in deglacial climate change” [Poster] In: 11th International Conference on Paleoceanography (ICP11) 2013, 01.-06.09.2013, Sitges - Barcelona, Spain. (2013)

Poggemann, D.-W.; Nürnberg, D.; Ronge, T.; Tiedemann, R.: „Plio/Pleistozäne Temperatur- und Salinitätsänderungen zwischen Oberflächenozean und Zwischenwasser im SE-Pazifik – Hinweise zum Wechsel von „permanenten El Niño“ zu modernen „La Niña – ähnlichen“ Bedingungen“ [Poster] In: Statusseminar Meeresforschung mit FS SONNE 2013, 13.-15.02.2013, Kiel. (2013)

Ronge, T.; Tiedemann, R.; Nürnberg, D.; Tapia Arroyo, R.; Poggemann, D.-W.; Uenzelmann-Neben, G.; Horn, M.: „SO213-SOPATRA – Fahrtbericht und erste Ergebnisse“ [Vortrag] In: SONNE Statusseminar 2013, 14.-15.02.2013, Kiel (2013).

Aguado, F.; Nürnberg, D.; Poggemann, D.-W.; Tiedemann, R.; Ronge, T.: “Southeast Pacific oceanographic change during the Plio/Pleistocene - implications from surface and subsurface temperature and salinity reconstructions” [Poster] In: GV & Sediment Meeting 2012, 23.-28.09.2012, Hamburg (2012).

Poggemann, D.-W.: “Early Pliocene to late Pleistocene seasurface and subsurface temperature development offshore Chile - Indications from planktonic foraminiferal $\delta^{18}O$ and Mg/Ca” (Diplomarbeit), Christian-Albrechts-Universität, Kiel, 79 pp. (2012).

Poggemann, D.-W.; Nürnberg, D.; Ronge, T.; Tiedemann, R.: “Plio/Pleistocene surface and subsurface temperature and salinity changes off South Chile – Responses to the transition from permanent El Niño-like to modern La Niña-like conditions” [Poster] In: GV & Sediment Meeting 2012, 23.-28.09.2012, Hamburg (2012).

Poggemann, D.-W.: „Tektonische und stratigraphische Untersuchungen im Gebiet Munt Müsella und Piz Mezzaun“ (Studienarbeit), Christian-Albrechts-Universität, Kiel, 56 pp. (2011).

Supplementary material

Supplement S1 for Scientific Chapter 1 as published and available online:

"Rapid Deglacial Injection of Nutrients into the tropical Atlantic via Antarctic Intermediate Water"

Authors: D.-W. Poggemann (corresponding author), E. C. Hathorne, D. Nürnberg, M. Frank, I. Bruhn, S. Reißig and A. Bahr.

Tab. S1.1) AMS dates calibrated using Calib 7.1 and Marine13

Depth (cm)	Measured Radiocarbon Age (BP)	+/- (BP)	Median Age (ka BP, 2σ)
3	569	31	0.24
43	2926	32	2.73
133	8424	44	9.06
188	10500	48	11.76
218	11586	48	13.10
298	13098	49	15.16
326	13850	60	16.21
358	15959	57	18.83
423	20139	93	23.79

Figure S1:

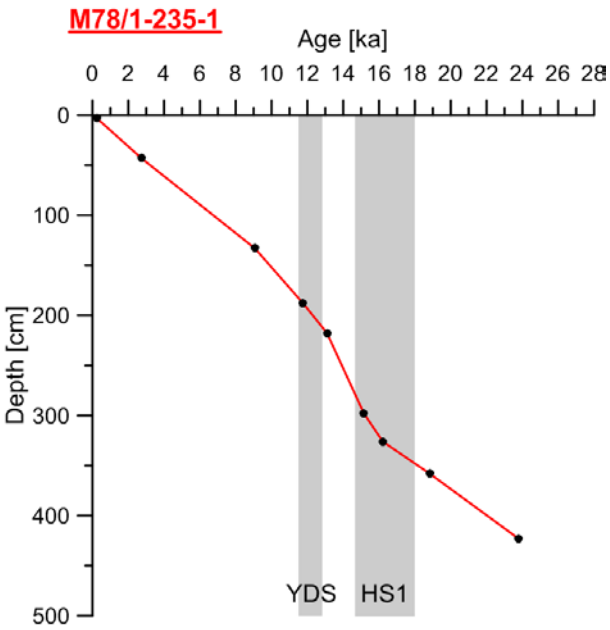

Figure S1.1) Age-model of Sediment core M78/1-235-1. YDS = Younger Dryas Stadial; HS1 = Heinrich Stadial 1. 9 AMS dates were used to create the age model by linear interpolation between the data points.

Cd_w data for sediment core M78/1-235-1 (*Uvigerina spp.*) as published and available online:

/* DATA DESCRIPTION:		
Citation:	Poggemann, David-Willem; Hathorne, Ed C; Nürnberg, Dirk; Frank, Martin; Bruhn, Imke; Reissig, Stefan; Bahr, André (2017): Seawater cadmium concentrations of sediment core M78/1-235-1. doi:10.1594/PANGAEA.872358,	
	In supplement to: Poggemann, D-W et al. (2017): Rapid deglacial injection of nutrients into the tropical Atlantic via Antarctic Intermediate Water. Earth and Planetary Science Letters, 463, 118-126, doi:10.1016/j.epsl.2017.01.030	
Coverage:	LATITUDE: 11.608833 * LONGITUDE: -60.964333	
	DATE/TIME START: 2009-03-22T14:54:00 * DATE/TIME END: 2009-03-22T14:54:00	
	MINIMUM DEPTH, sediment/rock: 0.305 m * MAXIMUM DEPTH, sediment/rock: 4.185 m	
Event(s):	M78/1_235-1 (235-1) * LATITUDE: 11.608833 * LONGITUDE: -60.964333 * DATE/TIME: 2009-03-22T14:54:00 * ELEVATION: -852.2 m * LOCATION: N. Tobago * CAMPAIGN: M78/1 (URI: doi:10.2312/cr_m78_1) * BASIS: Meteor (1986) (URI: https://de.wikipedia.org/wiki/Meteor_(Schiff,_1986)) * DEVICE: Piston corer (PC)	
Parameter(s):	DEPTH, sediment/rock [m] (Depth) * GEOCODE * PI: Poggemann, David-Willem (dpoggemann@geomar.de)	
	AGE [ka BP] (Age) * GEOCODE * PI: Poggemann, David-Willem (dpoggemann@geomar.de)	
	Cadmium [nmol/kg] (Cd) * PI: Poggemann, David-Willem (dpoggemann@geomar.de) * COMMENT: values with # are outliers	
License:	Creative Commons Attribution 3.0 Unported (CC-BY)	
Size:	144 data points	
*/		
Depth [m]	Age [ka BP]	Cdw [nmol/kg]
0.305	1.95	0.59
0.325	2.08	0.65
0.345	2.2	0.69
0.365	2.33	0.78
0.385	2.45	0.78
0.405	2.58	0.76
0.445	2.84	0.56
0.465	2.98	0.65
0.485	3.12	0.54
0.505	3.26	0.66
0.525	3.4	0.58
0.545	3.54	0.74
0.565	3.68	0.68
0.585	3.82	0.75
0.605	3.96	0.68
0.625	4.1	0.54
0.645	4.25	0.56
0.665	4.39	0.76
0.685	4.53	0.84
0.705	4.67	0.6

0.725	4.81	0.75
0.745	4.95	0.67
0.765	5.09	0.76
0.805	5.37	0.68
0.825	5.51	0.63
0.845	5.65	0.63
0.865	5.79	0.51
0.905	6.07	0.74
0.925	6.22	0.73
0.965	6.5	0.72
0.985	6.64	0.69
1.005	6.78	0.7
1.025	6.92	0.66
1.045	7.06	0.73
1.065	7.2	0.73
1.085	7.34	0.7
1.105	7.48	0.68
1.125	7.62	0.8
1.145	7.76	0.69
1.165	7.9	0.77
1.205	8.18	0.57
1.225	8.33	0.74
1.245	8.47	0.75
1.265	8.61	0.7
1.305	8.89	0.61
1.325	9.03	0.69
1.345	9.14	0.72
1.365	9.24	0.86
1.405	9.43	0.68
1.425	9.53	0.74
1.445	9.63	0.82
1.505	9.92	0.79
1.525	10.02	0.62
1.545	10.12	0.75
1.565	10.22	0.84
1.605	10.41	1.09
1.625	10.51	0.91
1.645	10.61	0.71
1.665	10.7	1.12
1.705	10.9	1.08
1.725	11	0.7
1.745	11.1	0.7
1.765	11.19	0.79
1.805	11.39	0.8
1.825	11.49	0.66
1.845	11.59	1.29
1.855	11.64	1.18
1.885	11.78	0.99

1.895	11.83	0.98
2.005	12.32	0.71
2.025	12.41	1.26
2.165	13.04	0.98
2.205	13.17	0.65
2.425	13.73	0.66
2.505	13.94	0.55
2.525	13.99	0.54
2.545	14.04	0.69
2.565	14.09	0.73
2.605	14.2	0.53
2.625	14.25	0.6
2.645	14.3	0.58
2.665	14.35	0.63
2.705	14.45	0.73
2.725	14.5	0.56
2.745	14.56	0.81
2.755	14.58	0.71
2.765	14.61	0.6
2.775	14.63	0.78
2.785	14.66	0.87
2.795	14.68	0.83
2.805	14.71	0.8
2.815	14.74	0.92
2.825	14.76	0.85
2.835	14.79	0.89
2.845	14.81	0.9
2.865	14.86	0.75
2.875	14.89	1.08
2.895	14.94	0.92
2.905	14.97	1.14
2.915	14.99	1.12
2.925	15.02	1.24
2.945	15.07	1.34
2.955	15.09	1.21
2.965	15.12	1.33
2.975	15.15	1.21
2.985	15.19	1.33
2.995	15.22	1.59
3.005	15.25	0.69
3.015	15.29	0.56
3.025	15.33	0.79
3.04	15.39	0.81
3.055	15.44	0.89
3.065	15.48	0.89
3.08	15.54	0.58
3.105	15.63	0.68
3.115	15.67	1

3.255	16.21	0.64
3.38	17.2	0.59
3.505	18.22	0.41
3.545	18.55	0.33
3.565	18.71	0.33
3.605	19.02	0.3
3.625	19.18	0.32
3.645	19.33	0.26
3.665	19.48	0.31
3.725	19.94	0.32
3.745	20.09	#0.91
3.765	20.24	0.52
3.805	20.55	0.18
3.865	21.01	0.33
3.905	21.31	0.32
3.925	21.47	0.22
3.985	21.92	0.24
4.005	22.08	0.28
4.025	22.23	0.28
4.045	22.38	0.28
4.055	22.46	0.24
4.065	22.53	0.36
4.085	22.69	0.41
4.105	22.84	0.23
4.125	22.99	0.37
4.145	23.15	0.35
4.165	23.3	0.29
4.185	23.45	0.31

$\delta^{13}C$ data for sediment core M78/1-235-1 (*Cibicidoides pachyderma*) as published and available online:

/* DATA DESCRIPTION:		
Citation:	Poggemann, David-Willem; Hathorne, Ed C; Nürnberg, Dirk; Frank, Martin; Bruhn, Imke; Reissig, Stefan; Bahr, André (2017): Stable carbon isotopes of sediment core M78/1-235-1. doi:10.1594/PANGAEA.872357,	
	In supplement to: Poggemann, D-W et al. (2017): Rapid deglacial injection of nutrients into the tropical Atlantic via Antarctic Intermediate Water. Earth and Planetary Science Letters, 463, 118-126, doi:10.1016/j.epsl.2017.01.030	
Coverage:	LATITUDE: 11.608833 * LONGITUDE: -60.964333	
	DATE/TIME START: 2009-03-22T14:54:00 * DATE/TIME END: 2009-03-22T14:54:00	
	MINIMUM DEPTH, sediment/rock: 0.305 m * MAXIMUM DEPTH, sediment/rock: 4.105 m	
Event(s):	M78/1_235-1 (235-1) * LATITUDE: 11.608833 * LONGITUDE: -60.964333 * DATE/TIME: 2009-03-22T14:54:00 * ELEVATION: -852.2 m * LOCATION: N. Tobago * CAMPAIGN: M78/1 (URI: doi:10.2312/cr_m78_1) * BASIS: Meteor (1986) (URI: https://de.wikipedia.org/wiki/Meteor_(Schiff,_1986)) * DEVICE: Piston corer (PC)	
Parameter(s):	DEPTH, sediment/rock [m] (Depth) * GEOCODE * PI: Poggemann, David-Willem (dpoggemann@geomar.de)	
	AGE [ka BP] (Age) * GEOCODE * PI: Poggemann, David-Willem (dpoggemann@geomar.de)	
	delta 13C, adjusted/corrected [per mil PDB] (d13C) * PI: Poggemann, David-Willem (dpoggemann@geomar.de) * COMMENT: values with # are outliers	
License:	Creative Commons Attribution 3.0 Unported (CC-BY)	
Size:	59 data points	
*/		
Depth [m]	Age [ka BP]	δ13C [per mil PDB]
0.305	1.95	0.836
0.405	2.58	0.799
0.505	3.26	0.896
0.605	3.96	0.915
0.705	4.67	0.939
0.805	5.37	0.977
0.905	6.07	0.813
1.005	6.78	0.721
1.105	7.48	0.651
1.205	8.18	0.717
1.305	8.89	0.44
1.405	9.43	0.416
1.505	9.92	0.37
1.605	10.41	0.283
1.705	10.9	0.286
1.805	11.39	0.211
1.845	11.59	0.133
1.885	11.78	0.09
1.915	11.92	#0.899
1.945	12.05	0.091

1.98	12.21	0.098
2.002	12.31	0.171
2.045	12.5	0.278
2.08	12.66	0.424
2.125	12.86	0.303
2.185	13.1	0.363
2.225	13.22	0.279
2.305	13.43	0.206
2.33	13.49	0.539
2.405	13.68	0.114
2.505	13.94	0.32
2.605	14.2	0.13
2.705	14.45	0.15
2.745	14.56	0.263
2.785	14.66	0.256
2.805	14.71	0.159
2.845	14.81	0.243
2.88	14.9	0.233
2.925	15.02	0.239
2.965	15.12	0.193
3.005	15.25	0.137
3.045	15.4	0.099
3.075	15.52	0.503
3.125	15.71	0.377
3.165	15.86	0.399
3.205	16.01	0.387
3.245	16.16	0.709
3.275	16.34	0.763
3.325	16.75	0.746
3.365	17.07	0.834
3.405	17.4	0.927
3.43	17.61	#-0.130
3.505	18.22	0.762
3.605	19.02	0.843
3.705	19.79	0.797
3.805	20.55	1.048
3.905	21.31	0.965
4.005	22.08	0.861
4.105	22.84	0.84

Cd_w data for sediment core MD99-2198 (*Uvigerina spp.*) as published and available online:

/* DATA DESCRIPTION:		
Citation:	Poggemann, David-Willem; Hathorne, Ed C; Nürnberg, Dirk; Frank, Martin; Bruhn, Imke; Reissig, Stefan; Bahr, André (2017): Seawater cadmium concentrations of sediment core MD99-2198. doi:10.1594/PANGAEA.872359,	
	In supplement to: Poggemann, D-W et al. (2017): Rapid deglacial injection of nutrients into the tropical Atlantic via Antarctic Intermediate Water. Earth and Planetary Science Letters, 463, 118-126, doi:10.1016/j.epsl.2017.01.030	
Coverage:	LATITUDE: 12.091833 * LONGITUDE: -61.233500	
	DATE/TIME START: 1999-08-01T00:00:00 * DATE/TIME END: 1999-08-01T00:00:00	
	MINIMUM DEPTH, sediment/rock: 0.035 m * MAXIMUM DEPTH, sediment/rock: 4.975 m	
Event(s):	MD99-2198 (6bis2G) * LATITUDE: 12.091833 * LONGITUDE: -61.233500 * DATE/TIME: 1999-08-01T00:00:00 * ELEVATION: -1330.0 m * Recovery: 35.53 m * LOCATION: Tobago basin * CAMPAIGN: MD114 (IMAGES V) (URI: hdl:10013/epic.42867.d001) * BASIS: Marion Dufresne (URI: http://www.institut-polaire.fr/ipev/bases_et_navires/le_marion_dufresne) * DEVICE: Calypso Corer (CALYPSO)	
Comment:	Age obtained from Pahnke et al., 2008 "Abrupt changes in Antarctic Intermediate Water circulation over the past 25,000 years". Nature Geoscience 1(12): 870-874.	
Parameter(s):	DEPTH, sediment/rock [m] (Depth) * GEOCODE * PI: Poggemann, David-Willem (dpoggemann@geomar.de)	
	AGE [ka BP] (Age) * GEOCODE * PI: Poggemann, David-Willem (dpoggemann@geomar.de)	
	Cadmium [nmol/kg] (Cd) * PI: Poggemann, David-Willem (dpoggemann@geomar.de)	
License:	Creative Commons Attribution 3.0 Unported (CC-BY)	
Size:	82 data points	
*/		
Depth [m]	Age [ka BP]	Cdw [nmol/kg]
0.035	0.01	0.42
0.185	0.42	0.5
0.335	0.83	0.55
0.485	1.24	0.51
0.635	1.65	0.4
0.935	2.48	0.48
1.085	2.93	0.43
1.235	3.48	0.43
1.385	4.02	0.62
1.535	4.56	0.43
1.835	5.64	0.43
1.985	6.18	0.55
2.135	6.72	0.62
2.285	7.26	0.51
2.435	7.8	0.42
2.585	8.34	0.52

2.735	8.88	0.54
2.885	9.43	0.4
3.075	10.08	0.5
3.125	10.25	0.49
3.175	10.41	0.47
3.225	10.57	0.46
3.275	10.74	0.5
3.325	10.9	0.42
3.375	11.06	0.46
3.425	11.35	0.56
3.455	11.53	0.57
3.465	11.59	0.61
3.475	11.65	0.46
3.485	11.71	0.73
3.505	11.83	0.46
3.515	11.89	0.69
3.525	11.95	0.59
3.525	11.95	0.4
3.535	12.01	0.6
3.575	12.23	0.48
3.585	12.29	0.44
3.615	12.46	0.5
3.625	12.51	0.45
3.625	12.51	0.46
3.675	12.79	0.56
3.685	12.85	0.43
3.725	13.07	0.39
3.775	13.35	0.4
3.825	13.63	0.47
3.875	13.91	0.33
3.925	14.19	0.55
3.975	14.47	0.5
3.985	14.53	0.46
4.005	14.64	0.42
4.015	14.7	0.49
4.025	14.75	0.5
4.025	14.75	0.45
4.035	14.81	0.55
4.055	14.92	0.52
4.065	14.98	0.44
4.075	15.03	0.44
4.085	15.09	0.51
4.095	15.14	0.55
4.105	15.2	0.43
4.125	15.31	0.52
4.125	15.31	0.48
4.135	15.43	0.39
4.145	15.6	0.47

4.205	16.55	0.45
4.215	16.64	0.44
4.235	16.81	0.3
4.255	16.98	0.46
4.275	17.16	0.43
4.325	18.16	0.28
4.375	18.59	0.36
4.425	19.02	0.36
4.475	19.49	0.21
4.525	19.97	0.32
4.575	20.38	0.3
4.625	20.79	0.25
4.675	21.12	0.32
4.725	21.45	0.32
4.775	21.78	0.29
4.875	22.49	0.28
4.925	22.92	0.31
4.975	23.36	0.3

Supplement S2 for Scientific Chapter 2:

"Deglacial heat deprivation from the atmosphere in the Southern Ocean via Antarctic Intermediate Water"

Authors: D.-W. Poggemann (corresponding author), D. Nürnberg, W. Rath, E. C. Hathorne, M. Frank, S. Reißig, A. Bahr

Age model of sediment core M78/1-222-9

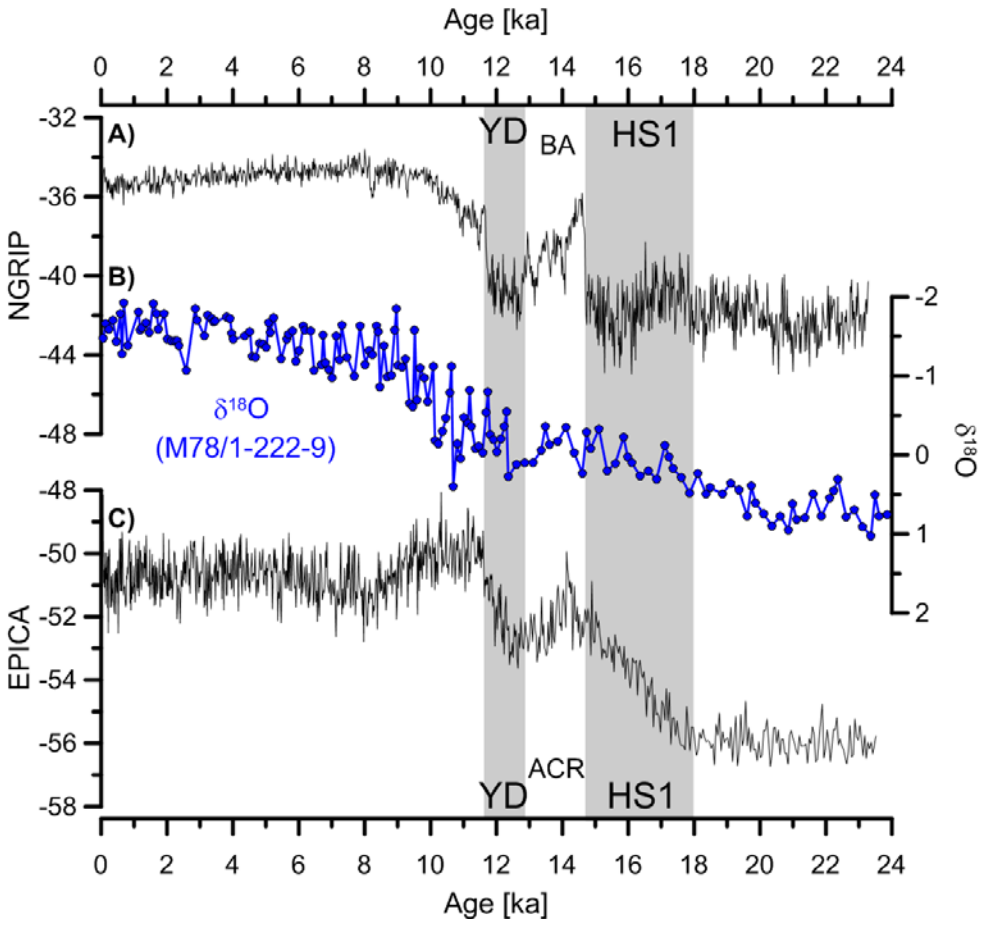

Figure S2.1: Comparison of stable oxygen isotopes to northern and southern hemisphere reference records. **A)** Oxygen isotope record of the Greenland NGRIP ice core (NGRIP Dating Group, 2006) as reference reflecting the northern hemisphere climate signal (black). **B)** Stable oxygen isotope record of sediment core M78/1-222-9 (blue). **C)** Oxygen isotope record of the Antarctica EPICA Dome C (Stenni et al., 2006) as reference reflecting the southern hemisphere climate signal (black). HS1 = Heinrich Stadial 1; YD = Younger Dryas Stadial; BA = Bølling-Allerød; ACR = Antarctic Cold Reversal;

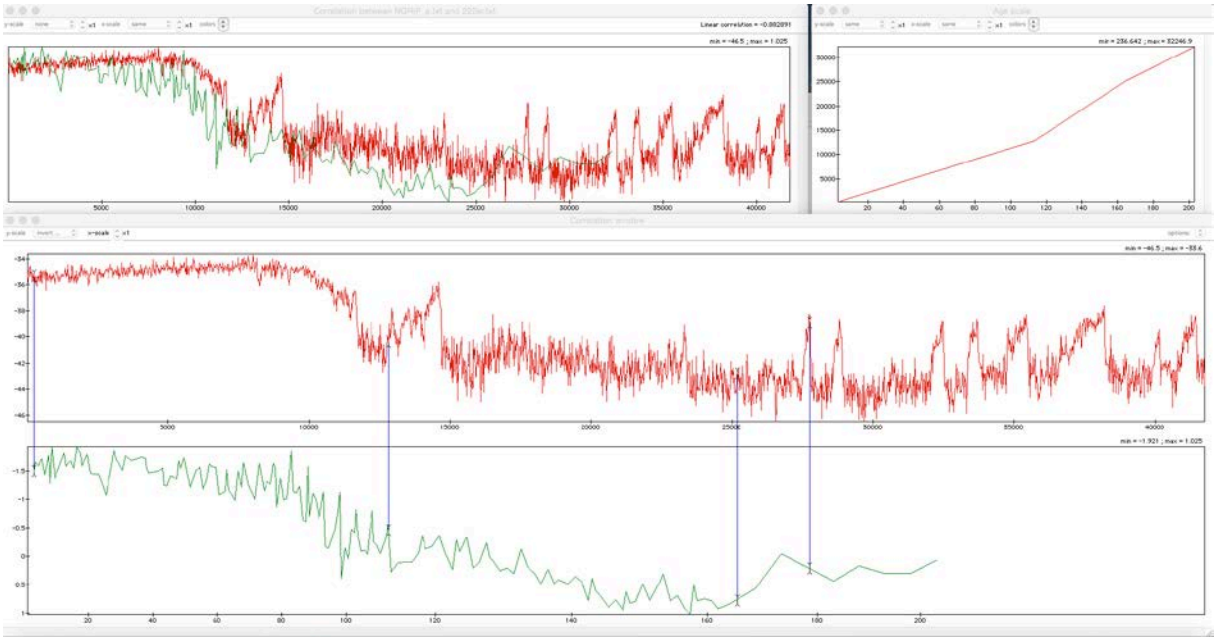

Figure S2.2: Optical referencing of the age model of sediment core M78/1-222-9 with NGRIP using AnalySeries 2.0.4.2. **Top left**: Oxygen isotope record of the Greenland NGRIP ice core (red, NGRIP Dating Group, 2006) with oxygen isotope record of sediment core M78/1-222-9 (green) placed on top of each other to monitor correlation (correlation factor is 0.883). **Top right:** depth versus age plot with depth below sediment surface on x-axis and age on y-axis. **Bottom:** Tuning of oxygen isotope record of sediment core M78/1-222-9 (green) to Greenland NGRIP ice core (red) using pointers for the measured and calibrated AMS ^{14}C dates. Please note: no additional pointers were selected. The age model therefore is created by linear interpolation between the AMS ^{14}C dates

Contamination check

To check for possible contamination by clay minerals or other element coatings we monitored Mn/Ca and Fe/Ca ratios in comparison to Mg/Ca ratios:

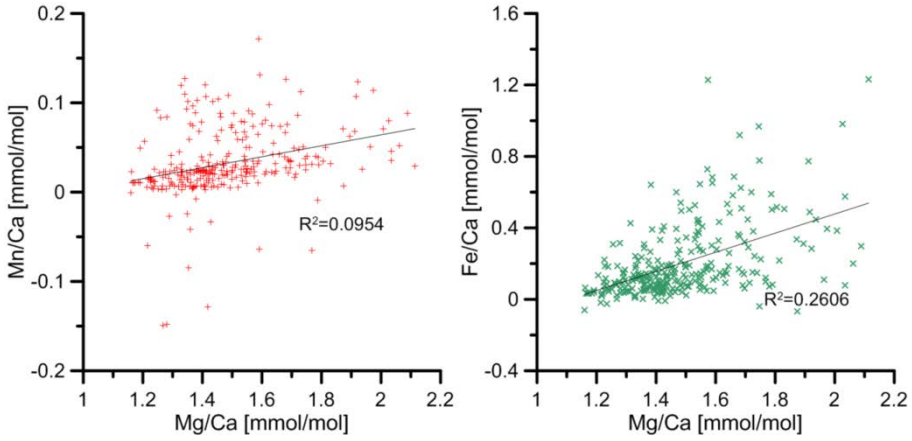

Figure S2.3: Element/Calcium ratio comparison for Mn/Ca vs. Mg/Ca (left, red) and for Fe/Ca vs. Mg/Ca (right, green). There is no correlation between Mn/Ca and Mg/Ca or for Fe/Ca and Mg/Ca and hence we assume no diagenetic alteration of our Mg/Ca data.

Data points rejected as outliers

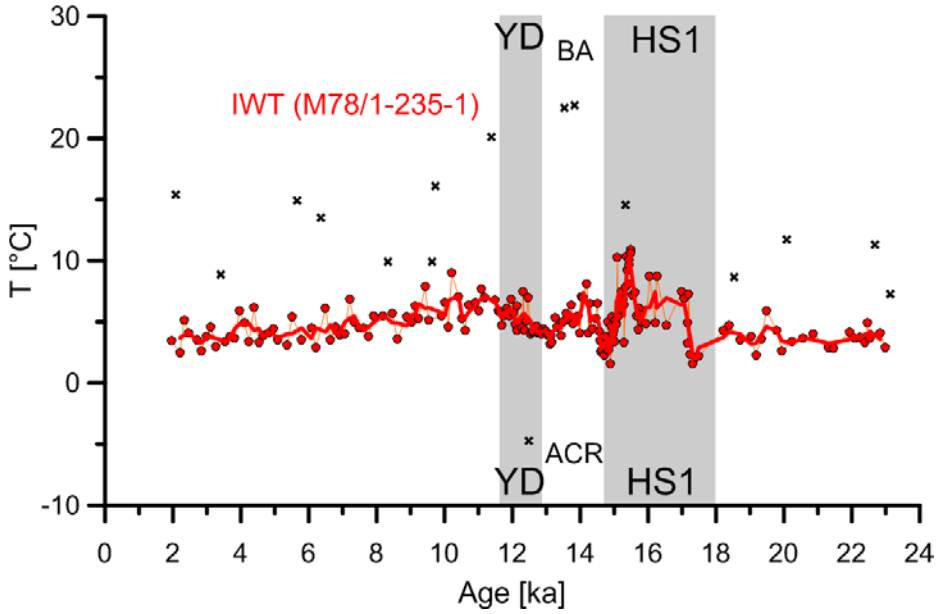

Figure S2.4: Mg/Ca based IWT data points for sediment core M78/1-235-1. Besides the high resolution IWT record (red) 16 data points seemed unrealistically high (or low) and were tested by a Grubb's test. Based on this, these data were rejected as outliers (black crosses).

Comparison of IWT-calibrations for *Uvigerina spp.*

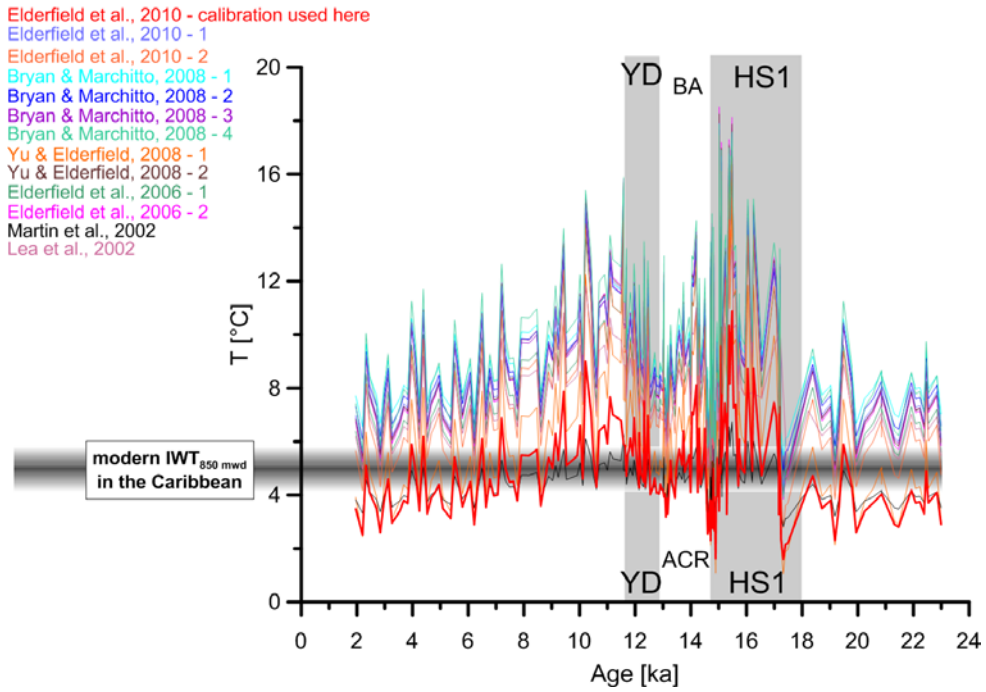

Figure S2.5: Comparison of available temperature calibrations for *Uvigerina spp*. Linear and exponential calibrations from previous studies (Lea et al., 2002; Martin et al., 2002; Elderfield et al., 2006; Yu & Elderfield, 2008; Brian & Marchitto, 2008; Elderfield et al., 2010).

Comparison of standard 400yr and local 277yr reservoir age calibration:

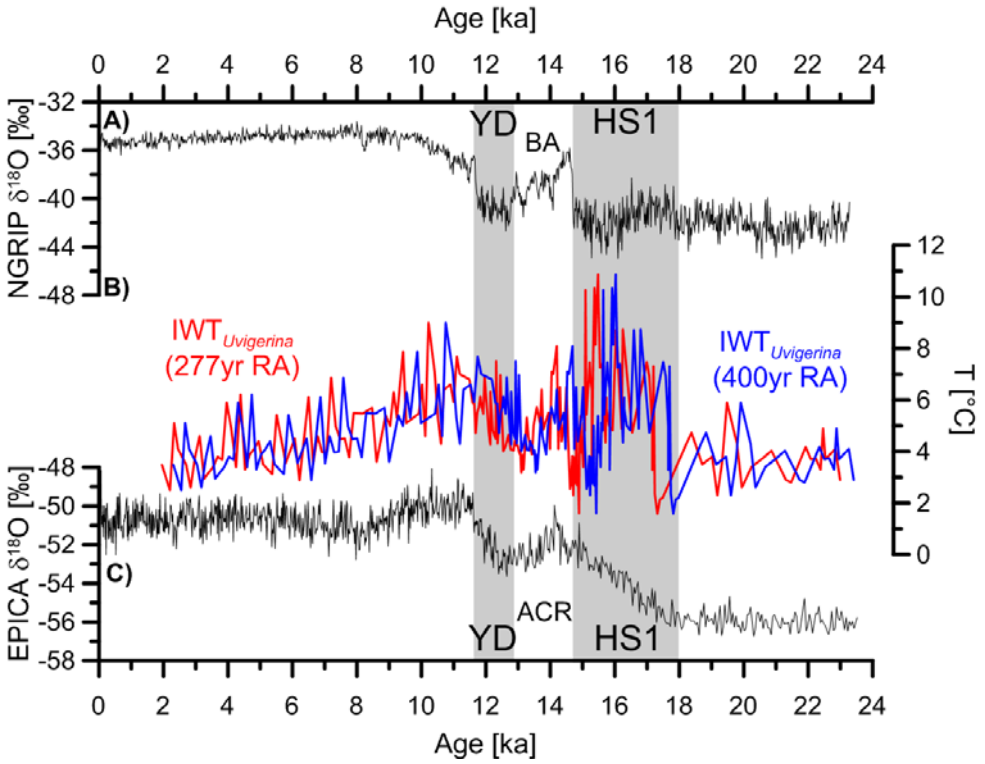

Figure S2.6: Comparison of different reservoir age corrections. **Blue**: IWT record with age model corrected using Calib 7.10 and the standard 400yr reservoir age (IntCal13). **Red**: IWT record with age model corrected using Calib 7.10 and the local 277yr reservoir age (MARINE13).

Additional references:

Elderfield et al.: "Calibrations for benthic foraminiferal Mg/Ca paleothermometry and the carbonate ion hypothesis." *Earth and Planetary Science Letters* 250.3 (2006): 633-649.

Lear et al.: "Benthic foraminiferal Mg/Ca-paleothermometry: A revised core-top calibration." *Geochimica et Cosmochimica Acta* 66.19 (2002): 3375-3387.

Martin et al.: "Quaternary deep sea temperature histories derived from benthic foraminiferal Mg/Ca." *Earth and Planetary Science Letters* 198.1 (2002): 193-209.

Yu, Elderfield: "Mg/Ca in the benthic foraminifera Cibicidoides wuellerstorfi and Cibicidoides mundulus: Temperature versus carbonate ion saturation." *Earth and Planetary Science Letters* 276.1 (2008): 129-139.

Mg/Ca based IWT data for sediment core M78/1-235-1 (*Uvigerina spp.*) as described in Scientific Chapter 2:

Depth [cm]	Age [ka BP]	Mg/Ca [mmol/mol]	IWT [°C]	IWT-Outlier [°C]	Al/Ca [mmol/mol]	Mn/Ca [mmol/mol]	Fe/Ca [mmol/mol]
30.5	1.95	1.35	3.5		0.04	-0.02	0.05
32.5	2.08	2.54		15.4			
34.5	2.20	1.25	2.5		0.02	0.09	0.07
36.5	2.33	1.51	5.1		0.02	0.09	0.07
38.5	2.45	1.41	4.1		0.02	0.11	0.09
42.5	2.70	1.35	3.5		0.02	0.09	0.13
44.5	2.84	1.26	2.6		0.01	0.08	0.09
46.5	2.98	1.38	3.8		0.11	0.09	0.19
48.5	3.12	1.46	4.6		0.07	0.09	0.13
50.5	3.26	1.30	3.0		0.01	0.04	0.06
52.5	3.4	1.89		8.9			
54.5	3.54	1.34	3.4		0.01	0.13	0.14
56.5	3.68	1.38	3.8		-0.02	0.10	0.08
58.5	3.82	1.37	3.7		0.03	0.07	0.05
60.5	3.96	1.59	5.9		-0.02	0.13	0.05
62.5	4.10	1.49	4.9		0.00	0.11	0.04
64.5	4.25	1.34	3.4		0.01	0.11	0.12
66.5	4.39	1.62	6.2		0.07	0.10	0.13
68.5	4.53	1.33	3.3		-0.02	0.12	0.13
70.5	4.67	1.39	3.9		0.00	0.07	0.05
72.5	4.81	1.41	4.1		0.06	0.12	0.17
74.5	4.95	1.44	4.4		0.03	0.10	0.12
76.5	5.09	1.35	3.5		0.05	0.10	0.10
80.5	5.37	1.31	3.1		-0.02	0.00	0.04
82.5	5.51	1.54	5.4		0.32	0.08	0.38
84.5	5.65	2.49		14.9			
86.5	5.79	1.36	3.6		0.00	0.06	0.00
90.5	6.07	1.45	4.5		0.03	0.10	0.18
92.5	6.22	1.29	2.9		0.01	-0.03	0.14
94.5	6.36	2.35		13.5			
96.5	6.50	1.61	6.1		0.30	0.08	0.43
98.5	6.64	1.35	3.5		0.01	-0.08	0.11
100.5	6.78	1.46	4.6		0.03	0.08	0.15
102.5	6.92	1.40	4.0		0.00	0.04	0.05
104.5	7.06	1.40	4.0		0.04	0.08	0.16
106.5	7.20	1.69	6.9		0.31	0.04	0.51
108.5	7.34	1.50	5.0		0.07	0.08	0.18
110.5	7.48	1.45	4.5		-0.01	0.06	0.02
112.5	7.62	1.45	4.5		0.06	0.06	0.15
114.5	7.76	1.38	3.8		-0.01	-0.01	0.06
116.5	7.90	1.55	5.5		0.11	0.01	0.14
120.5	8.18	1.55	5.5		0.02	0.05	0.05

122.5	8.33	1.99		9.9			
124.5	8.47	1.57	5.7		0.07	0.07	0.16
126.5	8.61	1.36	3.6		-0.02	-0.04	0.05
130.5	8.89	1.54	5.4		0.09	0.07	0.30
132.5	9.03	1.50	5.0		0.09	0.07	0.20
134.5	9.14	1.63	6.3		0.02	0.07	0.16
136.5	9.24	1.53	5.3		0.12	0.08	0.34
140.5	9.43	1.79	7.9		0.47	-0.01	0.59
142.5	9.53	1.51	5.1		0.05	0.07	0.19
144.5	9.63	1.99		9.9			
146.5	9.73	2.61		16.1			
150.5	9.92	1.55	5.5		0.15	0.02	0.65
152.5	10.02	1.66	6.6		0.11	0.07	0.69
154.5	10.12	1.46	4.6		-0.01	0.07	0.10
156.5	10.22	1.90	9.0		0.06	0.06	0.31
160.5	10.41	1.71	7.1		0.09	0.05	0.45
162.5	10.51	1.53	5.3		-0.01	0.06	0.14
164.5	10.61	1.43	4.3		0.03	-0.03	0.15
166.5	10.70	1.64	6.4		0.11	0.05	0.53
170.5	10.90	1.66	6.6		0.12	0.04	0.58
172.5	11.00	1.59	5.9		-0.02	-0.06	0.11
174.5	11.10	1.77	7.7		-0.02	-0.07	0.10
176.5	11.19	1.70	7.0		0.11	0.04	0.32
180.5	11.39	3.01		20.1			
182.5	11.49	1.68	6.8		0.06	0.03	0.35
184.5	11.59	1.59	5.9		0.15	0.03	0.45
185.5	11.64	1.59	5.9		0.04	0.03	0.20
186.5	11.68	1.47	4.7		0.01	0.03	0.06
187.5	11.73	1.55	5.5		0.00	0.02	0.08
188.5	11.78	1.57	5.7		-0.01	0.03	0.05
189.5	11.83	1.61	6.1		0.01	0.02	0.15
190.5	11.87	1.58	5.8		0.00	0.02	0.19
191.5	11.92	1.55	5.5		-0.01	0.02	0.11
192.5	11.96	1.69	6.9		0.01	0.02	0.15
194.0	12.03	1.57	5.8		0.02	0.02	1.23
195.5	12.09	1.48	4.8		0.05	0.02	0.10
196.5	12.14	1.43	4.3		0.02	0.04	0.07
196.5	12.14	1.63	6.3		-0.20	0.02	0.09
198.0	12.21	1.48	4.8		0.03	0.02	0.21
200.0	12.30	1.45	4.5		0.00	0.03	0.04
200.5	12.32	1.75	7.5		0.10	0.04	0.22
201.5	12.36	1.43	4.3		0.00	0.02	-0.01
202.5	12.41	1.51	5.1		0.02	0.03	0.07
203.5	12.45	1.70	7.0		0.04	0.03	0.06
204.5	12.5	0.53		-4.74			
205.5	12.54	1.40	4.0		0.03	0.04	0.13
206.5	12.59	1.41	4.2		-0.04	0.01	0.04
207.0	12.61	1.42	4.2		-0.01	0.03	0.06

209.0	12.70	1.46	4.6		0.06	0.02	0.17
210.5	12.77	1.41	4.1		-0.19	0.01	-0.01
211.0	12.79	1.41	4.1		0.03	0.02	0.15
212.5	12.86	1.40	4.0		0.03	0.02	0.04
213.5	12.90	1.44	4.4		-0.02	0.02	0.13
214.5	12.95	1.42	4.2		0.01	0.02	0.04
215.5	12.99	1.42	4.2		0.01	0.02	0.05
216.5	13.04	1.39	3.9		0.01	0.02	0.07
217.5	13.07	1.40	4.0		-0.01	0.02	0.06
218.5	13.10	1.32	3.2		0.01	0.02	0.11
219.5	13.14	1.39	3.9		0.06	0.02	0.39
220.5	13.17	1.33	3.3		0.06	0.02	0.12
224.5	13.27	1.53	5.3		0.06	0.02	0.10
226.5	13.32	1.46	4.6		-0.09	0.02	0.06
230.5	13.43	1.39	3.9		-0.06	0.02	0.14
232.5	13.48	1.5	5.0		0.03	0.01	0.18
234.5	13.53	3.25		22.5			
236.5	13.58	1.57	5.7		0.18	0.03	0.73
240.5	13.68	1.51	5.1		0.03	0.02	0.09
242.5	13.73	1.64	6.4		0.04	0.02	0.19
244.5	13.78	1.48	4.9		0.34	0.02	0.49
246.5	13.84	3.27		22.7			
250.5	13.94	1.55	5.5		0.01	0.03	0.12
252.5	13.99	1.41	4.1		0.07	0.02	0.33
254.5	14.04	1.71	7.1		0.02	0.02	0.29
256.5	14.09	1.70	7.0		0.04	0.03	0.14
260.5	14.20	1.81	8.1		0.13	0.03	0.51
262.5	14.25	1.41	4.1		0.01	0.03	0.11
264.5	14.30	1.65	6.5		0.08	0.02	0.49
266.5	14.35	1.44	4.4		0.04	0.03	0.19
270.5	14.45	1.53	5.3		0.14	0.03	0.53
272.5	14.50	1.65	6.5		0.01	0.03	0.26
274.5	14.56	1.42	4.2		0.08	0.02	0.19
275.5	14.58	1.35	3.5		0.00	0.02	0.13
276.5	14.61	1.25	2.6		0.02	0.02	0.31
277.5	14.63	1.27	2.7		0.00	0.02	0.19
278.5	14.66	1.33	3.3		0.01	0.03	0.24
279.5	14.68	1.38	3.8		0.01	0.03	0.64
280.5	14.71	1.23	2.3		0.02	0.01	0.19
281.5	14.74	1.38	3.8		0.00	0.02	0.11
282.5	14.76	1.28	2.8		-0.01	0.02	0.10
283.5	14.79	1.28	2.8		-0.01	0.02	0.10
284.5	14.81	1.50	5.0		-0.03	0.02	0.02
285.5	14.84	1.27	2.7		0.00	0.02	0.00
286.5	14.86	1.31	3.1		-0.01	0.02	0.08
287.5	14.89	1.16	1.6		0.00	0.02	0.06
288.5	14.91	1.47	4.7		0.06	0.03	0.39
289.5	14.94	1.54	5.4		0.17	0.03	0.44

290.5	14.97	1.39	4.0		0.03	0.02	0.17
291.5	14.99	1.42	4.2		0.03	0.02	0.10
292.5	15.02	1.34	3.4		0.05	0.02	0.22
293.5	15.04	1.51	5.1		0.17	0.03	0.50
294.5	15.07	1.48	4.8		0.04	0.03	0.28
295.5	15.09	2.03	10.3		0.41	0.08	0.98
296.5	15.12	1.54	5.4		0.13	0.04	0.45
297.5	15.15	1.60	6.0		0.11	0.05	0.28
298.5	15.19	1.68	6.8		0.20	0.04	0.36
299.5	15.22	1.75	7.5		0.25	0.04	0.97
300.5	15.25	1.68	6.8		0.07	0.07	0.17
301.5	15.29	1.33	6.4		2.17	0.02	0.02
301.5	15.29	1.64	3.3		0.01	0.04	0.14
302.5	15.33	2.46		14.55			
302.5	15.33	1.78	7.8		0.68	0.04	0.07
303.5	15.37	2.03	10.4		0.27	0.05	0.08
304.0	15.39	1.92	9.2		0.05	0.12	0.28
304.5	15.4	1.81	8.2		0.10	0.05	0.22
305.5	15.44	1.96	10.1		0.12	0.05	0.11
305.5	15.44	1.96	9.6		0.08	0.07	0.38
306.5	15.48	2.06	10.9		0.22	0.05	0.20
306.5	15.48	2.06	10.6		0.19	0.09	0.30
308.0	15.54	1.72	7.3		0.03	0.05	0.15
310.0	15.61	1.74	7.4		-0.02	0.05	0.15
311.5	15.67	1.54	5.5		0.01	0.03	0.08
312.5	15.71	1.43	4.3		0.02	0.03	0.09
313.5	15.74	1.56	6.1		0.09	0.03	0.07
313.5	15.74	1.56	5.6		0.25	0.02	0.33
315.5	15.82	1.50	5.0		0.10	0.03	0.35
318.5	15.93	1.48	4.8		-0.03	0.04	0.54
321.5	16.04	1.87	8.7		0.01	0.07	0.34
325.5	16.21	1.49	4.9		-0.01	0.04	0.07
326.5	16.25	1.87	8.7		-0.64	0.01	-0.07
330.0	16.54	1.47	4.7		0.13	0.03	0.25
335.5	16.99	1.75	7.5		-0.90	0.03	-0.04
336.5	17.07	1.69	6.9		-0.01	0.03	0.08
337.5	17.16	1.33	4.9		-0.10	0.03	0.01
337.5	17.16	1.49	3.3		10.61	0.00	0.14
338.0	17.20	1.73	7.3		-0.03	0.11	0.24
338.5	17.24	1.24	2.4		6.65	0.00	-0.03
339.5	17.32	1.16	1.6		12.51	0.00	-0.06
340.5	17.4	1.21	2.2		7.79	0.01	-0.02
341.5	17.48	1.22	2.2		0.00	0.02	0.03
350.5	18.22	1.43	4.3		0.07	0.01	0.13
352.5	18.38	1.47	4.7		0.39	0.01	0.33
354.5	18.55	1.87		8.7			
356.5	18.71	1.35	3.5		0.03	0.01	0.14
360.5	19.02	1.38	3.8		0.01	0.01	0.12

362.5	19.18	1.23	2.3		0.04	0.01	0.12
364.5	19.33	1.36	3.6		0.00	0.01	0.08
366.5	19.48	1.59	5.9		0.08	0.01	0.17
370.5	19.79	1.43	4.3		-0.01	0.01	0.05
372.5	19.94	1.26	2.6		0.02	0.00	0.09
374.5	20.09	2.17		11.7			
376.5	20.24	1.34	3.4		0.03	0.01	0.13
380.5	20.55	1.37	3.7		0.06	0.00	0.14
384.5	20.86	1.40	4.0		0.04	0.02	0.08
390.5	21.31	1.29	2.9		0.05	0.01	0.12
392.5	21.47	1.28	2.8		-0.01	-0.15	0.04
398.5	21.92	1.42	4.2		0.00	-0.13	0.03
400.5	22.08	1.37	3.7		0.03	0.00	0.12
402.5	22.23	1.37	3.7		0.16	0.01	0.22
404.5	22.38	1.33	3.3		0.01	0.01	0.11
405.5	22.46	1.49	4.9		0.01	0.01	0.09
406.5	22.53	1.37	3.7		0.01	0.01	0.07
408.5	22.69	2.13		11.3			
410.5	22.84	1.41	4.1		0.08	0.01	0.22
412.5	22.99	1.29	2.9		-0.01	0.02	0.09
414.5	23.15	1.73		7.3			

εNd data for sediment core M78/1-222-9 (mixed planktonic foraminiferal tests) as described in Scientific Chapter 2:

Depth [cm]	**Age [ka BP]**	**εNd**	**±, error**
17.0	1.63	-11.5	0.1
33.0	3.41	-11.6	0.1
49.0	5.19	-11.7	0.3
65.0	6.97	-11.9	0.3
81.0	8.74	-11.3	0.3
86.0	9.30	-11.4	0.3
92.0	9.97	-11.2	0.1
98.0	10.63	-11.2	0.2
104.0	11.30	-11.3	0.3
110.0	11.97	-11.0	0.3
115.5	12.86	-11.2	0.4
120.5	14.11	-11.1	0.1
125.5	15.36	-10.9	0.1
130.5	16.61	-10.4	0.5
135.5	17.86	-10.2	0.1
142.5	19.61	-10.0	0.3
147.5	20.86	-9.6	0.4
152.5	22.12	-9.8	0.3
157.5	23.37	-9.9	0.3
162.5	24.62	-9.9	0.3
167.5	25.37	-10.2	0.3
172.5	26.01	-9.9	0.3
177.5	26.64	-10.1	0.3
182.5	27.36	-10.2	0.3
187.5	28.11	-10.4	0.3

$\delta^{18}O$ data for sediment core M78/1-222-9 (*Globigerinoides ruber*) as described in Scientific Chapter 2:

Depth [cm]	Age [ka BP]	δ18-O [‰]
3.5	0.13	-1.659
4.5	0.25	-1.588
5.5	0.36	-1.706
6.5	0.47	-1.431
7.5	0.58	-1.782
8.5	0.69	-1.921
9.5	0.8	-1.376
12.5	1.13	-1.81
13.5	1.25	-1.605
14.5	1.36	-1.673
15.5	1.47	-1.545
16.5	1.58	-1.911
17.5	1.69	-1.786
19.5	1.91	-1.783
20.5	2.02	-1.46
21.5	2.13	-1.442
22.5	2.24	-1.443
23.5	2.36	-1.375
25.5	2.58	-1.063
28.5	2.91	-1.708
30.5	3.13	-1.509
31.5	3.24	-1.769
32.5	3.36	-1.722
33.5	3.47	-1.69
36.5	3.8	-1.741
37.5	3.91	-1.726
38.5	4.02	-1.462
41.5	4.36	-1.504
43.5	4.58	-1.243
44.5	4.69	-1.233
45.5	4.8	-1.408
46.5	4.91	-1.401
47.5	5.02	-1.358
48.5	5.13	-1.543
49.5	5.24	-1.736
51.5	5.47	-1.212
53.5	5.69	-1.522
54.5	5.8	-1.57
55.5	5.91	-1.179
56.5	6.02	-1.315
57.5	6.13	-1.625
59.5	6.36	-1.563
60.5	6.47	-1.072

62.5	6.69	-1.142
63.5	6.8	-1.159
64.5	6.91	-1.078
65.5	7.02	-0.973
66.5	7.13	-1.502
67.5	7.24	-1.208
69.5	7.47	-1.239
71.5	7.69	-0.995
74.5	8.02	-1.142
75.5	8.13	-1.313
76.5	8.24	-1.265
77.5	8.36	-1.63
78.5	8.47	-0.862
79.5	8.58	-1.38
80.5	8.69	-0.988
81.5	8.8	-1.008
82.5	8.91	-1.578
83.5	9.02	-1.133
84.5	9.13	-1.111
85.5	9.24	-1.218
86.5	9.36	-0.648
87.5	9.47	-0.606
88.5	9.58	-0.694
89.5	9.69	-1.095
90.5	9.8	-0.971
91.5	9.91	-0.668
93.5	10.13	-0.181
94.5	10.24	-0.138
95.5	10.36	-0.293
96.5	10.47	-0.459
97.5	10.58	-0.791
98.5	10.69	0.396
99.5	10.8	-0.141
100.5	10.91	0.048
101.5	11.02	-0.473
102.5	11.13	-0.398
103.5	11.24	-0.36
104.5	11.36	-0.083
105.5	11.47	-0.111
106.5	11.58	-0.028
107.5	11.69	-0.537
108.5	11.8	-0.255
109.5	11.91	-0.196
110.5	12.02	-0.038
111.5	12.13	-0.199
112.5	12.24	-0.357
113.5	12.36	0.276
114.5	12.61	0.117

115.5	12.86	0.098
116.5	13.11	0.097
117.5	13.36	-0.054
118.5	13.61	-0.128
119.5	13.86	-0.172
120.5	14.11	-0.349
121.5	14.36	-0.027
122.5	14.61	0.233
123.5	14.86	-0.077
124.5	15.11	-0.33
125.5	15.36	0.201
126.5	15.61	0.105
127.5	15.86	-0.226
128.5	16.11	0.103
129.5	16.36	0.263
130.5	16.61	0.204
131.5	16.86	0.305
132.5	17.11	-0.12
133.5	17.36	0.176
134.5	17.61	0.286
135.5	17.86	0.489
136.5	18.11	0.236
137.5	18.36	0.493
139.5	18.86	0.492
140.5	19.11	0.361
141.5	19.36	0.448
142.5	19.61	0.78
143.5	19.86	0.605
144.5	20.11	0.747
145.5	20.36	0.899
146.5	20.61	0.772
147.5	20.86	0.949
148.5	21.11	0.823
149.5	21.36	0.797
150.5	21.61	0.49
151.5	21.86	0.78
152.5	22.12	0.55
153.5	22.37	0.312
154.5	22.62	0.785
155.5	22.87	0.695
156.5	23.12	0.911
157.5	23.37	1.025
158.5	23.62	0.776
159.5	23.87	0.751

Supplement S3 for Scientific Chapter 3:

"Antarctic Intermediate Water effectively cooled the Gulf of Mexico during rapid deglacial northern hemisphere cooling events"

Authors: D.-W. Poggemann (corresponding author), D. Nürnberg, E. C. Hathorne, M. Frank, S. Reißig,

Age model of sediment core M78/1-180-1

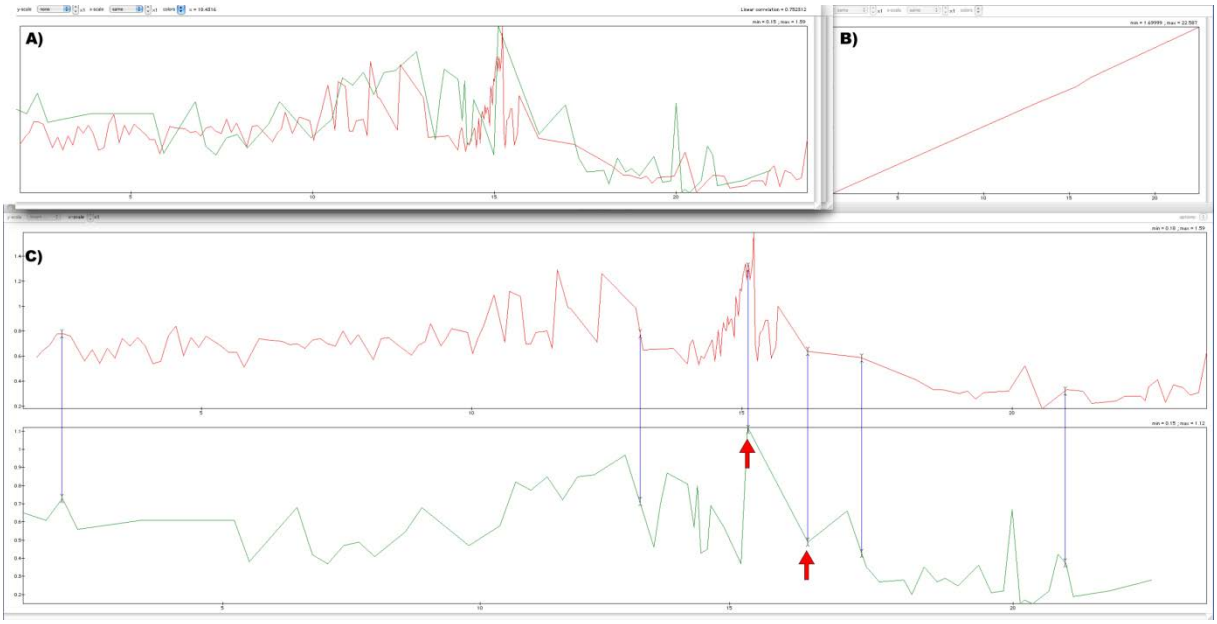

Figure S3.1: Visual referencing of the age model of sediment core M78/1-180-1 using AnalySeries 2.0.4.2. **A)** Cd_w record of sediment core M78/1-235-1 (red, Poggemann et al., 2017) with appropriate Cd_w record of sediment core M78/1-180-1 (green) placed on top of each other to monitor correlation (correlation factor is 0.75). **B)** depth versus age plot with depth below sediment surface on x-axis and age on y-axis. **C)** Visual referencing of Cd_w record of sediment core M78/1-180-1 (green) to Cd_w record of core M78/1-235-1 (red) using pointers for the measured and calibrated AMS ^{14}C dates. Please note: two additional pointers were selected to improve the age model of sediment core M78/1-180-1 between 13.37 and 16.94 ka (red arrows). The age model was created by linear interpolation between the AMS ^{14}C dates and the two additional pointers.

Table S3.1: AMS dates calibrated using Calib 7.1 and Marine13

Depth [cm]	Measured Radiocarbon Age (BP)	+/- (BP)	Median Age (ka BP)
1.5	1690	30	1.27
40.5	11610	50	13.12
69.5	14520	60	17.21
118.5	17770	70	20.98
148.5	21090	100	24.96

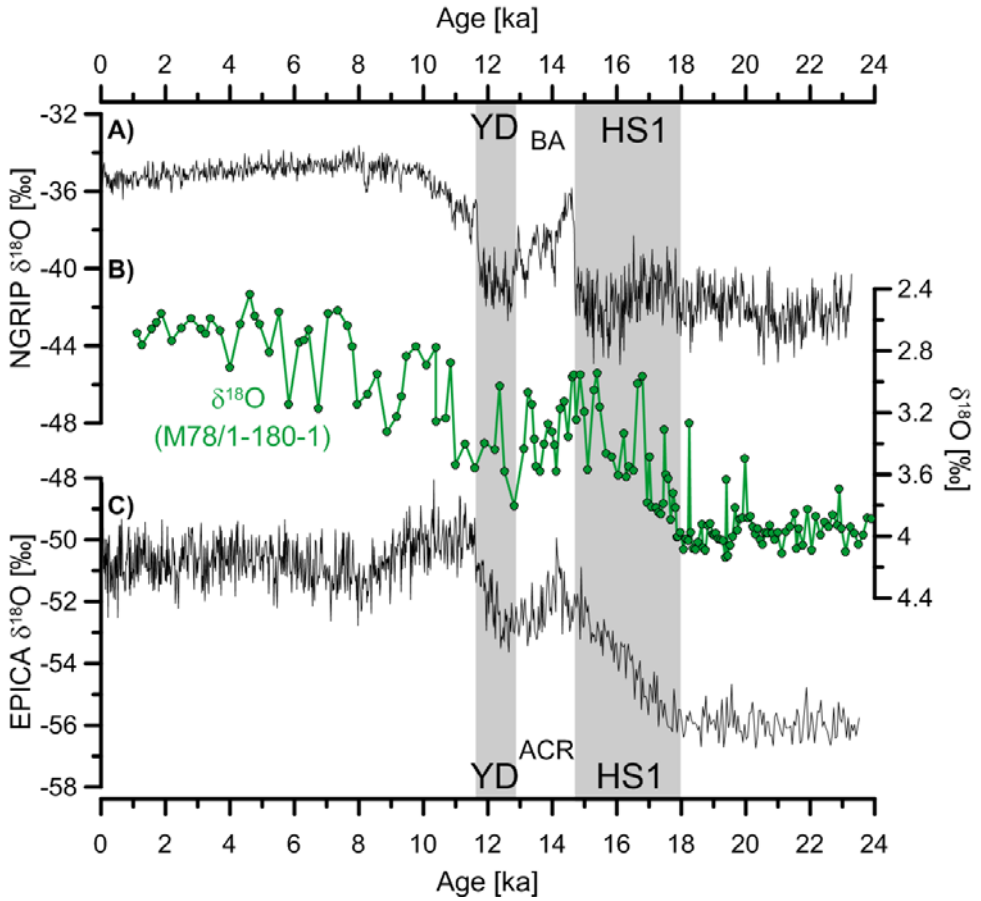

Figure S3.2: Comparison of stable oxygen isotopes to northern and southern hemisphere reference records. **A)** Oxygen isotope record of the Greenland NGRIP ice core (NGRIP Dating Group, 2006) as reference reflecting the northern hemisphere climate signal (black). **B)** Stable oxygen isotope record of sediment core M78/1-180-1 (green) obtained from the benthic foraminiferal species *Uvigerina spp.* **C)** Oxygen isotope record of the Antarctica EPICA Dome C (Stenni et al., 2006) as reference reflecting the southern hemisphere climate signal (black). HS1 = Heinrich Stadial 1; YD = Younger Dryas Stadial; BA = Bølling-Allerød; ACR = Antarctic Cold Reversal;

Comparison of IWT-calibrations for *Cibicides lobatulus*

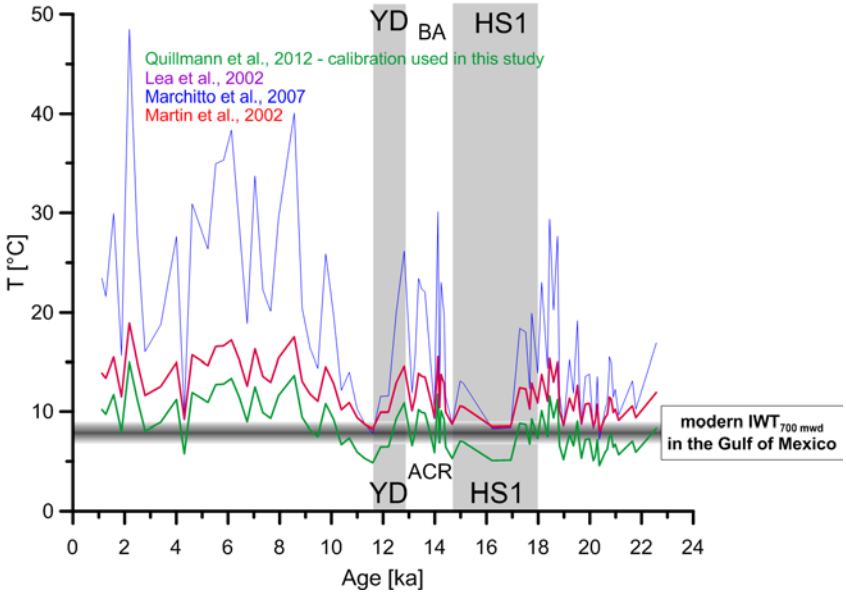

Figure S3.3: Comparison of available temperature calibrations for *Cibicides lobatulus* from previous studies (Lea et al., 2002; Martin et al., 2002; Marchitto et al., 2007; Quillmann et al., 2012). Note: the purple and the red curve are almost identical and therefore plot on each other.

Contamination check

To check for possible contamination by clay minerals or other element coatings we monitored Mn/Ca, Al/Ca and Fe/Ca ratios in comparison to Mg/Ca ratios:

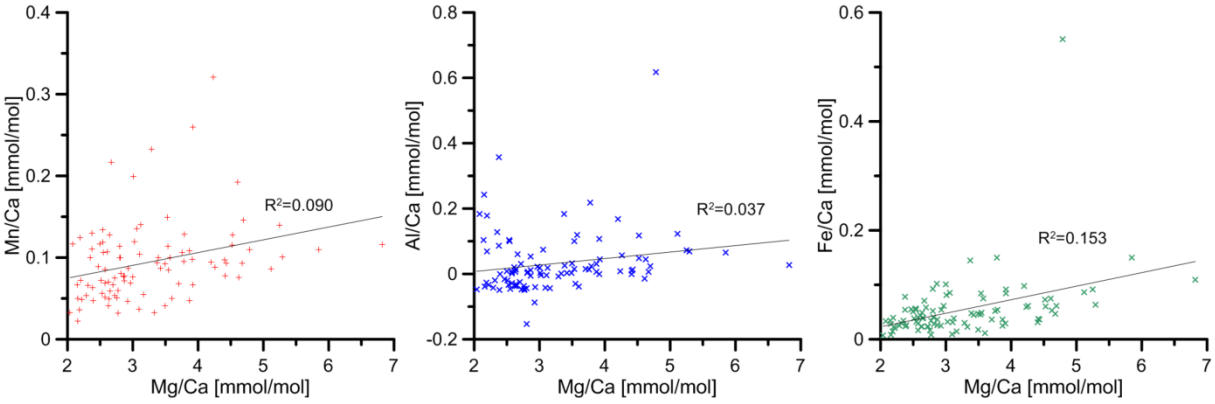

Figure S3.4: Element/Calcium ratio comparison for Mn/Ca vs. Mg/Ca (left, red), for Al/Ca vs. Mg/Ca (middle, blue) and for Fe/Ca vs. Mg/Ca (right, green). There is no correlation between Mg/Ca and Mn/Ca, Al/Ca, or Fe/Ca. Hence we assume no diagenetic alteration of our Mg/Ca data.

Additional references:

Lear et al.: "Benthic foraminiferal Mg/Ca-paleothermometry: A revised core-top calibration." *Geochimica et Cosmochimica Acta* 66.19 (2002): 3375-3387.

Marchitto et al.: "Mg/Ca temperature calibration for the benthic foraminifer Cibicidoides pachyderma." *Paleoceanography* 22.1 (2007).

Martin et al.: "Quaternary deep sea temperature histories derived from benthic foraminiferal Mg/Ca." *Earth and Planetary Science Letters* 198.1 (2002): 193-209.

Mg/Ca based IWT and Cd_w data for sediment core M78/1-180-1 (*Cibicides lobatulus*) as described in Scientific Chapter 3:

Depth [cm]	Age [ka]	Mg/Ca [mmol/ mol]	IWT [°C]	Cd_w [nmol/ kg]	Al/Ca [mmol/ mol]	Mn/Ca [mmol/ mol]	Fe/Ca [mmol/ mol]
0.5	1.12	3.92	10.2	0.65	0.11	0.07	0.09
1.5	1.27	3.70	9.7		0.01	0.07	0.04
2.5	1.57	4.67	11.7	0.61	0.01	0.09	0.05
3.5	1.88	3.01	7.9	0.73	0.00	0.20	0.08
4.5	2.18	6.82	15.0	0.56	0.03	0.12	0.11
5.5	2.49	4.43	11.3		0.01	0.09	0.04
6.5	2.79	3.06	8.1		0.07	0.14	0.09
8.5	3.40	3.38	8.9	0.61	0.18	0.09	0.14
10.5	4.00	4.41	11.2		0.01	0.10	0.03
11.5	4.31	2.34	5.8				
12.5	4.61	4.79	11.9		0.62	0.11	0.55
13.5	4.92	4.52	11.4		0.12	0.12	0.07
14.5	5.22	4.26	10.9	0.61	0.06	0.09	0.06
15.5	5.52	5.25	12.7	0.38	0.07	0.14	0.09
16.5	5.83	5.29	12.8		0.07	0.10	0.06
17.5	6.13	5.65	13.4				
18.5	6.44	4.53	11.4	0.68	0.05	0.13	0.06
19.5	6.74	3.39	9.0	0.42	0.03	0.10	0.05
20.5	7.04	5.12	12.5	0.37	0.12	0.09	0.09
21.5	7.35	3.78	9.9	0.47	0.22	0.09	0.15
22.5	7.65	3.54	9.3	0.49	0.10	0.11	0.08
23.5	7.95	4.62	11.6	0.41	0.04	0.08	0.05
25.5	8.56	5.85	13.7	0.55	0.06	0.11	0.15
26.5	8.87	3.58	9.4	0.68	0.12	0.10	0.08
27.5	9.17	3.10	8.2		0.00	0.10	0.03
28.5	9.47	2.87	7.5		0.05	0.08	0.03
29.5	9.78	4.20	10.8	0.47	0.17	0.09	0.10
30.5	10.08	3.50	9.2		0.03	0.09	0.05
31.5	10.39	2.61	6.7	0.69	0.02	0.11	0.04
32.5	10.69	2.82	7.4	0.82	-0.15	0.11	0.09
33.5	10.99	2.39	5.9	0.95	0.02	0.14	0.04
34.5	11.30	2.22	5.3	0.90	0.07	0.12	0.04
35.5	11.60	2.11	4.9	0.72	0.18	0.12	0.03
36.5	11.90	2.54	6.5	0.85	0.10	0.12	0.06
37.5	12.21	2.54	6.5	0.86	0.10	0.13	0.05
38.5	12.51	3.53	9.3		0.02	0.15	0.05
39.5	12.82	4.24	10.9	0.97	0.01	0.32	0.06
40.5	13.12	2.58	6.6		0.00	0.09	0.03
41.5	13.25	3.02	8.0		0.00	0.12	0.03
42.5	13.37	3.92	10.2	0.46	0.00	0.10	0.03
43.5	13.49	3.79	9.9	0.70	0.02	0.13	0.05
44.5	13.62	3.76	9.8	0.87	0.01	0.11	0.05

46.5	13.87	2.82	7.4		0.01	0.08	0.03
47.5	13.99	2.38	5.9	0.81	0.13	0.10	0.03
48.5	14.12	4.69	11.8	0.57	0.02	0.15	0.06
49	14.18	2.67	6.9	0.80	-0.03	0.13	0.04
49.5	14.24	3.87	10.1	0.43	0.03	0.11	0.04
50.5	14.36	3.49	9.2	0.45	0.00	0.04	0.02
51	14.42	2.54	6.5	0.69	0.01	0.12	0.05
53	14.67	2.22	5.3	0.57	0.18	0.07	0.02
55.5	14.98	2.72	7.1	0.37	0.03	0.05	0.02
56.5	15.10	2.70	7.0	1.12	0.06	0.22	0.07
62.5	16.22	2.16	5.1	0.49	0.24	0.05	0.03
67.5	16.94	2.18	5.1	0.66	0.10	0.07	0.03
70.5	17.29	3.33	8.8	0.35	0.00	0.03	0.02
73.5	17.52	3.29	8.7	0.27	-0.01	0.23	0.03
75.5	17.67	2.63	6.8		0.01	0.04	0.02
76.5	17.75	3.51	9.3				
79.5	17.98	2.81	7.3	0.28	0.00	0.10	0.04
81.5	18.13	3.87	10.1	0.20	0.01	0.05	0.02
84.5	18.36	2.87	7.5	0.35	-0.01	0.07	0.04
85.5	18.44	4.61	11.6		-0.02	0.19	0.07
87.5	18.59	3.55	9.3	0.27	-0.03	0.08	0.05
89.5	18.75	4.41	11.2	0.29	0.00	0.08	0.04
90.5	18.83	2.57	6.6		0.01	0.07	0.04
92.5	18.98	2.19	5.2	0.25	-0.03	0.04	0.01
95.5	19.21	2.97	7.8		0.02	0.07	0.06
97.5	19.36	2.58	6.6	0.36	-0.03	0.05	0.02
99.5	19.52	3.42	9.0		0.00	0.09	0.04
100.5	19.60	2.64	6.8	0.21	0.01	0.05	0.05
101.5	19.67	2.22	5.3		-0.03	0.05	0.02
103.5	19.83	2.77	7.2	0.22	-0.05	0.03	0.01
105.5	19.98	2.80	7.3	0.67	-0.04	0.10	0.05
107.5	20.13	2.16	5.1	0.15	-0.04	0.02	0.01
108.5	20.21	2.29	5.6	0.17	-0.04	0.05	0.02
109.5	20.29	2.77	7.2		-0.05	0.06	0.03
110.5	20.36	2.04	4.6	0.15	-0.05	0.03	0.01
113.5	20.60	2.39	6.0		0.00	0.05	0.03
114.5	20.67	2.47	6.2	0.22	-0.02	0.09	0.05
115.5	20.75	2.86	7.5		0.01	0.08	0.10
116.5	20.83	2.93	7.7	0.42	-0.04	0.09	0.05
117.5	20.90	2.53	6.4		-0.03	0.06	0.06
118.5	20.98	2.62	6.7	0.37	-0.04	0.07	0.02
119.5	21.11	2.32	5.7	0.19	-0.02	0.07	0.03
123.5	21.64	2.72	7.1		-0.05	0.07	0.02
124.5	21.78	2.39	5.9	0.22	-0.05	0.06	0.02
130.5	22.57	3.16	8.4	0.28	-0.04	0.06	0.01

$\delta^{18}O$ data for sediment core M78/1-180-1 (*Uvigerina spp.*) as described in Scientific Chapter 3:

Depth [cm]	Age [ka BP]	δ18O [‰]
0.5	1.12	2.69
1.5	1.27	2.76
2.5	1.57	2.66
3.0	1.73	2.62
3.5	1.88	2.56
4.5	2.18	2.73
5.5	2.49	2.65
6.5	2.79	2.59
7.5	3.09	2.66
8.0	3.25	2.69
8.5	3.40	2.59
9.5	3.70	2.67
10.5	4.00	2.91
11.5	4.31	2.63
12.5	4.61	2.43
13.0	4.76	2.57
13.5	4.92	2.63
14.5	5.22	2.81
15.5	5.52	2.55
16.5	5.83	3.15
17.5	6.13	2.75
18.0	6.28	2.73
18.5	6.44	2.67
19.5	6.74	3.18
20.5	7.04	2.56
21.5	7.35	2.54
22.5	7.65	2.64
23.0	7.80	2.78
23.5	7.95	3.15
24.5	8.26	3.08
25.5	8.56	2.95
26.5	8.87	3.32
27.5	9.17	3.23
28.0	9.32	3.10
28.5	9.47	2.84
29.5	9.78	2.77
30.5	10.08	2.89
31.5	10.39	2.78
31.5	10.39	3.26
32.5	10.69	3.23
33.0	10.84	2.88
33.5	10.99	3.54
34.5	11.30	3.40

35.5	11.60	3.56
36.5	11.90	3.40
37.5	12.21	3.44
38.0	12.36	3.03
38.5	12.51	3.58
39.5	12.82	3.80
40.5	13.12	3.43
41.5	13.25	3.07
42.5	13.37	3.15
43.0	13.43	3.37
43.5	13.49	3.55
44.5	13.62	3.58
45.5	13.74	3.41
46.5	13.87	3.27
47.5	13.99	3.33
48.0	14.06	3.41
48.5	14.12	3.58
49.5	14.24	3.17
50.5	14.36	3.13
51.5	14.48	3.36
52.5	14.61	2.97
53.0	14.67	2.96
53.5	14.73	3.25
54.5	14.86	2.95
55.5	14.98	3.20
56.5	15.10	3.57
57.5	15.29	3.05
58.0	15.38	2.94
58.5	15.47	3.16
59.5	15.66	3.47
60.5	15.85	3.49
61.5	16.03	3.61
62.5	16.22	3.34
63.0	16.29	3.62
63.5	16.36	3.55
64.5	16.51	3.58
65.5	16.65	3.01
66.5	16.80	2.97
67.5	16.94	3.78
68.0	17.01	3.49
68.5	17.08	3.81
69.5	17.21	3.81
70.5	17.29	3.84
71.5	17.36	3.86
72.5	17.44	3.79
73.0	17.48	3.31
73.5	17.52	3.60
74.5	17.59	3.63

75.5	17.67	3.89
76.5	17.75	3.72
77.5	17.83	3.82
78.0	17.86	4.01
78.5	17.90	4.00
79.5	17.98	3.97
80.5	18.06	4.08
81.5	18.13	4.02
82.5	18.21	4.03
83.0	18.25	3.27
83.5	18.29	3.98
84.5	18.36	4.08
85.5	18.44	4.09
86.5	18.52	4.04
88.0	18.63	3.93
88.5	18.67	4.07
89.5	18.75	4.09
90.5	18.83	3.93
91.5	18.90	3.92
92.5	18.98	3.99
93.0	19.02	3.99
93.5	19.06	3.98
94.5	19.13	4.02
95.5	19.21	4.02
96.5	19.29	4.03
97.5	19.36	4.14
98.0	19.40	3.63
98.5	19.44	4.13
99.5	19.52	4.06
100.5	19.60	4.00
101.5	19.67	3.81
102.5	19.75	3.96
103.5	19.83	3.89
104.5	19.90	3.88
105.5	19.98	3.50
106.5	20.06	3.88
107.5	20.13	3.87
108.5	20.21	3.94
109.5	20.29	3.99
110.5	20.36	3.95
111.5	20.44	4.02
112.5	20.52	4.06
113.5	20.60	3.97
114.5	20.67	3.98
115.5	20.75	3.93
116.5	20.83	3.98
117.5	20.90	4.02
118.5	20.98	3.98

119.5	21.11	4.11
120.5	21.25	3.97
121.5	21.38	3.94
122.5	21.51	3.85
123.0	21.58	4.08
123.5	21.64	3.95
124.5	21.78	4.06
125.5	21.91	3.82
126.5	22.04	4.09
127.5	22.17	3.87
128.5	22.31	3.99
129.5	22.44	3.91
130.5	22.57	3.94
131.5	22.70	3.86
132.5	22.84	3.93
133.0	22.90	3.70
133.5	22.97	3.95
134.5	23.10	4.10
135.5	23.24	3.94
136.5	23.37	3.98
137.5	23.50	4.05
138.5	23.63	3.99
139.5	23.77	3.88
140.5	23.90	3.89